Model-based Wavelength Estimation with Tunable Color Filter and Single Photodiode

T.E Agbana

Master of Science Thesis

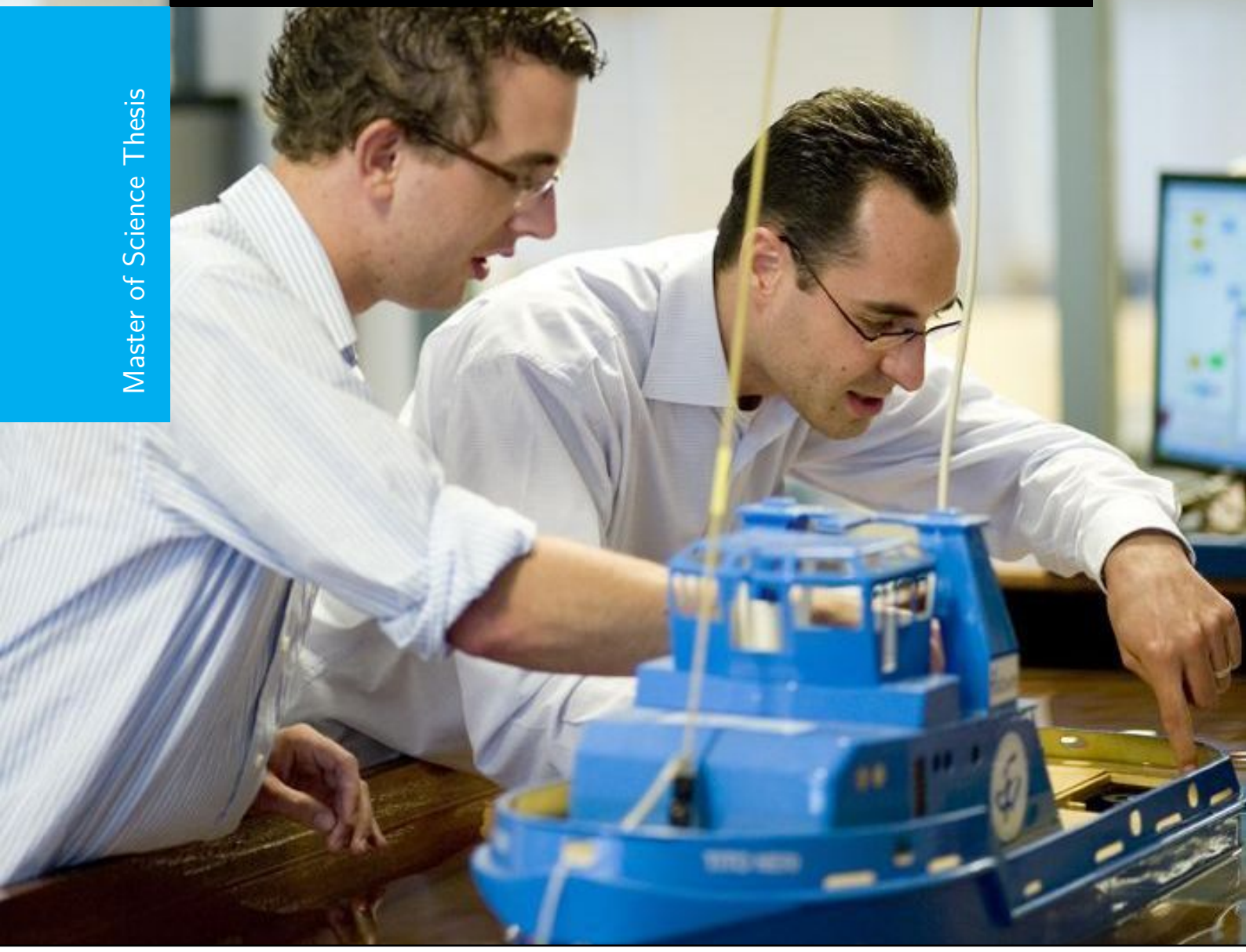

TU Delft Delft University of Technology

Delft Center for Systems and Control

Model-based Wavelength Estimation with Tunable Color Filter and Single Photodiode

Master of Science Thesis

For the degree of Master of Science in Electrical Engineering at Delft University of Technology

T.E Agbana

5th July 2013

Faculty of Electrical Engineering · Delft University of Technology

Delft University of Technology
Department of
Department of Telecommunications(eemcs)

The undersigned hereby certify that they have read and recommend to the Faculty of Electrical Engineering for acceptance a thesis entitled

Model-based Wavelength Estimation with Tunable Color Filter and Single Photodiode

by

T.E Agbana

in partial fulfillment of the requirements for the degree of

Master of Science Electrical Engineering

Dated: 5th July 2013

Supervisor(s):

prof.dr.ir. M. Verhaegen

prof.dr. O. Yaravoy

Reader(s):

prof.dr.ir. J. Spronck

dr.ir. J. Kalkman

Abstract

Wavelength measurement and control of lasers is of paramount importance and has found vast application in areas such as linear and nonlinear spectroscopy, multichannel wavelength division multiplexing, laser meteorology and applications which involve testing of laser and LED light sources to ensure spectral purity and power distribution.

While the state of the art optical wavelength measuring devices such as the AQ6317 Yokogowa Optical spectrum analyzer have high spectral resolution of about 0.015nm at the cost price of 50,000 euro,and the Thorlabs FT Michelson Spectrometer with a resolution of about 0.001nm has a cost price of about 23,000 euros, other easy to use table top Wavelength Meter developed in recent time provide limited resolution and accuracy. The trade off is cost, resolution, size and accuracy.

The major research question in this thesis is how do we realize an optical wavelength measurement machine which has the capability of providing a spectral resolution better than 0.015nm with an accuracy better than 0.1nm at a low-cost?

In this thesis we presents a novel and simple approach to optical wavelength measurement and the working principles is demonstrated with a tunable color filter and a single photodiode. A simple and lowcost solution that could lead to realising the functionality of the state of the art equipment at a cost of less than 700 euros is therefore proposed in this thesis work.

Table of Contents

Acknowledgements **xiii**

1 Introduction **1**

1-1 The Need for Optical Wavelength Measurement Devices 2

1-2 Principles of Optical Wavelength Measurements 3

1-3 Interferometric Spectrometers 4

1-3-1 Michelson interferometer based Spectrometer 4

1-3-2 Advantages of the Fourier Transform Spectrometer 10

1-3-3 Disadvantages of the Fourier Transform Spectrometer 10

1-4 Resonance based Spectrometer 11

1-4-1 Fabry-Perot Interferometer 11

1-4-2 Advantage of the Fabry-Perot Interferometer 14

1-4-3 Disadvantage of the Fabry-Perot Interferometer 14

1-5 Spatial dispersion based Spectrometer 14

1-5-1 Wavelength Tuning 18

1-5-2 Tuning Techniques 19

1-5-3 Advantage of the Diffraction grating Spectrometer 19

1-5-4 Disadvantages of the Diffractiong grating Spectrometer 19

1-6 Optical Spectrum Analyzer Using the Combination of Grating and Fabry Perot Interferometer 19

1-7 Specification of Optical Wavelength Measurement devices. 20

1-7-1 Resonance based principles for wavelength estimation 22

1-7-2 The Look-up table approach 23

1-7-3 Our proposed Wavelength estimation approach 23

1-8 Motivation and Goal for this thesis 23

1-8-1 Goal of this thesis 24

1-8-2 Main contributions 24

2 Model-based Wavelength Meter Theory **25**
2-1 Introduction . . . 25
2-2 Overview of system components . . . 26
2-2-1 Bandpass Filter (Tunable Color Filter) . . . 26
2-2-2 Light sensor . . . 28
2-3 Strategy . . . 30
2-3-1 Step 1 : Formulation of the Problem . . . 31
2-3-2 Step 2 : Calibration of the Spectral Function $(f(\lambda_0, v_k))$ . . . 32
2-3-3 Step 3: System set-up and Generation of Data . . . 33
2-3-4 Step 4 : Wavelength estimation . . . 34
2-4 Validation of the proposed strategy . . . 37
2-4-1 Design of a Tunable laser source using a Laser Pointer . . . 38
2-4-2 Design of Tunable Light Source with a Bandpass Filter . . . 39
2-5 Concluding Remarks . . . 43

3 Wavelength Estimation **45**
3-1 Experimental set-up of Tunable light source . . . 45
3-1-1 Experiment and Results . . . 46
3-1-2 Calibration of the tunable color filter . . . 47
3-2 Wavelength Estimation Methods . . . 47
3-2-1 Non-Linear Least square Optimisation approach based on Neural Network 47
3-2-2 The Neural Network Approach . . . 49
3-2-3 The Hybrid Method . . . 50
3-3 Performance Measures . . . 51
3-3-1 Variance-Accounted-For . . . 51
3-3-2 Sum of Squares . . . 52
3-4 Experiments and results . . . 52
3-5 Data for calibration and wavelength estimation . . . 53
3-5-1 Data set A . . . 53
3-5-2 Validation Data set B . . . 54
3-5-3 Data set C . . . 54
3-5-4 Data set D . . . 55
3-6 Data Processing . . . 55
3-6-1 Normalizing the transmission data points . . . 55
3-6-2 System of equation . . . 55
3-7 Results for Data Set A and Data Set B . . . 57
3-7-1 Result of trained Neural Network with validation data set A . . . 57
3-7-2 Result of trained Neural Network with validation data set B . . . 57
3-7-3 Neural Network algorithm validation data set B Normalized . . . 57
3-7-4 Hybrid (Neural Network - Nonlinear least square optimisation) algorithm validation data set B Normalized . . . 58

3-7-5 Results for Data Set C and Validation Data Set D 59
3-7-6 Neural Network Algorithm with Dataset D 59
3-7-7 Non-linear least square optimisation algorithm 60
3-7-8 Hybrid solution (Educated - iterative method) 60
3-8 Concluding Remarks 61

4 Temperature Drift **77**
4-1 Bandpass Filter Performance 77
4-1-1 Impact of Temperature on the performance of Bandpass filter 77
4-2 Experimental details 79
4-2-1 Function $\hat{F}(\lambda, U)_{RT}$ with Validation dataset generated at high temperature. 79
4-2-2 Case Scenarios 81
4-3 Concluding Remarks 83

5 Conclusions **89**
5-0-1 Thesis Contribution 90
5-1 Conclusions 90
5-2 Recommendation 91

A Basic idea of the Neural Network **93**
A-1 An Appendix Section 93
A-1-1 Advantages of the Artificial Neural Network. 93
A-1-2 Non-linear model of a neuron 94
A-1-3 Knowledge Representation of the Neural Network 95
A-1-4 Learning Process of a Neural Network 96
A-1-5 The Back Propagation Algorithm 98

B Methods for solving the Non Linear Least Square **99**
B-0-6 Gradient Descent Method 99
B-0-7 Gauss-Newton Method 99
B-0-8 Levenberg-Marquardt Method 100

Bibliography **101**

List of Abbreviations **101**

List of Figures

1-1 *Schematic of the Michelson interferometer.The input light beam is splitted into two. While $E_1(z,t)$ is transmitted to the moving mirror, the other half $E_2(z,t)$ is reflected to the fixed mirror. The variation of the distance d of the moving mirror causes a consequent sinusoidal variation in the output intensity and the combined intensity from the mirrors m_1 and m_2 is therefore measured at the output of the interferometer by the detector [6].* 4

1-2 *Illustration of the intensity of the light beam at the exit of the Michelson interferometer as a function of optical path difference. As observed in the figure above, Maximum intensity is obtained when the path difference is equal to $n\lambda$ where n is an integer. When $d_1 = d_2$ as shown in fig 1.2, then the two beams are in phase and this consequently yields a constructive interference depicted in this schematic as a peak. Conversely destructive interference represented by the dip in the diagram is experienced when the path difference is half the wavelength.* 5

1-3 *Normalized photocurrent versus differential arm length for wavelength $\lambda = 1550nm$*[19] 8

1-4 *Schematic diagram showing the working principle of the Fabry Perot Interferometer. The input electric field E_{in} enters the cavity and it is reflected multiple times until the amplitude of the field is significantly reduced.* 11

1-5 *Illustration of a circular fringes pattern when a noncollimated light source is launched onto a screen through a Fabry Perot Interferometer.*[18] 12

1-6 *Block diagram of an optical spectrum measurement using a scanning Fabry Perot Interferometer*[18] 14

1-7 *The Incident beam is separated by the input beam into a number of outputs.Within the output beam, except the zero order beam, different wavelengths are separated. [2]* 15

1-8 *Diffraction grating with period l. The first order diffraction angle appears when delay between reflections from the neighbor grooves is equal to one wavelength Λ.[6]* 16

1-9 *Monochromator optical scheme: d_i and d_o are the sizes of the input and output slits respectively, F is the focal length of the mirrors and φ is the angle between the incident and the diffracted beam and α denotes the incident angle of the light on the grating.* 17

1-10 *High resolution Spectrometer design based on the combination of the Fabry Perot Interferometer and dispersion grating optical devices.*[18] 20

2-1 Overview of a Bandpass filter (purchased from Thorlabs and used in our system set-up) showing the transmission of the well defined wavelength band of light [27]. 26

2-2 Filter operation overview showing the filter structure. Picture gotten from Thorlabs [27],a manufacturer of the tunable color filter used in our system model. 27

2-3 Diagram showing a typical photodiode and its current-voltage charateristics depicting the increasing in photocurrent of the photodiode when the illumination of the PN junction increases.[28]. 29

2-4 A junction photodiode model with basic discrete components depicting the main characteristics of the operation of photodiodes. Picture gotten from Thorlabs [],a manufacturer of the photodiode used in our system model. 30

2-5 A pictoral representation of noise sources in a photodetector [25] 30

2-6 Schematic of the proposed wavelength measurement method.Control signal $v(k)$ is applied to the TCF and intensity $y(k)$ is measured from the photodiode. . . . 31

2-7 Figure showing a typical set up for irradiance measurement. The incoming light source is coupled to the AvaSpec through a fibre optics cable,the CC-UV/VIS and the Avasphere-50-IRRAD enables the coupling of the incoming light into the spectrometer. The spectrometer is connected to the computer via a USB cable and the read out of the wavelength is obtained on the computer through the Avasoft software installed for wavelength and intensity measurement. 34

2-8 Schematic of the tunable light laser source using a laser pointer. 38

2-9 *The schematic diagram of the Tunable Light Source. The light from the red Light Emitting Diode is collimated by the collimating Lens system and then incident on the tunable color filter mounted on a stepper motor, the output from the tunable color filter is collimated again and passed through a beam splitter where. The incoming light is splitted and part is reflected to the spectrometer and part is further transmitted into the wavelength meter*[18] 40

3-1 Figure showing the plot of wavelength obtained by tuning the tunable color filter,the color filter is mounted on a stepper motor which provides the control input signal θ thus generating a total of 18 wavelengths when the angle is displaced from normal angle. Maximum wavelength obtained is 632.3nm and the minimum is 609.3nm. For our application, 15 wavelengths were selected and the rest discarded. Although this does not proffer a very accurate tunable light source for the calibration of our system, it however gives an opportunity to develop a proof of concept in the DSCS Optics Lab. 63

3-2 Figure showing the system set-up comprising of the tunable light source 64

3-3 Spectra curve $f(\lambda, v)$ for different motor angle u at fixed wavelength λ. 1 angle step is approximately equal to 1 degree. Intensity varies from 0 (all blocked),to maximum; 64

3-4 Spectra curve $f(\lambda, u)$ for different motor angle u at varying wavelength λ. 65

3-5 Top: Figure showing the system set-up comprising of the tunable light source and the wavelength meter on the optical bench in the DSCS Lab; bottom: Figure showing the system set-up comprising of the tunable light source. 66

3-6 Top: the plot of wavelength estimation error in the modeling data set; bottom: histogram of the wavelength estimation error in the modeling data set. 67

3-7 Top: the plot of wavelength estimation error using the data set B generated 72 hours later; bottom: histogram of the wavelength estimation error in the data set B. 68

3-8 Top: the plot of wavelength estimation error using the normalised data set B generated 72 hours later; bottom: histogram of the wavelength estimation error in the normalised data set B. 69

3-9 Top: the plot of wavelength estimation error using the normalised data set B recorded 72 hours later; bottom: histogram of the wavelength estimation error in the normalised data set B. Hybrid solution (NN+NLLS)is used to estimate unknown wavelength 70

3-10 Top: the plot of wavelength estimation error using data set D ; bottom: the plot of the wavelength estimation error as plotted against wavelength.Neural Network trained with data set C and validated with data set D 71

3-11 Top: the histogram of wavelength estimation error using data set D. 72

3-12 Top: the plot of wavelength estimation error using data set D ; bottom: the plot of the wavelength estimation error when an initial guess of 625nm is used for the wavelength estimation algorithm. Nonlinear least squares algorithm used to estimate unknown wavelength in data D at an intial guess of 625 nm 73

3-13 Top: the histogram of wavelength estimation error plotted against wavelength. . 74

3-14 Top: the plot of wavelength estimation error using data set D ; bottom: the plot of the wavelength estimation error when NN is used to predict the initial guess needed to deduce the optimal wavelength. Using the Hybrid algorithm to estimate unknown wavelength in Data D 75

3-15 The wavelength estimation error plotted wavelength. 76

4-1 Wavelength estimation error and the corresponding histogram at Filter temperature of 50 degrees (top left: Wavelength estimation error with offset), 2 (top right:Wavelength estimation error histogram with offset), 3 (bottom left:Wavelength estimation error with offset of the photodiode removed) and 4 (bottom right:Wavelength estimation error histogram with offset removed). Case 1 :The performance of the Non-linear least square algorithm is validated when temperature drift is introduced to the system. 81

4-2 Wavelength estimation error and the corresponding histogram at Filter temperature of 50 degrees (top left: Wavelength estimation error with offset), 2 (top right:Wavelength estimation error histogram with offset), 3 (bottom left:Wavelength estimation error with offset of the photodiode removed) and 4 (bottom right:Wavelength estimation error histogram with offset removed). Case 1 :The performance of the Neural Network algorithm is validated when temperature drift is introduced to the system. 82

4-3 Wavelength estimation error and the corresponding histogram at Filter temperature of 70 degrees (top left: Wavelength estimation error with offset), 2 (top right:Wavelength estimation error histogram with offset), 3 (bottom left:Wavelength estimation error with offset of the photodiode removed) and 4 (bottom right:Wavelength estimation error histogram with offset removed). Case 1 :The performance of the Non-linear least square algorithm is validated when temperature drift is introduced to the system. 83

4-4 Wavelength estimation error and the corresponding histogram at Filter temperature of 70 degrees (top left: Wavelength estimation error with offset), 2 (top right:Wavelength estimation error histogram with offset), 3 (bottom left:Wavelength estimation error with offset of the photodiode removed) and 4 (bottom right:Wavelength estimation error histogram with offset removed). Case 1 :The performance of the Neural Network algorithm is validated when temperature drift is introduced to the system. 84

4-5 Wavelength estimation error and the corresponding histogram at Filter temperature of 90 degrees (top left: Wavelength estimation error with offset), 2 (top right:Wavelength estimation error histogram with offset), 3 (bottom left:Wavelength estimation error with offset of the photodiode removed) and 4 (bottom right:Wavelength estimation error histogram with offset removed). Case 1 :The performance of the Non-linear least square algorithm is validated when temperature drift is introduced to the system. 85

4-6 Wavelength estimation error and the corresponding histogram at Filter temperature of 90 degrees (top left: Wavelength estimation error with offset), 2 (top right:Wavelength estimation error histogram with offset), 3 (bottom left:Wavelength estimation error with offset of the photodiode removed) and 4 (bottom right:Wavelength estimation error histogram with offset removed). Case 1 :The performance of the Neural Network algorithm is validated when temperature drift is introduced to the system. 86

4-7 Plot of Estimated wavelength compared with the calibrated wavelength using the NNLS 3 (bottom :Plot of Estimated wavelength compared with calibrated wavelength using NN.) 87

4-8 Plot of Estimated wavelength compared with the calibrated wavelength using the NNLS estimation algorithm (bottom :Plot of Estimated wavelength compared with calibrated wavelength using NN algorithm.) 88

A-1 *The schematic diagram of the Neural Network error correction learning*[18] . . . 96

A-2 *The schematic diagram of the Neural Network error correction learning*[18] . . . 97

List of Tables

3-1 Wavelengths obtained at control input (θ) to the Tunable color filter. 46

3-2 Four data set used for system calibration and wavelength estimation 55

3-3 Summary of Neural Network training process. 58

3-4 Results of the Neural Network estimation Algorithm. 58

3-5 Table 3.4: Results of the Hybrid (NNNLS). 58

3-6 Results of the estimation algorithm on Data set C and D.. 61

4-1 Dataset measured at various temperatures drift. 80

4-2 Results of the estimation algorithm at Temperature 50 degrees with the photodiode offset (dark current) removed. 80

4-3 Results of the estimation algorithm at Temperature 70 degrees with the photodiode offset (dark current) removed. 80

4-4 Results of the estimation algorithm at Temperature 70 degrees with the photodiode offset (dark current) removed. 80

4-5 Results of the estimation algorithm at Temperature 90 degrees.$\|Y_{90} - \hat{F}(\lambda, U)_{RT}\|_2^2$ 86

4-6 Results of the estimation algorithm at Temperature 90 degrees.$\|Y_{90} - \hat{F}(\lambda, U)_{90}\|_2^2$ 86

Acknowledgements

In this short note, I will would like to acknowledge the help and support of the people who made this work possible. The first person I wish to thank is Prof. Michel to whom I am very grateful for being my supervisor and for giving me the possibility of achieving all of this. The trust and support that he gave me in the course of my study here in Delft is absolutely overwhelming and furthermore,I have really appreciated the freedom I enjoyed while working in the Lab and his patience with me when I did not understand what I had to do. Conclusively in this regard, I am greatly indebted to Michel for modelling me to appreciate the tenets of commitment to being a scientist even when I thought I could not be one.

Next, I would like to thank Prof. Yarovoy who did not just provided supervision in the course of my thesis work but also taught me some courses that stimulated my thought process and has further motivated me in certain scientific directions.

I would like to thank Hong Song who gave me some insight into this work when I took over the responsibility of developing this system from Him. Many thanks to my colleagues Jeroen for always being able to listen to me and answer my questions even when my questions were quite unreasonable. A special thanks to Hans V, who was ever willing to support me in getting this thesis to this point. Your questions and suggestions are absolutely wonderful. I appreciate you greatly for always being there to make valid input when I come knocking.

I should not forget to mention Prof. Jo Spronck for your valid contribution from time to time, thanks for making your library accessible to me without any form of hesitation. I sincerely appreciate Jacopo and Hans Yoo for their support through this project work. Your questions, guide and making your optical equipment available for my use is greatly appreciated. To my colleagues from the PME department (Arjen and Rudolf) thanks for your support and making your tools available for use when I needed them. To the DCSC technical team : Kees, Wills and Ron,thanks for your patience and your constant support. Patrick, Harry and Rob, thanks for helping with all my lab fabrications.

This work will not have been possible without the support I enjoyed from my lovely wife (Irene Agbana), Your love, prayers and constant encouragement kept me going even when I felt like quitting. You are indeed a rare gem.

To my mother in-law (Fester Imoh), and my lovely children (Anthony, Kelvin, Jeremy and Yaella), thanks for your patience. Great things are ahead!! My heart goes to all my dear friends and members of the Compassion Global Ministries, thanks for standing with me, praying for me and encouraging me regularly. God bless you all.

Finally, to my lovely parents, Dr Steve and Pastor Yemi Agbana, thanks for your daily prayers and constant support. Kayode, Grace and Timi, you guys remain the best siblings in the entire world.

I love you all.

Delft, University of Technology T.E Agbana
5th July 2013

"There is a spirit in man, the inspiration of the Almighty God giveth him understanding."

— *Job 32 vs.8*

Chapter 1

Introduction

Wavelength measurement and control of lasers is of paramount importance and has found vast application in areas such as linear and nonlinear spectroscopy, multichannel wavelength division multiplexing, laser meteorology and applications which involve testing of laser and LED light sources to ensure spectral purity and power distribution.

This thesis investigates how to simplify the optical wavelength measurement device such that wavelength metering with high spectral resolution is achieved at a very low cost. The spectral resolution in this context refers to the minimum separation required between two spectral features in order to resolve them as two separate lines.(i.e the ability of the wavelength measurement device to display two signals closely spaced in wavelength as two distinct responses) [4,17].

While the state of the art optical wavelength measuring devices such as the AQ6317 Yokogowa Optical spectrum analyzer have high spectral resolution of about 0.015nm at the cost price of 50,000 euro, and the Thorlabs FT Michelson Spectrometer with a resolution of about 0.001nm has a cost price of about 23,000 euros, it is the goal of this thesis to realize an optical wavelength measurement machine which has the capability of providing a spectral resolution better than 0.015nm at a low cost of about 700 euros.

This chapter introduces the fundamental on optical wavelength measurement devices, it summarizes the state- of-the art in wavelength measurement, discussing the limitation of existing approaches and motivates this thesis. This chapter provides specific answers to the following questions:

- The need for wavelength measurement.
- How wavelength meter works?
- What is the state of the art in spectrum analysis?
- What are the shortcomings of existing wavelength measurement device?
- What is the goal of this thesis and how is the goal achieved?
- What are the main contributions of the thesis?

1-1 The Need for Optical Wavelength Measurement Devices

Light is an electromagnetic radiation (an electric and a magnetic field perpendicular one to each other moving in the vacuum at the speed depending on the medium) and behave as a particle or as a wave (but not as both at the same time). Due to its duality, it shares all the properties of a wave and a particle and it carries energy because it moves.

If light is perceived as a wave, then we can represent it by its wavelength (λ) (the distance from two successive crest) and the quantity of crests that succeed in a second is the frequency (f).

$$E = \frac{hc}{\lambda} \tag{1-1}$$

The energy of light is then the product of the frequency and the Planck constant h The frequency is expressed in terms of wavelength since $f = \frac{c}{\lambda}$. Thus light energy can be observed experimentally by using photodetector to measure the intensity (energy per unit area and unit time) and the intensity of light is proportional to the square of the amplitude of the electric field of the light wave. The intensity arrives at an optical receiver (photodetector) as discrete units called photons. Photons are the particle of light and therefore the photonic characteristics of light enables it to act as a particle [1,3,15].

Light has found significant application in diverse fields ranging from metrology, medical imaging, astronomy to data transmission etc. As a matter of fact, the current demands for high data rates transmission in terms of internet connections, and computer speed is gradually becoming insatiable by the available electronics particularly when attempts are made to increase the speed of data transfer via cables and through microwave channels or when attempt is being made to speed-up the rates of computing and data storage [5].

Since the capabilities of current electronics necessary for meeting the demand for high bandwidths and data storage are approaching their ultimate limits a proper control of the spectral and temporal properties of light therefore provides a solution to this overwhelming demands. The control of the spectral and temporal properties of light has provided valuable contribution to the speed of the computers and also enhanced internet connections considering the fact that the fastest internet connections which are commercially available at the moment are the so-called fiber-to-the-home internet links which provides data rates of up to 500Mbit/s. [5]

With such contributions, it is obvious that advanced light sources will play a dominant role in the future speed or density of data requirement. This will however be feasible if light output with high spectral purity, wide wavelength tuning, phase control or temporal control are developed.

Based on this, several methods have currently been developed to realize cheap laser sources which will enable the possibility of combining a wide wavelength tunability, narrow optical bandwidth, the possibility for mass production at low manufacturing costs of about 20 euros and at small sizes suitable for optical integration.

Despite the advantages provided by such low-cost semiconductor tunable lasers, the tendency of experiencing significant wavelength drift as a function of temperature introduces the possibility of instability in the tunable laser and of course the spectral purity of the Laser is

compromised [12]. To stabilise such semiconductor lasers, it is important to have an instrument to determine the output wavelength quickly and with an acceptable level of accuracy at a cost less than 700 Euro since the essence of fabricating a lowcost semiconductor laser which can be purchased at the cost price of about 20 euros will be lost if its optical properties and spectral purity can only be measured accurately using a spectrometer which cost about 20,000 euro (a thousand times the cost of manufacturing the semiconductor laser).

Different methods of wavelength measurements have been developed in time past and these measurement methods involves collecting the light to be measured and sending it into a spectrometer or grating monochromator for the measurement of its spectral components. High accuracy measurement with these previously developed optical wavelength measurement device however required cumbersome long-path instruments and wavelength measurement of light under this condition was a time-consuming task [12].

With the increased need in ensuring the spectral purity of semiconductor diode lasers to meet up the need for its common application in recent past, table-top easy to use wavemeter is of uttermost importance. In this thesis, we describe the core principles of tunable color filter, present a representative spectrometer system design, we examine its performance in terms of its essential properties such as precision, resolution and accuracy. We also compare to currently available products and evaluate the possibilities for maximizing portability and efficiency while cost is minimized.

1-2 Principles of Optical Wavelength Measurements

In this section, three common mechanisms used for the isolation of spectral information from optical signals are reviewed from [6,7,8,9,10,19]

- Interferometry: The interferometric spectrometers modulate light in fourier or modal space contrary to the spatial dispersion based spectrometers which modulates light in the image plane. The fourier transform spectrometers are particularly very useful when there is a need to measure a spectrum using one detector.

- Resonance:Resonant effect can be created by the use of optical cavities or by quantum mechanical material processes. The resonant effect is used to create spectroscopic filters such as the thin film filters, metal nano particles, organic dyes, etc. Using these devices, spectral analysis can be achieved by using electronic detectors with intrinsically spectral sensitivity.

- Spatial dispersion : Employs the use of dispersive elements such as gratings and prisms (which redirects, refracts and diffracts waves as a function of wavelengths) to spread light into a spectrum such that the spectral components can be measured.

Since spectral analysis is of uttermost interest due to its application in various fields, the introduction to optical wavelength measurement techniques provide background information on how spectrometers and wavelength meters works in general.

1-3 Interferometric Spectrometers

Wavemeters have been designed based on several underlying principles since its evolution. To realize wavemeters with absolute accuracy and precision however, the interferometric techniques have proven to be the most practical design principles.

This section provides a review of optical wavelength measurement devices based on the scanning of the Michelson Interferometer.

1-3-1 Michelson interferometer based Spectrometer

The working principle of the Michelson interferometer based spectrometer is illustrated in the schematic diagram in [Figure 1.1] below.

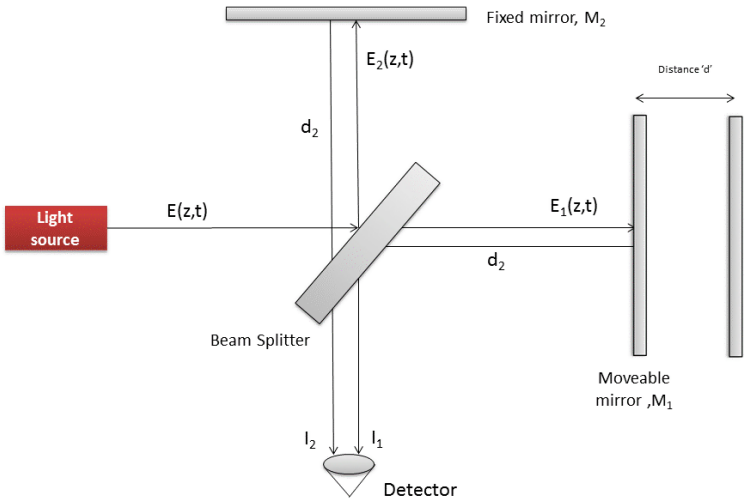

Figure 1-1: *Schematic of the Michelson interferometer. The input light beam is splitted into two. While $E_1(z,t)$ is transmitted to the moving mirror, the other half $E_2(z,t)$ is reflected to the fixed mirror. The variation of the distance d of the moving mirror causes a consequent sinusoidal variation in the output intensity and the combined intensity from the mirrors m_1 and m_2 is therefore measured at the output of the interferometer by the detector [6].*

The Michelson multiplex spectrometer has a collimated light from a source transmitted through a beam splitter (a special material which transmits half of the radiation striking its surface and reflects the other half) [4,6].

The two beams separated by the beam splitter are coherent and are reflected from two flat mirrors m_1 and m_2. As a result of the coherence, the combined amplitudes are added. Due to the variation in the position of the moving mirror, the path difference is changed and consequently the transmitted intensity of a monochromatic light source varies sinusoidally [6]. As a perfectly collimated light beam from a monochromatic source enters into the system, the beam splitter (BS) which is located between the two mutually perpendicular plane mirrors (m_1

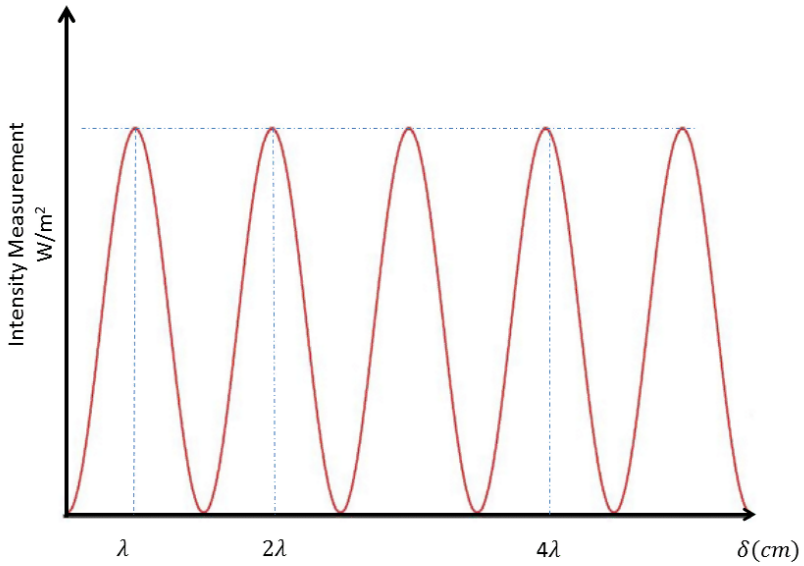

Figure 1-2: *Illustration of the intensity of the light beam at the exit of the Michelson interferometer as a function of optical path difference. As observed in the figure above, Maximum intensity is obtained when the path difference is equal to $n\lambda$ where n is an integer. When $d_1 = d_2$ as shown in fig 1.2, then the two beams are in phase and this consequently yields a constructive interference depicted in this schematic as a peak. Conversely destructive interference represented by the dip in the diagram is experienced when the path difference is half the wavelength.*

and m_2) divides the input beam into two beams such that the input light beam is partially reflected to the fixed mirror and partially transmitted to a moveable mirror as shown the figure [1.1]. The mobility of the moveable mirror through distance $'d'$ causes a variability of the optical path length between the fixed mirror and the moveable mirror. This variation generates an interference pattern (an overall pattern that results when two or more waves interfere with each other showing regions of constructive and of destructive interference [9]) at the detector.

The effect of interference causes variations in the output intensity as the difference in the path length changes. The difference between the two optical path lengths d_1 and d_2 is the optical path difference which is equal to the product of the physical distance travelled by the moving mirror and 'n' the refractive index of the medium filling the interferometer arms.

Let the intensity of the input beam be denoted as I and the reflectance of the beam splitter represented as R, then the intensity of the reflected beam by the beam splitter is RI and the intensity of the transmitted light is $(1-R)I$. Following the propagation of the transmitted beam, the moving mirror m_1 is adjusted such that the reflected beam from the moving mirror returns back to the beam splitter by the same path.Therefore the reflected beam will coincide with the incoming beam (which has an intensity (I_{in})) at exactly the same point on the beam splitter [6].

The intensity which is reflected from the mirror is depicted in fig.1.1 is $I_1 = R(1-R)I$. Following the propagation of the reflected beam from the beam splitter however, the mirror m_2 is adjusted in similar manner and the intensity which crosses the beam splitter is represented as $I_2 = R(1-R)I$. Having properly adjusted the Michelson Interferometer, then it is able to split the incoming beam which has an intensity I_{in} into two beams of equal intensities I_1 and I_2 propagating in the same direction towards the optical detector [6,7,9,10].

The resulting output intensity (which is a function of the optical path difference) is detected as an interference signal with an optical receiver and fed into a data processing unit where the interference signal is converted into optical spectrum waveform by means of fast Fourier transform. The resultant optical spectrum waveform is processed such that the output wavelength and power data of the input signal is obtained.To obtain the output intensity of the interferometer from the resulting field however, the electric fields created by the two beams $E_1(z,t)$ and $E_2(z,t)$ must be summed.

Assuming that the light input as shown in Fig 1.1 is from a monochromatic light source and with the beams propagating in the same direction along the z-axis, the mathematical model of the system functionality can be represented according to [6] as follows:

Let the electric field created by one of the beams on the output of the interferometer be denoted as E_{out} then,

$$E_1(z,t) = E_{out}e^{i(wt-\kappa z-\varphi_1)} \tag{1-2}$$

and

$$E_2(z,t) = E_{out}e^{i(wt-\kappa z-\varphi_2)} \tag{1-3}$$

φ_1 and φ_2 are the phases which depends on the propagation distance of the beam from the beam splitter to the reflectors (fixed mirror and moving mirror) φ_1 and φ_2 can be written as $2\kappa d_1$ and $2\kappa d_2$ respectively where κ is the wave number which is $\frac{2\pi}{\lambda}$ (it determines the wave

propagation direction) and the multiplier 2 implies that each beam travels twice the distance from the beam splitter to the corresponding Mirrors [9,10].

Thus the field E at the output of the interferometer is the summation of both fields E_1 and E_2 and can be written as :

$$E = E_{out}(e^{i(wt-\kappa z-2\kappa d_1)}) + E_{out}(e^{(i(wt-\kappa z-2\kappa d_2)}) \tag{1-4}$$

Therefore,

$$E = E_{out}e^{i(wt-\kappa z)}(e^{-2i\kappa d_1} + e^{-2i\kappa d_2}) \tag{1-5}$$

Since the square of the amplitude of the electric field is proportional to the light intensity, then the output intensity of the interferometer can be deduced from the output electric field using equation 1.5.

$$I_{out} = \langle E.E^* \rangle \tag{1-6}$$

Therefore,

$$I_{out} = E_{out}^2 e^{i(wt-\kappa z)}(e^{-2i\kappa d_1} + e^{-2i\kappa d_2})e^{-i(wt-\kappa z)}(e^{2i\kappa d_1} + e^{2i\kappa d_2}) \tag{1-7}$$

$$I_{out} = 2E_{out}^2(2 + e^{-2i\kappa(d_1-d_2)} + e^{2i\kappa(d_1-d_2)}) \tag{1-8}$$

$$I_{out} = 2E_{out}^2(1 + cos2\kappa(d_1 - d_2)) \tag{1-9}$$

By smooth changing of the distance d_1 or d_2 and counting the interference maxima, which is a cosine function of the distance, the wavenumber can be determined as the number of maxima per unit length and the wavelength is derived as an inverse of wavenumber. Therefore the intensity as derived in (equation 1.9) can be written in terms of wavelength by converting the wavenumber κ to wavelength.

Substituting $\kappa = \frac{2\pi}{\lambda}$ into equation 1.9 yields,

$$I_{out} = 2E_{out}^2(1 + cos4\pi\frac{(d_1 - d_2)}{\lambda}) \tag{1-10}$$

From equation (1.10) It can be observed that the output intensity I_{out} consist of two parts. While the first component is constant and contains no useful information for the deduction of the wavelength, the second part is modulated and thus useful for spectroscopic measurement. The modulated part is referred to as the inteferogram which is the resulting signal that exits the interferometer as a result of interference caused by the optical path difference due to the displacement of the moving mirrors. The interferogram has the unique property that every data point (a function of the moving mirror position) which makes up the signal has information about the wavelength.

To estimate the wavelength of the input beam, we first consider the simplest option where the optical signal has a single wavelength. From the derived equation, (equation 1.10), A change

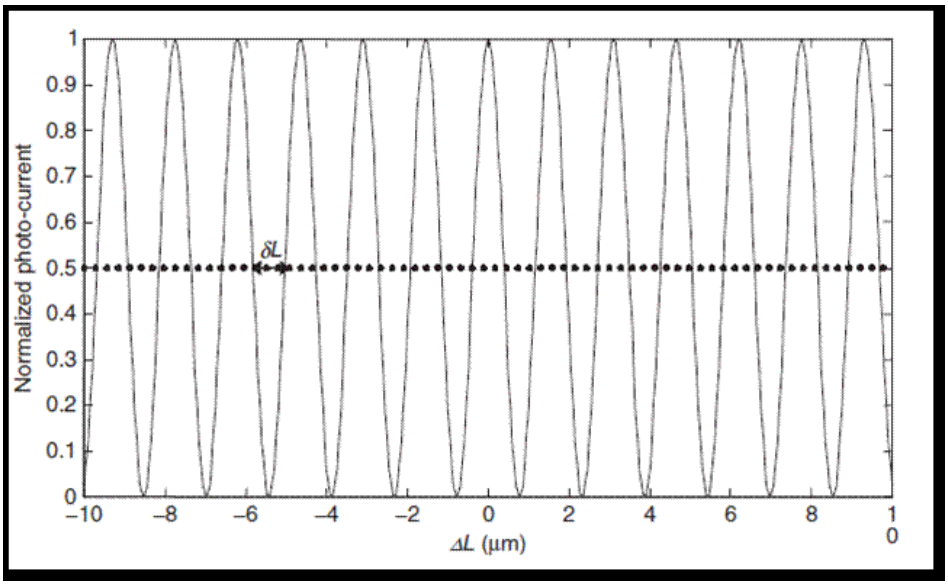

Figure 1-3: *Normalized photocurrent versus differential arm length for wavelength* $\lambda = 1550nm$[19]

in length corresponds to a change in photocurrent $'I'$ measured as intensity of the beam. From Fig. 1.3, [19] The photocurrent passes through maximum and minimums alternatively.

By deriving the photocurrent $'I'$ as a function of the change in optical path length, then the wavelength of the signal can be estimated. For example, every time the photocurrent crosses the half-maximum point, equation 1.10 becomes $(cos4\pi(\frac{d_1-d_2}{\lambda})) = 0$

The interval between adjacent crossings $\delta L = \delta d$ as shown in Fig 1.3 above is then recorded satisfying the equation $4\pi\frac{\delta d}{\lambda} = \pi$ and therefore the wavelength of the signal is estimated. This wavelength measurement techniques is also known as fringe counting and the key to this technique is the accurate knowledge of the differential length variation of the interferometer arm.

Since $4\pi\frac{\delta d}{\lambda} = \pi$ therefore the signal wavelength can be found as $\lambda = 4\delta d$.

To measure an optical signal with multiple wavelengths however, the fast fourier transform is used to determine the wavelengths. The Fast fourier transform is used to convert the measured data from the length (δd) domain into the frequency (f) domain. The wavelength coverage and the spectral resolution of the wavelength meter can then be determined by the step size and the total range of the scanning interferometer arm, respectively.

Estimating the spectral details of the optical signal with multiple wavelengths requires taking into consideration the performance characteristics of the optics. Therefore taking the reflection coefficient (i.e a description of the intensity of a reflected wave relative to an incident wave) of the beam splitter and the reflection coefficient of the mirrors into consideration. Writing equation 1.9 in terms of the reflectance of the beam splitter BS, we obtain:

$$I_{out} = 2I_{in}R(1-R)(1+cos4\pi(\frac{d_1-d_2}{\lambda})) \tag{1-11}$$

The above equation can be written as

$$I_{out} = 2I_{in}R(1-R) + 2I_{in}R(1-R)(cos4\pi(\frac{d_1 - d_2}{\lambda})) \tag{1-12}$$

Disregarding the first part of equation 1.12, we obtain the interferogram represented by equation 1.13 (the modulated part which contains the spectral details of the waveform.)

$$I_{out} = 2I_{in}(1-T_{BS})R_m T_{BS} cos2\kappa\delta \tag{1-13}$$

Where T_{BS} is the transmission coefficient (the description of the intensity, or total power of a transmitted wave relative to an incident wave) of the beam splitter, R_m is the reflection coefficient of the mirrors and δ represents d_1 - d_2. Furthermore, we take into account the responsivity of the detector which is dependent on the wavelength (i.e it changes at different wavelength). The responsivity of the optical detector is defined as the amount of photocurrent (Ip) that results from an optical input of 1 W [1].

Hence for a broadband wavelength dependent source, the interferogram becomes:

$$I_{out} = \int_{-\infty}^{+\infty} U(\kappa) cos2\pi\delta d\kappa \tag{1-14}$$

Where $U(\kappa) = 2(1 - T_{BS}(\kappa)R_m(\kappa)T_{BS}(\kappa)G(\kappa))$ and $G(\kappa)$ represents the response of the optical detector to the incident light beam.

The spectrum of the light source producing the interferogram taking into consideration the instrument function (i.e the properties of the devices ranging from the beam splitter to the mirror along the transmission path towards the optical detector) is denoted as $U(\kappa)$ in equation (1.14).

The intensity, therefore can be obtained from equation 1.14 by performing the Fourier transform of the interferogram I_{out}. Fourier transform maps a function defined on physical space to a function defined on the space of frequencies whose values quantify the amount of each periodic frequency contained in the original function.The original function can be recovered from its transformed frequency components by Inverse Fourier transform [13].

Therefore the sum of the monochromatic interferograms simply turns into an integral as indicated below.

$$U(\kappa) = \int_{-\infty}^{+\infty} I(\delta) e^{-i2\pi\kappa\delta} d\delta \tag{1-15}$$

Since the integral equation obtained in equation 1.15 above ranges to infinity, it is obviously impossible to achieve an infinite path difference, therefore the application of fourier theory is impossible because of the non infinite boundaries. To provide an infinite resolution to the infinite integral however, a boxcar function which is a truncation function with a value equal to 1 between 0 and a chosen finite number V' and thus equal to zero everywhere else.

With the truncation function, equation 1.15 can be written as :

$$T(\kappa) = \int_{-\infty}^{+\infty} I(\delta) f(\delta) cos(2\pi\kappa\delta d\delta) \tag{1-16}$$

Where $T(\kappa)$ is the total fourier transform of the finite path difference interferogram.

In conclusion, the essential idea is that there is a 1-to-1 correspondence between spectra and interferogram. Each particular light spectrum is related to a unique interferogram, and each interferogram corresponds to a unique spectrum and the mathematical relationship between the two is the Fourier transform.

1-3-2 Advantages of the Fourier Transform Spectrometer

- The Multiplex Advantage: Since the interferometer does not separate energy into individual wavelength, the interferogram therefore contains information from each wavelength of light that is being measured. A scan of the entire light spectrum is equivalent to every stroke of the moving mirror and therefore, averaging of the signal can be done by combining all the individual scans.This makes this type of spectrometer suitable for high speed measurement as contrary to the Dispersive Instrument where every wavelength across the spectrum must be measured by the scanning of the grating.The multiplex advantage implies that many scans can be completed and averaged using an FT Spectrometer in a shorter time as compared to the dispersion based spectrometer [4,18].

- Since no slit is required for higher resolution in the hardware design of the FT spectrometer, it thus implies that the amount of light reaching the detector is not limited therefore making the amount of energy reaching the detector in the Michelson Interferometer much higher than what is obtained in the dispersion based spectrometer. In retrospect, higher signal-to-noise ratio is obtained and this account for the better sensitivity in the performance of the fourier transform spectrometers [4,18].

- Precision Advantage : Since an internal reference laser HeNe (helium neon) is used to control the velocity of the moving mirror and to time data collection throughout the mirror scan, the calibration of the wavenumber of the interferometer is much more accurate and has much long term stability as compared with other spectrometer that requires external calibration standards [18].

- Reduced sensitivity to stray light: Since Fourier Transform is used for the spectrum analysis then only interference signals are allowed to contribute to spectrum. Background light have little or no effect on the measurement results [18].

1-3-3 Disadvantages of the Fourier Transform Spectrometer

- One major drawback in the Fourier transform spectrometers is their sensitivity to their environment. Fourier transform spectrometers are particularly sensitive to temperature variation and vibrations as a result of the tight tolerances inside the interferometer. Although various design methods (such as thermostatting the interferometer and dynamic alignment) have been developed to counteract these deficiencies, the inherent sensitivity makes these instruments unsuitable for process applications unless they are located within an environmentally controlled shelter [19].

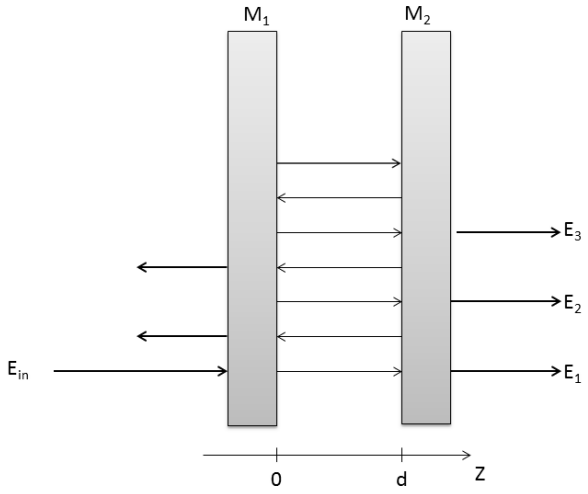

Figure 1-4: *Schematic diagram showing the working principle of the Fabry Perot Interferometer. The input electric field E_{in} enters the cavity and it is reflected multiple times until the amplitude of the field is significantly reduced.*

- Complex and expensive hardware are needed for the processing of the interferogram. Furthermore, the incorporation of the reference laser also increases the cost of the equipment. Typical Fourier transformed spectrometer cost about 30,000 euros.

1-4 Resonance based Spectrometer

The resonant devices in recent past have introduced qualitatively novel features into optical systems. The design, fabrication and tools for analysis of the resonant devices are evolving rapidly and these has made them suitable for optical spectroscopy. This section gives an overview of the resonance based spectrometer, its advantages and disadvantages are also discussed.

1-4-1 Fabry-Perot Interferometer

The Fabry-Perot etalon is the simplest example of a resonant interferometer. It consists of two partially transmissive and partially reflective surfaces which is separated by a dielectric gap of thickness d as shown in Fig [1.4]. The optical cavity can tightly enclose a light field in all directions and this makes it suitable for the design of high-resolution optical spectrometer. The resonance frequencies of the Fabry-Perot resonator or interferometer can be tuned by changing the cavity length (the distance between the mirror) [14].

An incident wave which is partially reflected by the first surface and partially transmitted

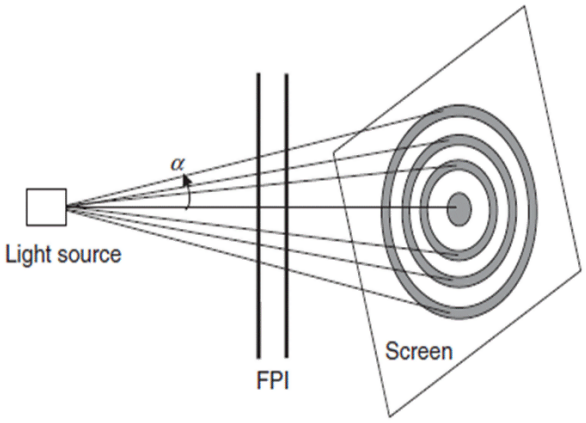

Figure 1-5: *Illustration of a circular fringes pattern when a noncollimated light source is launched onto a screen through a Fabry Perot Interferometer.*[18]

into the cavity experiences an infinite series of partial reflection and transmission event at each surface.

Let the intensity of the incident light be represented as $E_{in} = e^{i(wt-\kappa z)}$ and the reflection of the two mirrors with approximately same reflection be expressed as 'r' for the electric field flow. Taking the two mirrors into consideration, the intensity reflection becomes $R = r^2$ and the corresponding transmittance for the electric field component of the wave is $T = \sqrt{1-r^2}$. The interference pattern at the output of the interferometer is formed as a result of multiple reflections (repetition of the reflection within the cavity until the amplitude of the beam is significantly reduced) of the incoming beam between the mirrors [6,7].

Figure 1.5 above shows a point light source which is illuminated on a Fabry Perot Interferometer. A group of bright rings which appears on the screen behind the Fabry Perot Interferometer depicts the light fringes and the diameters of the rings depend on the thickness of the Fabry Perot Interferometer as well as on the signal wavelength [18].

Denote the electric field created by the incoming plane wave just before the first mirror M_1 as $E_{in} = e^{i(wt-\kappa z)}$, since (z=0) then $E_{in} = e^{iwt}$.

Taking the transmittance of mirror M_1 into account, the emerging electric field of the incident light becomes Te^{iwt} where T is the transmittance of mirror M_1. Since the field propagates over a distance $z = d$ towards the second mirror M_2, the electric field at M_2 becomes $Te^{i(wt-\kappa d)}$, thus $E_1 = T^2e^{i(wt-\kappa d)}$ is transmitted field by M_2, and it is the first beam participating in the interference of the interferometer output.

$Tre^{i(wt-\kappa d)}$ is the light reflected back to the mirror M_1 and a portion of it is reflected back to M_2 The field of the reflected light is $E_2 = Tr^2e^{i(wt-2\kappa d)}$. The field is transmitted by mirror M_2 to form the second participating beam $E_2 = T^2r^2e^{i(wt-3\kappa d)}$ this equals $E_1r^2e^{-i2\kappa d}$

Re-reflection process continues over and over again thus producing beams with fields, $E_3, E_4, ...E_n$. Therefore for beam n, the electric field becomes $E_n = E_1 r^{2(n-1)} e^{-i2\kappa d(n-1)}$ The sum of all the beam is the resulting electric beam after mirror M_2 and according to [6,19] it is therefore obtained as follows:

$$E_{out} = E_1 \sum_{n=0}^{+\infty} (r^2 e^{-i2\kappa d})^n = \frac{E_1}{1 - r^2 e^{-i2\kappa d}} \tag{1-17}$$

Intensity of the transmitted beam is therefore obtained as follows

$$I_{out} = \langle E_{out} E_{out}^* \rangle = \frac{(1 - r^2)^2}{(1 - r^2)^2 + 4r^2 sin^2 \kappa d} \tag{1-18}$$

since $\kappa = \frac{2\pi}{\lambda}$ and $R = r^2$, then the equation above can be converted to intensity reflection.

$$I_{out} = I_{in}(\frac{(1 - R)^2}{(1 - R)^2 + 4R sin^2 \frac{2\pi d}{\lambda}}) \tag{1-19}$$

The transfer function (the ratio of the output intensity to the input intensity) is therefore defined by the equation below, and this is equivalent to the transmission of the Fabry Perot Interferometer.

$$\frac{I_{out}}{I_{in}} = T(\lambda) = (\frac{(1 - R)^2}{(1 - R)^2 + 4R sin^2 \frac{2\pi d}{\lambda}}) \tag{1-20}$$

From the transfer function, the wavelength λ_m which corresponds to the m^{th} transmission peak (which is the highest intensity measurement with respect to the transmission of the mirror)is found as

$$\lambda_m = \frac{2nd}{m} \tag{1-21}$$

where $'d'$ is the space between the mirrors and the $'n'$ is the refractive index of the mirrors. The peak transmission wavelength is moved when the length of the cavity is varied [19].

The block diagram shown [Fig.1.6] depicts an optical spectrum measurement device using a scanning Fabry Perot Interferometer. The Fabry Perot Interferometer mirror is linearly scanned by a sawtooth voltage waveform (A non-sinusoidal waveform which ramps upward and sharply drops) which consequently causes the linear scanning of the peak transmission of the Fabry Perot Interferometer transfer function. To measure the output waveform, a photodiode is used at the output of the Fabry Perot Interferometer to convert the optical signal into electrical waveform and this is then displayed on an oscilloscope.

To convert the measured oscilloscope waveform into an optical spectrum a precise calibration method is required to determine the relationship between time and frequency.

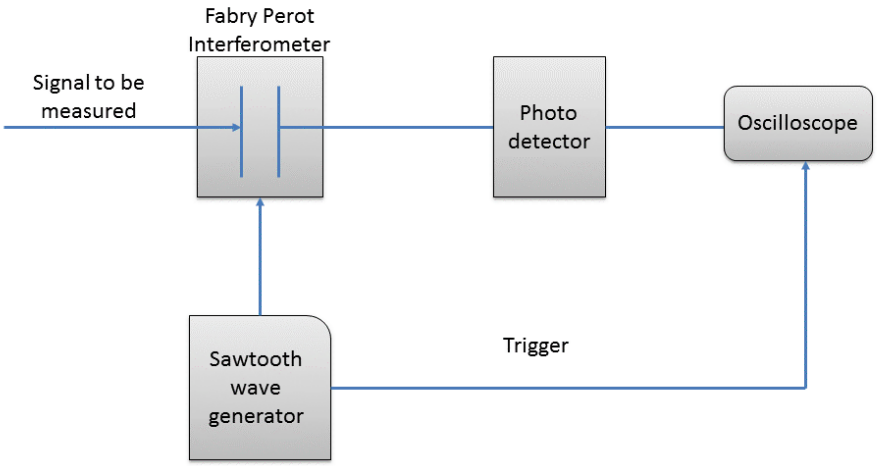

Figure 1-6: *Block diagram of an optical spectrum measurement using a scanning Fabry Perot Interferometer*[18]

1-4-2 Advantage of the Fabry-Perot Interferometer

- The major advantage of the Fabry-Perot interferometer is that it has a very narrow spectral resolution (typically in the range of 0.01nm and 0.001nm). The narrow spectral feature enables Fabry-Perot interferometer to be very useful in the measurement of laser Chirp (an abrupt change of the center wavelength of a laser, caused by laser instability) [1].
- It also provides superior spectral resolution as compared to the diffraction grating spectrometers which has a spectral resolution of about 0.08nm.

1-4-3 Disadvantage of the Fabry-Perot Interferometer

- The Fabry Perot interferometers have narrow wavelength coverage [18].
- Due to their narrow resolution range, these devices may allow many wavelengths to pass through their filter at any one point, presenting an interference issue.

1-5 Spatial dispersion based Spectrometer

Diffraction Gratings are optical components used to separate light into its component wavelengths. Diffraction gratings consist of a series of closely packed grooves that have been

engraved or etched into the grating surface [6]. It is an optical component which can either be transmissive or reflective. As light transmits through or reflects off a Grating, the grooves causes the light to diffract, dispersing the light into its component wavelengths.

An incident beam striking the surface of the diffraction grating device is reflected in a number of directions. The first reflection is referred to as the zero-order beam (m=0). The performance characteristics of the diffraction grating device at this point of zero-order reflection is equivalent to a plane mirror such that no diffraction of the input beam is observed. Therefore, the input beam is not separated into different wavelengths neither is the beam used by the optical spectrum analyzer [2,12,14].

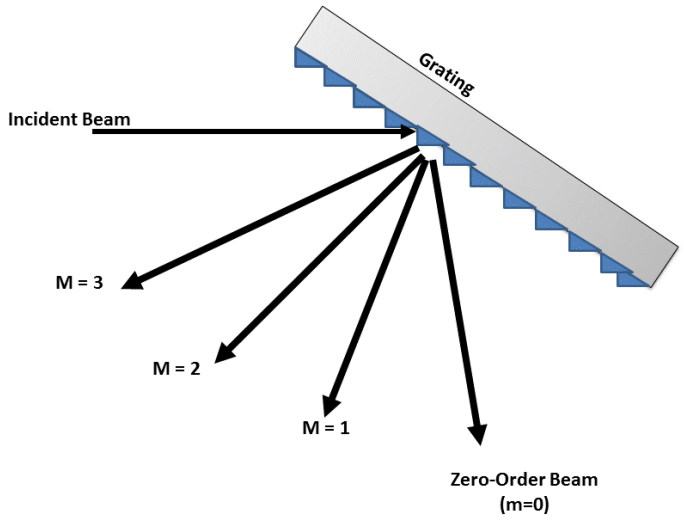

Figure 1-7: *The Incident beam is separated by the input beam into a number of outputs.Within the output beam, except the zero order beam, different wavelengths are separated. [2]*

The first order beam (m=1) is created by the constructive interference of reflections off each groove [2], and constructive interference occurs when the difference in path-length between reflections from adjacent grooves equals to one wavelength.

If an input light containing more than one wavelength component is incident on the diffraction grating device, then the beam will have some angular dispersion, (i.e each wavelength exhibits a different reflection angle so as to satisfy the requirement that the path-length difference off the adjacent grooves is equal to one wavelength). When the path-length difference from adjacent grooves is equal to two wavelengths then the second-order beam (m=2) is defined. Consequently,a three wavelength differences defines the third-order beam and so forth.

Lets assume a normal light incidence and one wavelength shift between the reflection as depicted in figure 1.7, then the angular position of the diffraction maxima is expressed in equation 1.22.

$$sin\theta = \frac{m\lambda}{l} \tag{1-22}$$

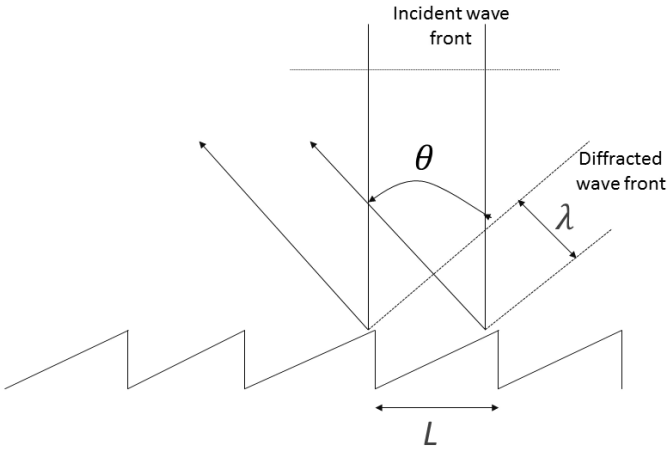

Figure 1-8: *Diffraction grating with period l. The first order diffraction angle appears when delay between reflections from the neighbor grooves is equal to one wavelength* Λ*.[6]*

Therefore a flat incident wavefront is reflected from the grating at a number of angles θ which is determined by the grating period and the wavelength as expressed in equation 1.22 above.

Wavefronts passing through the grating that are parallel to the incident light wave are referred to as zero order (undiffracted) or direct light. Diffracted higher-order wavefronts are inclined at an angle θ according to the equation 1.22 where λ is the wavelength of the wavefront, l is the grating period and m is an integer termed the diffraction order (e.g., $m = 0$ for direct light, Âś1 for first order diffracted light, etc.) of light waves deviated by the grating. The combination of diffraction and interference effects on the light wave passing through the periodic grating produces a diffraction spectrum, which occurs in a symmetrical pattern on both sides of the zero order direct light wave [6,20]. Therefore the diffraction angle can also be expressed in terms of the grooves number such that

$$sin\theta = m\lambda(g) \tag{1-23}$$

The diffraction grating based Optical spectrum analyzer uses the monochromator (an optical device which works as narrow band wavelength filter with mechanically adjustable transmission wavelength)as the tunable optical filter. The monochromator is an optical device which works as narrow band wavelength with mechanically adjustable transmission wavelength. As depicted in the schematic diagram in Figure 1.9, an incoming light crossing the input slit (i.e the opening through which the incoming wavefront is transmitted to the grating) is collected by a spherical mirror with a focal length F located at a distance F, from the slit. The mirror produces a flat wavefront and this directs the wavefront to a diffraction grating device (an optical device which spread light into a spectrum).

The flat wavefront is reflected from the grating at a number of angles determined by the grating period and the wavelength. From equation 1.22 the angular Period of the diffraction

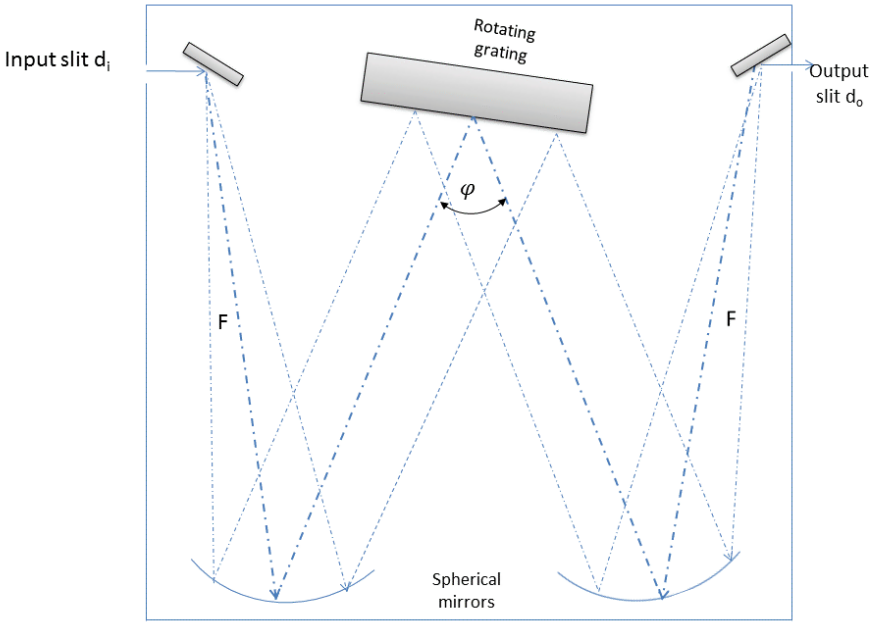

Figure 1-9: *Monochromator optical scheme: d_i and d_o are the sizes of the input and output slits respectively, F is the focal length of the mirrors and φ is the angle between the incident and the diffracted beam and α denotes the incident angle of the light on the grating.*

maxima are $sin\theta = \frac{m\lambda}{l}$ where l is the grating period and m is the diffraction order of the rotating diffraction grating used in the monochromator. The grating produces a diffracted light which is collected by the second mirror and thus focused to the output slit d_0 and the output wavelength at the slit can be changed by simply tuning the grating.

Considering the geometry in Fig. [1.9] and thus taking into account the incident angle of light on the grating and the angle between the incident and diffracted beams (an angle which is fixed as a result of the geometry of the instrument), the angle of reflection $sin(\theta)$ can be expressed as $sin(\alpha) + sin(\varphi + \alpha)$.Therefore, the equation of the light transmission wavelength can be now be expressed as :

$$l(sin\alpha + sin(\varphi + \alpha)) = m\lambda \tag{1-24}$$

Here α is the incident angle of the light on the grating and φ is the angle between the incident and diffracted beams. expressing the above equation in terms of grooves number yields

$$sin\alpha + sin(\varphi + \alpha) = m\lambda g \tag{1-25}$$

From Trigonometric identities, $sin\alpha + sin(\varphi + \alpha) = sin\alpha + sin\alpha cos\varphi + cos\alpha sin\varphi$ Thus equation 1.25 is simplified thus :

$$sin\alpha(1 + cos\varphi) + cos(\alpha sin\varphi) = \alpha(1 + cos\varphi) + sin\varphi = m\lambda g \tag{1-26}$$

where g is the groove number which is the reciprocal of the grating period. Considering a normal incidence of light on the grating, which implies light incidence angle α is approximately equal to zero, (i.e alpha is small α) the simplified equation becomes :

$$sin\alpha(1 + cos\varphi) + cos(\alpha sin\varphi) = \alpha(1 + cos\varphi) + sin\varphi = m\lambda g \tag{1-27}$$

$$\lambda = (\alpha\frac{1 + cos\varphi}{mg} + \frac{sin\varphi}{mg}) \tag{1-28}$$

Equation (1.26) is known as the monochromator dispersion equation and it shows the linear relationship between the incident angle of the light on the grating and the wavelength. This linear dependence explains why the wavelength scale is very common for spectroscopy devices. The spectral resolution of the monochromator is determined by the slit size and the spectral resolution of the monochromator is expressed as follows :

$$\Delta\lambda = d_i\frac{1 + cos\phi}{Fmg} \tag{1-29}$$

while F = focal distance.

The intensity of the diffracted light is measured by a photodetector and the tuning of the diffraction based optical spectrum analyzer is achieved by rotating the diffraction grating.

The spectrum resolution of the monochromator can be improved by doing the following:

- Decreasing the size of the input slit. This however implies that smaller amount of light will enter into the monochromator and as the slits size approaches the wavelength the monochromator efficiency is gradually reduced.
- Making use of mirrors with longer focal distance. Although this increases the resolution of the monochromator, however the physical dimension of the monochromator is also increased thus creating a disadvantage.
- Increasing the number of grooves on the grating also increases the resolution of the monochromator.

1-5-1 Wavelength Tuning

The wavelength tuning of the dispersion based spectrometer is achieved by rotating the diffraction grating element. Each angle of the diffraction grating element causes a corresponding wavelength of light to be focused directly to the centre of the slit. An initial angle and a final angle can be determined and recorded such that a the equipment can sweep across a given span of wavelength. Precisely controlling the diffraction-grating angle provides accurate tuning of the diffraction grating element.

1-5-2 Tuning Techniques

The tuning techniques employed for the rotation of the diffraction grating element in dispersion based optical spectrometer is the gear reductions system. The gear reduction system is used to obtain the required angular resolution of the diffraction grating. The Agilent Technologies Optical spectrum analyzers have employed the use of the direct-drive motor system. This tuning system provides very good wavelength accuracy (1nm) and a very fast tuning speed [2].

1-5-3 Advantage of the Diffraction grating Spectrometer

- The diffraction grating spectrometer has a wide wavelength coverage.
- The diffraction grating also provide good measurement accuracy, precision, resolution and sensitivity.

1-5-4 Disadvantages of the Diffractiong grating Spectrometer

- The diffraction grating spectrometer spectral resolution is limited by the groove-line density of the grating and also by the size of the collimated optical beam on the grating.
- To obtain high resolution diffraction grating optical spectrum analyzers, the focal distance has to be increased and this constitute a disadvantage as such diffraction grating spectrum analyzers are usually bulky and typically have a weight of 19kg.

1-6 Optical Spectrum Analyzer Using the Combination of Grating and Fabry Perot Interferometer

Having discussed the resonance based spectrometers and the dispersion based spectrometers, we came to a conclusion that the dispersion based spectrometer has wide wavelength coverage but limited in its spectral resolution due to the groove-line density of the grating and the size of the collimated beam of the grating. The Fabry Perot Interferometer based spectrometers can however provide high spectral resolution by using long cavity length but since its transfer function is periodic, the spectral coverage is limited to a free spectral range.

To achieve both high spectral resolution and wide wavelength coverage however, a spectrometer which combines a Fabry Perot Interferometer and a grating can be designed.

Figure 1.10 depicts the operating principle of the high resolution spectrometer using the combination of the Fabry Perot interferometer and a grating.

The Fabry Perot Interferometer transforms the incident optical signals into discrete narrow band slices with the wavelength separation equals to the free spectral range (the frequency separation between adjacent transmission peaks of a Fabry Perot interferometer). After the wavelength separation, the transmission grating disperses each wavelength slice into a beam at a certain spatial angle $\delta\phi$. $\Delta\phi$ is theoretically determined by the convolution between spectral bandwidth of the fabry perot interferometer and the angle resolution of the grating.

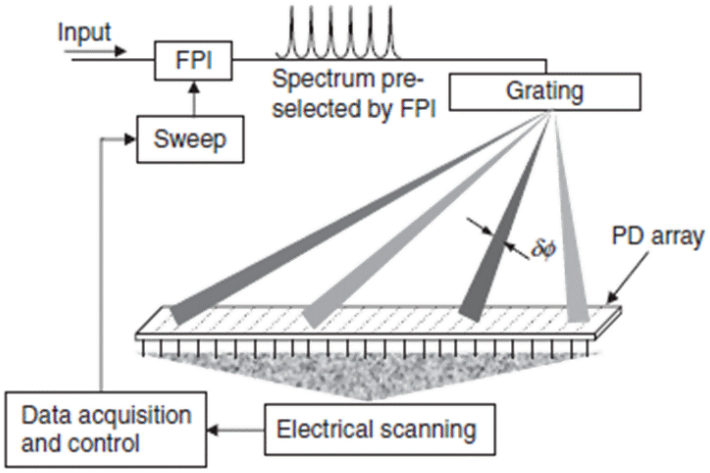

Figure 1-10: *High resolution Spectrometer design based on the combination of the Fabry Perot Interferometer and dispersion grating optical devices.*[18]

Due to the angular width, a beam with width ΔL is produced at the surface of the photodiode array. Assuming the photodiode has a width d there will be $n = \frac{\Delta L}{d}$ photodiodes simultaneously illuminated by this light beam. Summing up the photocurrents generated by all the n associated photodiodes, an electrical signal which linearly is proportional to the optical power within the optical bandwidth selected by each transmission peak of the fabry perot interferometer is obtained.

Assuming there are m light beams where the number of beam $m = 4$ as shown in figure 1-10, each beam corresponds to a specific transmission peak of the Fabry Perot Interferometer transfer function. For each Fabry Perot Interferometer setting, the signal's optical spectral density can be measured simultaneously at separate wavelengths. If each transmission peak of the Fabry Perot Interferometer is linearly swept across a free spectral range, the measurement will be able to cover a continuous wavelength range of m times free spectral range.

In this type of spectrometer, the frequency sweep of the Fabry Perot interferometer is converted into angular sweep of the light beams at the output of the grating and thus the spatial position on the surface of the photodetector is estimated. This optical wavelength measurement device is able to provide a high spectral resolution as well as wide spectral coverage if the signal processing unit of the device is properly configured.

1-7 Specification of Optical Wavelength Measurement devices.

The selection of an appropriate optical wavelength measurement devices is impossible when the important specification of the measurement device is unknown. As such this section give

a brief review of the cogent specification of optical wavelength measurement device.[19]

The most important qualities of an Optical wavelength measurement devices can be specified by the following parameters:

- Wavelength range: The wavelength range of an optical wavelength measurement device is the maximum wavelength range the device can cover while ensuring that its specified performance is not violated. Optical Filters play a major role in the wavelength range of a wavelength meter as such the desire to have an optical wavelength measurement device with a large wavelength range has not been actualized due to the limited application window of optical filters, photodetectors and other optical devices necessary for the design and development of such spectrometers. Typical wavelength range of commercially available grating-based Optical Spectrum analyzer is 400nm to 1700nm.

- The Wavelength Accuracy : It is a specification of the optical wavelength measurement device that specifies how accurately the device measures the wavelength of the light under test. Most commercial wavelength measurement devices separately specify absolute wavelength accuracy and relative wavelength accuracy. Absolute wavelength accuracy specifies how accurate the measured absolute wavelength value is, this is often affected by the wavelength calibration. Relative wavelength accuracy tells how accurate the measured wavelength separation between two optical signals is, it is mainly determined by the nonlinearity of the optical filters. In typical Wavelength measurement device, wavelength accuracy of less than 0.1 nm can be achieved.

- Resolution Bandwidth. Defines how fine an optical wavelength measurement device slices the signal optical spectrum during the measurement. Hence a smaller resolution bandwidth means more detailed characterization of the optical signal. The finest optical resolution bandwidth of a grating based optical wavelength measurement device ranges from 0.1nm to 0.01nm. The minimum resolution bandwidth is usually limited by the narrowest bandwidth of the optical system the measurement device can provide and also limited by the lowest detectable optical power of the receiver.

- Sensitivity : It specifies the minimum measurable signal optical power before the background noise floor influences the measurement signal. Hence the noise characteristics of the photodetector used in the measurement device determines the detection sensitivity. Short wavelength range (typically from 400nm to 1000nm) are detected by the photodiode with less noise interference, for wavelength ranging from 1000nm to 1700nm an InGaAs photodiode is required. Commercially available Wavelength measurement device can provide a detection sensitivity of -120dBm in the 400-1700 wavelength range.

- Maximum power. The maximum allowable signal optical power before the wavelength measurement device detection system is saturated.

- Calibration accuracy. Specifies how accurate the absolute optical power reading is in the measurement. Typically a calibration accuracy of less than 0.5 dB can be achieved in a commercial optical wavelength measurement device.

Some limitations of existing optical wavelength measurement device are summarized below:

- The Rotating Grating Spectrometer: A very common type of the diffraction grating based spectrometer is the AQ6370C Optical spectrum analyzer produced by Yokogawa. A rotating grating and a photon-diode is used as the optical measurement device. The spectrum of the input light is measured by scanning the whole spectrum of the incident light. This device has the capacity to measure a spectrum range of 600nm to 1750nm and it also has a resolution of 0.01nm. Due to the hardware configuration of this system, the AQ6370C cost about 50,000 euros with a weight of about 19kg which makes it unaffordable and not easily transferable. Furthermore, the option of integrating this device with a semiconductor tunable laser is absolutely impractical.

- The Fixed Grating Spectrometer: The Oriel spectrometer is an example of such an optical measurement device which measures the spectrum of an incident light by employing the use of static grating and a CCD array using dispersion of light. This device has measurement range of 550nm to 1600nm, and has an accuracy of about 0.5nm, its resolution is however limited by the discretization of the spectrum in the hardware such that the size of the CCD pixel causes a limitation to the discretization. The Oriel spectrometer is also expensive costing about 20,000 euro to purchase one of such device.

- Interference Based Spectrometer : WS5-IR2 is a type of spectrometer based on the interferometric technique. The wavelength of a monochromatic light is measured by comparing a reference interference pattern with the one formed by the light with unknown wavelength. This device measures wavelength within 1100nm to 2250 nm range and it offers an accuracy of about 0.01nm at the cost of 30,000 euro. Though this device provides the required accuracy needed for lots of spectroscopic application, again the cost of purchase and optical integration remains a major limitation. Although it is possible to save cost in the methods described above, however cost saving will be done at the expense of measurement accuracy.

  Cheaper spectrometers with ease of optical integration have been developed in time past. A common example is the OMH-6727B from ILX Light wave.This spectrometer employs the use of two fixed color filters and two photon-detectors for wavelength and power estimation. The transfer function of the color filters and photon detectors are calibrated a priori and stored in a look-up table.

  An unknown wavelength of an incident monochromatic light is estimated by checking the lookup table and looking at the ratio between the measurements from the two photon-detectors. This optical wavelength measurement device is affordable as compared to the others described above, costing about 4500 euros its measurable wavelength range is 900 nmâĂŞ1650 nm and the best accuracy it can provide is about 1nm.

From the state of the art of the equipment described above, several methods have been employed in the measurement of optical wavelengths and power but obtaining a low-cost measurement device with high accuracy has not been attainable and hence only certain trade-offs were possible.

1-7-1 Resonance based principles for wavelength estimation

From the principles of optical wavelength measurements highlighted above, the Resonance based Optical wavelength measurement methodology has been selected as the underlying

principles for our proposed wavelength meter.Although other conventional small optical wavelength estimation machines are also built on this principle our approach however provides better accuracy and better resolution at low cost as compared to the other conventional wavelength measurement device. This section provides a quick overview on the principles of operation of simple Look up table technique for wavelength estimation.

1-7-2 The Look-up table approach

The conventional small and low-cost optical wavelength measurement device which employs the resonance based optical wavelength measurement principles employs the look-up table approach for unknown wavelength estimation. In these types of wavelength measurement devices,a tunable color filter and two photodiodes are deployed to provide the measurements necessary for the determination of the wavelength of an incoming light with an unknown wavelength.

An incoming light with an unknown wavelength passes through the precisely characterised colored filter glass assembly. The photodiodes attached to the assembly generate independent photocurrents.[22] The ratio of the two generated currents depends on wavelength and this ratio is translated to a wavelength using a calibration lookup table stored with each colored filter glass assembly. The measured number is then transmitted to the display electronics [22]. Hence the look up table uses two spectra curves (output of two photodiodes) to construct a table. Although this approach employs a simple and low-cost technique for wavelength estimation, yet its accuracy is limited to 1 nm and the resolution provided by this system is about 0.5 nm due to the method of wavelength estimation which employs the use of limited data for calibration.

1-7-3 Our proposed Wavelength estimation approach

Using the resonance based optical wavelength measurement methodology as our underlying principles, we proffer a system which estimates the unknown wavelength of an incoming light with better accuracy (better than 1 nm) and better resolution (better than 0.01 nm). In our approach, a nonlinear model will be built and this nonlinear model will have approximately 30 inputs (30 photodiode measurements) and one output (wavelengths). Since our approach provides more spectra curves and more data for calibration with an appropriate estimation algorithm to estimate unknown wavelength, it will therefore provide a wavelength estimation methods with accuracy and resolution better than the look-up table technique of wavelength measurement.

1-8 Motivation and Goal for this thesis

This thesis focuses on a simple approach to optical wavelength measurement with a single tunable color filter and a single photo detector. From our literature survey, several design methods employed for spectral analysis have been reviewed. Although some of these existing systems provide good accuracy in measurement, the system hardware configuration causes

some limitations which make them unsuitable for routine laboratory applications which require accuracy of a few tenths of a nanometer. From the analysis of the prior art above, the goal of the thesis is summarized as follows:

1-8-1 Goal of this thesis

- To develop a simple, compact and low-cost optical wavelength measurement device (spectrometer) which provides a high spectral resolution (better than 0.01nm) and an accuracy (better than 1nm) in an integrated optical design using a single color filter and photodiode.

1-8-2 Main contributions

- In our model based wavelength meter with single tunable color filter and single photodiode, a novel and simple approach to optical wavelength measurement has been proposed. This makes a high performance simple, low-cost optical wavelength measurement device available for optical integration.
- A novel method is proposed for the determination of the unknown wavelengths as the photo detector signals are analyzed using neural network and nonlinear optimization algorithm.
- An optical wavelength measurement device proof of concept experimental setups have been developed and this experimental validation proves that the proposed wavelength measurement technique is not only efficient in improving the simplicity of the device but also, interface with the computer to produce an immediate readout of the wavelength to a level of accuracy that rivaled the best monochromator systems.

Chapter 2

Model-based Wavelength Meter Theory

This chapter aims at improving the simplification of high precision optical wavelength measurement system by the use of a single tunable color filter and a single photo detector. The improvement is achieved by tuning the spectral transmission of the Tunable color filter and identifying the combined spectral sensitivity of both the tunable color filter and the photodiode at different incident wavelength and control signals from the measurement data. Based on the identified model, spectral sensitivity curves obtained from the photodiode measurement are approximated using an appropriate curve fitting method. Experimental result shows that the system is capable of providing an accuracy which is comparable to the accuracy provided by high cost optical spectrum analyzer.

2-1 Introduction

Application of modern spectroscopy technologies include astronomy, medicine, research, remote sensing etc. Despite the diverse application fields, there is still a common dependency on the technological advances in the field of spectroscopy specifically in the area of cost and portability as established in the previous chapter. Although significant efforts have been focused on miniaturizing the traditional laboratory spectrometer and decreasing its cost in recent years, these efforts have however resulted to a subsequent decrease in the functionality of the equipment specifically in terms of accuracy and resolution capabilities.

Based on the review of the methodologies on which the state of the art spectrometers are based, the Resonance spectroscopy has been selected for the design of our optical wavelength meter. Our choice of employing the resonance spectroscopy methodology in realizing our system design is based on the availability and the simplicity of the optical device. Furthermore, its ability to provide good resolution which is better than the resolution provided by the grating based spectroscopy makes it a device of choice for our proposed system.

In this chapter we continue in the line of improving the accuracy and sensitivity of a conventional simple wavelength meter by means of developing a nonlinear model using the performance characteristics of the Fabry Perot tunable color filter and a single photodiode . Fabry Perot etalon filters consist of two highly reflective mirrors separated by a distance. The separation distance of the cavity and the refractive index of the mirrors determines the finesse of the filter. The Fabry Perot tunable color filter is considered in this thesis because of the tunability function of the filter when voltage is applied. Also its free spectral and tunable range, high resolution and low driving voltage also enhance its consideration for our system design (this will be discussed in later sections).

The main contribution of this chapter is to develop a high precision simple wavemeter using the tunable color filter and photodiode. This chapter is organized as follows: In section 2.2, a general overview of the system component is discussed,the problem and the strategy is formulated in section 2.3 while Section 2.4 focuses on the theory of the design of a tunable light source to validate our model.

2-2 Overview of system components

It is part of the goal of this thesis to achieve the design of our system with a single color filter (bandpass filter) and a single photodiode. In this regard, this section provides a description of the components used for the design of our wavelength meter.

2-2-1 Bandpass Filter (Tunable Color Filter)

Bandpass filters provide one of the simplest ways to transmit a well-defined wavelength band of light, while rejecting other unwanted radiation. Their design is essentially that of a thin film Fabry-Perot Interferometer formed by vacuum deposition techniques and consists of two reflecting stacks, separated by an even-order spacer layer. These reflecting stacks are constructed from alternating layers of high and low refractive index materials, which can have a reflectance in excess of 99.99. By varying the thickness of the spacer layer or the number of reflecting layers, the central wavelength and bandwidth of the filter can be altered [27].

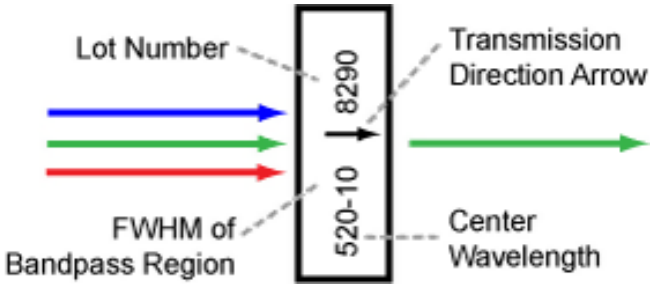

Figure 2-1: Overview of a Bandpass filter (purchased from Thorlabs and used in our system set-up) showing the transmission of the well defined wavelength band of light [27].

A bandpass filter is created by depositing layers of material on the surface of the substrate. Typically, there are several dielectric stacks separated by spacer layers. The dielectric stack

is composed of a large number of alternating layers of low-index and high-index dielectric material. The thickness of each layer in the dielectric stack is $\frac{\lambda}{4}$, where λ is the central wavelength of the bandpass filter (i.e. the wavelength with the highest transmittance through the filter). The spacer layers are placed in between the dielectric stacks and have a thickness of $\frac{n\lambda}{2}$, where n is an integer. A Fabry-Perot cavity is formed by each spacer layer sandwiched between dielectric stacks. The filter is mounted in an engraved metal ring for protection and ease of handling [27].

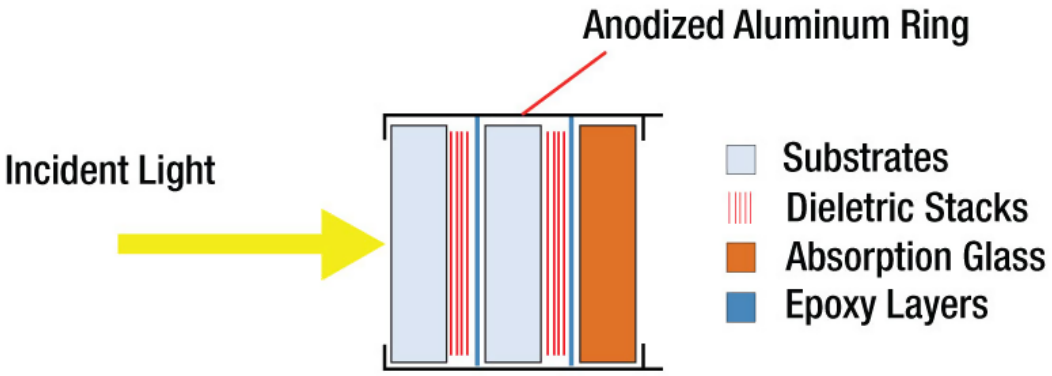

Figure 2-2: Filter operation overview showing the filter structure. Picture gotten from Thorlabs [27],a manufacturer of the tunable color filter used in our system model.

Filter Operation

The constructive interference conditions of a Fabry-Perot cavity allow light at the central wavelength, and a small band of wavelengths to either side, to be transmitted efficiently, while destructive interference prevents the light outside the passband from being transmitted. Although these materials effectively block out of band transmission of incident radiation they also decrease the transmission through the filter in the passband [27]. The filter is intended to be used with collimated light normally incident on the surface of the filter. For uncollimated light or light striking the surface and an angle not normally incident to the surface, the central wavelength (wavelength corresponding to peak transmission) will shift toward lower wavelengths and the shape of the transmission region (passband) will change [27],[33]. Varying the angle of incidence by a small amount can be used to effectively tune the passband over a narrow range. Large changes in the incident angle will cause larger shifts in the central wavelength but will also significantly distort the shape of the passband and, more importantly, cause a significant decrease in the transmittance of the passband.

An engraved arrow on the edge of the filter is used to indicate the recommended direction for the transmission of light through the filter. Although the filter will function with either side facing the source, it is better to place the coated side toward the source. This will minimize any thermal effects or possible thermal damage that blocking intense out-of-band radiation might cause due to the absorption of the out-of-band radiation by the substrate or colored glass filter layers.

Filter Temperature

The central wavelength of the bandpass filter can be tuned slightly (1 nm over the operating range of the filter) by changing the temperature of the filter. This is primarily due to the slight thermal expansion or contraction of the layers.

2-2-2 Light sensor

A Light Sensor generates an output signal indicating the intensity of light by measuring the radiant energy that exists in a very narrow range of frequencies basically called "light", and which ranges in frequency from "Infrared" to "Visible" up to "Ultraviolet" light spectrum. The light sensor is a passive devices that convert this "light energy" whether visible or in the infrared parts of the spectrum into an electrical signal output. Light sensors are more commonly known as "Photoelectric Devices" or "Photo Sensors" because they convert light energy (photons) into electricity (electrons).

Of particular interest to our design is the photodiode.The photodiode is made from silicon semiconductor PN-junctions (An interface between two regions in a semiconductor crystal which have been treated so that one is a positive-type semiconductor and the other is an negative-type semiconductor) which are sensitive to light and which can detect both visible light and infrared light levels. It uses light to control the flow of electrons and holes across the PN-junction. Photodiode is classified as a photojunction device and it is specifically designed for detector application. It is also used as a light sensor with its spectral response tuned to the wavelength of incident light.

The Photodiode

The Photodiode is a light sensor that has an outer casing which is transparent or has a clear lens to focus the incoming light onto the PN junction for increased sensitivity. When light falls upon the junction more hole/electron pairs are formed and the leakage current increases. This leakage current increases as the illumination of the junction increases. Thus,the junction will respond to light and the photodiode current is directly proportional to light intensity falling onto the PN-junction [28].

The fast response of a photodiode to changes in the light levels is its main advantage when it is used as a light sensor , but one disadvantage is the relatively small current flow even when it is fully illuminated.

Noise in the Photodiode

The following subsection describes the source of noise in a photodiode.

1. Johnson noise : Johnson noise is generated by thermal fluctuations in conducting materials. It is also referred to as thermal noise sometimes. It results from the random motion of electrons in a conductor. Cooling of the system can reduce the magnitude of Johnson noise [24]. The Johnson noise (thermal noise) is given by:

$$I_j = (\frac{4KTB}{R})^{\frac{1}{2}} \tag{2-1}$$

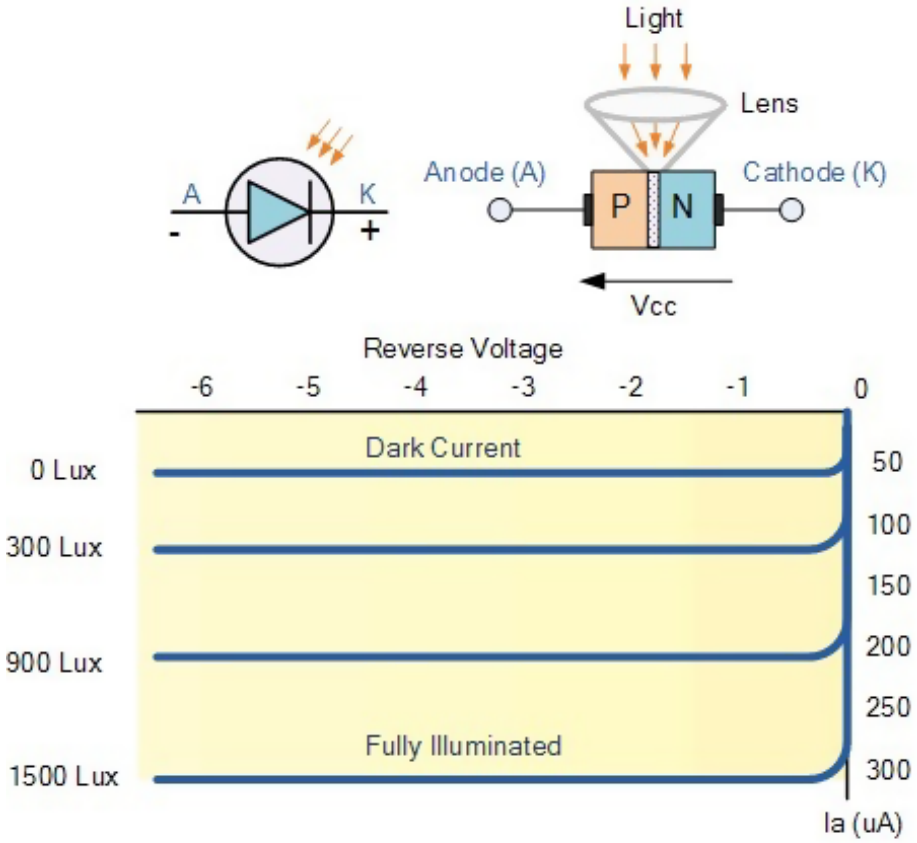

Figure 2-3: Diagram showing a typical photodiode and its current-voltage charateristics depicting the increasing in photocurrent of the photodiode when the illumination of the PN junction increases.[28].

where : I_j = Johnson noise current K = Boltzmann constant [1.38*10 JK], T = absolute temperature [K], R = resistance giving rise to noise, Ohms, B = bandwidth of system,Hz.

2. Dark current: Dark current is the current through the photodiode in the absence of light, when it is operated in photoconductive mode. The dark current includes photocurrent generated by background radiation and the saturation current of the semiconductor junction. Dark current must be accounted for by calibration [23]. Dark current contributes to the total system noise and gives random fluctuations about the average photocurrent [25].

3. Shot noise: Is a measure of the intensity variation in the signal itself and it occurs when the finite number of particles that carry energy (such as electrons in an electronic circuit or photons in an optical device) is small enough to give rise to detectable statistical fluctuations in a measurement. Shot noise tends to be more visible at low intensity because relative fluctuations in number of photons is more significant when the brightness of light is reduced [24,25,26].

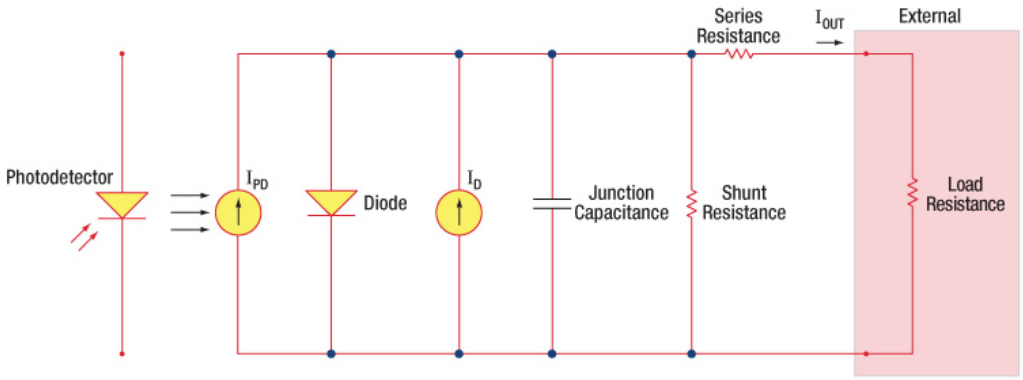

Figure 2-4: A junction photodiode model with basic discrete components depicting the main characteristics of the operation of photodiodes. Picture gotten from Thorlabs [],a manufacturer of the photodiode used in our system model.

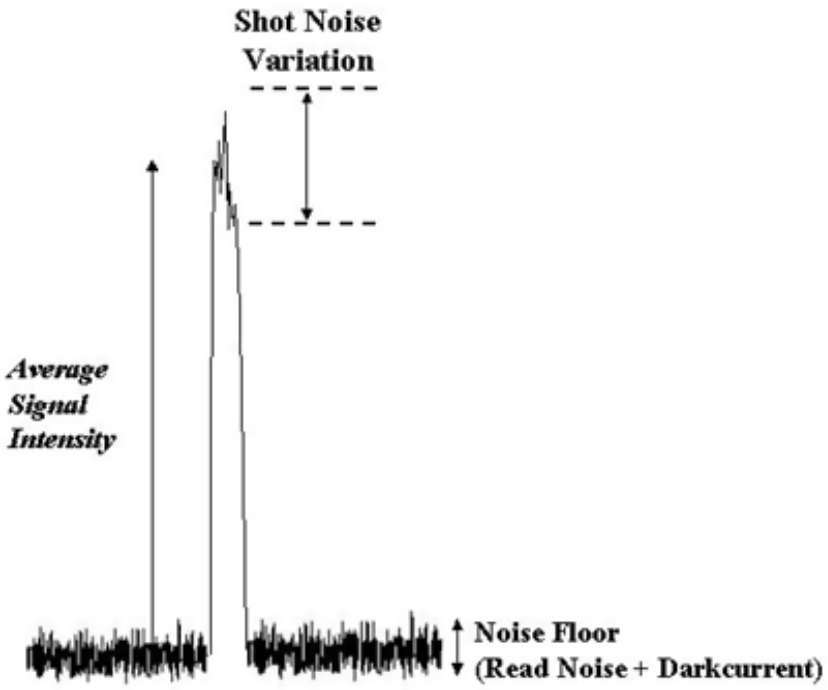

Figure 2-5: A pictoral representation of noise sources in a photodetector [25]

2-3 Strategy

To realise our goal of developing a low-cost model based wavelength meter with a Tunable Color Filter and a single photodiode, we proceed in four steps as indicated below :

1. Step 1 : Formulation of the Problem.
2. Step 2 : Calibration of the device (System Identification).
3. Step 3 : Initialization and Generation of Data.
4. Step 4 : Wavelength estimation using the Neural Network Approach and the Non Linear Least Square Approach.

2-3-1 Step 1 : Formulation of the Problem

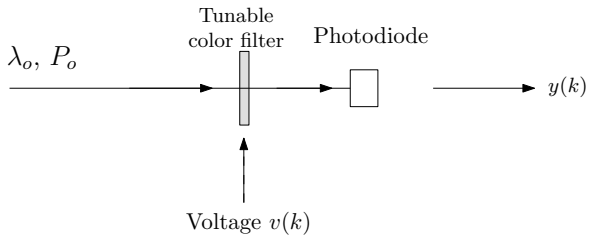

Figure 2-6: Schematic of the proposed wavelength measurement method.Control signal $v(k)$ is applied to the TCF and intensity $y(k)$ is measured from the photodiode.

The schematic of our wavelength estimation method is depicted in figure 2.6. Incident light with an unknown wavelength λ_0 and power P_0 passes through the tunable color filter and illuminates a photodiode. The intensity of the transmitted light is measured by the photodiode at discrete time instant k and the intensity is denoted by y_k. To tune the spectral transmission of the tunable color filter, a control signal (represented by v_k) is applied to the TCF. The spectral transmission of the Tunable color filter is denoted as $T(\lambda_0, v)$ because it is a function of wavelength and the control signal.

The input intensity spectrum denoted by $f(\lambda_0)$ which is incident on the tunable color filter with spectral transmission $T(\lambda_0, v_k)$ produces a photo current $I_p(\lambda_0)$ at a photodetector with responsivity $R(\lambda_0)$ and the generated photocurrent at the photodiode in our system is reffered to as the intensity of the incoming light. The intensity of the measurement is therefore represented in equation 2.2 below.

$$y(\lambda_0) = R(\lambda_0)T(\lambda_0, v_k) + \eta_k \tag{2-2}$$

The product of the photodiode spectral sensitivity and the spectral transmission of the tunable color filter at control input signal is referred to as the combined spectral sensitivity and it is denoted as

$$R(\lambda)T(\lambda, v_k) = f(\lambda_0, v_k) \tag{2-3}$$

.

Hence equation 2.2 becomes

$$y(\lambda_0) = f(\lambda_0, v_k) + \eta_k \tag{2-4}$$

where η_k is the measurement noise. The Photodetector spectral sensitivity can be defined as the ratio of the output signal to the input signal and it is represented as :

$$R = (\frac{Output_signal}{input_signal}) \tag{2-5}$$

where

$$R = \frac{\eta q \lambda}{hc} \tag{2-6}$$

where η in this context is the quantum efficiency of the photodetector, q is the charge of an electron, h is the planck constant and c is the vacuum speed of light. The responsivity is a function of wavelength λ through spectral variation in the quantum efficiency.

2-3-2 Step 2 : Calibration of the Spectral Function $(f(\lambda_0, v_k))$

The combined spectral sensitivity function $f(\lambda_0, v_k)$ plays a dominant role in the estimation of the unknown wavelength of an incoming light, hence the first step is to obtain all relevant information on the transmission function. There are several strategies for calibrating the spectral sensitivity curves $f(\lambda_0, v_k)$ amidst are:

1. Using Measurements to obtain the model structure and parameters at once (black-box modelling) by minimising the prediction error.
2. Developing a set of physical equations based on some available physical insight whilst some parameters such as the wavelength needs to be determined from the observed data.

Deriving the combined spectral function $f(\lambda_0, v_k)$ by physical equation as recommended in the second point above is possible but the accuracy of the result is limited. To obtain high accuracy however the combined spectral sensitivity function is calibrated with tunable light source of known wavelength highlighted as the first strategy above (black-box modelling).

The combined spectral sensitivity curves $f(\lambda_0, v_k)$ is approximated by fitting an analytical function for the recorded data. Neural network fitting method is selected for use for our data analysis amidst others such as as spline fitting, polynomial fit, etc because it is able to fit a broad range of nonlinear curves with a minimum number of fit parameters.(Refer to Appendix A for a more information on the basic idea of the Neural Network Algorithm.)

For fitting, a choice of a 2 layer Neural Network with q neurons in the first layer and one neuron in the second layer is made. Output $\hat{y}_k(\lambda_0)$ of the neural network is determined as

$$\hat{y}_k(\lambda_0) = \hat{f}(\lambda_0, v_k) = w_1 tanh(w_2 \lambda + s_1) + s_2 \tag{2-7}$$

where $\hat{f}(\lambda_0, v_k)$ is the estimate of the $f(\lambda_0, v_k)$, $w_2 \in \mathbb{R}^{Q*1}$ and $w_1 \in \mathbb{R}^{(1*Q)}$ contain the input and the output weight of the neural network respectively.

The input and output neurons have biases represented as $s_1 \in \mathbb{R}^{(Q*1)}$ and $s_2 \in \mathbb{R}$ while tanh is the hyperbolic tangent function. The parameters $w_1, w_2,, s_1$ and s_2 are optimised by training the neural network with sufficient data points λ, y and v.

Obtaining a good compromise between a maximum quality of the fit and a minimum number of fit parameter requires varying the number of neurons that describe a single transmission curve. The numerical implementation of the neural network algorithm produces a fit curves $\hat{f}(\lambda_0, v_k)$ which are approximation of the true transmission function $f(\lambda_0, v_k)$

2-3-3 Step 3: System set-up and Generation of Data

Step 3 of our strategy for wavelength estimation involves system set-up and data generation. The following data (necessary for wavelength estimation) were generated from our system set-up.

1. Control signal v_k (degrees) : Control input signal generated from the stepper motor which causes angular displacement of the tunable color filter so that the spectral transmission function of the filter can be altered.
2. Intensity data y_k (volts): Intensity of the incoming light is the only property of light that we can measure and use for the estimation of the unknown wavelength. At control signal v_k , the intensity of the incoming light which represents the combined spectral sensitivity function of the tunable color filter and the photodiode is measured.
3. For the purpose of calibration, The unknown Wavelength λ_0 (nm)of the incoming light source is measured using the purchased Avantes Spectrometer.
4. At certain instances, the need to measure the Power (watts) of the incoming light source is necessary. The power of the incoming light source is estimated from the voltage and current values obtained from the power source.

The data generated serves two purposes:

1. Approximation of the combined spectral sensitivity function.
2. Development of an algorithm that estimates an unknown wavelength of incoming light source with great accuracy.

Wavelength Calibration Device - Avantes Spectrometer

To generate the data needed for the estimation of the unknown wavelength, the need for the use of a functional spectrometer was necessary therefore, a low-cost spectrometer was purchased from Avantes (A manufacturers of fiber optic spectroscopy instruments). The purchased spectrometer is known as AvaSpec-3648 Fiber Optic Spectrometer and it is designed based on the AvaBench-75 symmetrical Czerny-Turner design with 3648 pixel CCD Detector Array. The spectrometer has a fiber optic entrance connector, collimating and focusing mirror and diffractional grating.

The AvaSpec-3648 has a USB2 interface with the computer and therefore the wavelength of an incoming light coupled through the fiber ($400\mu m$) to the spectrometer can be measured with the Avasoft (a software purchased from the company and installed on the computer for the measurement of the wavelength). The specification of the used Calibration Device is given below :

- The spectrometer covers the visible optical region (360 -860 nm).
- The irradiance calibrated spectrometer has a 0.5nm resolution.
- The accuracy of the spectrometer is 1nm.

It is important to note that the specification of the spectrometer (in terms of accuracy and resolution) is a limitation to the performance (desired resolution and accuracy) of our model since the data measured by this equipment is used for calibration is limited in accuracy and resolution.

The picture below depicts the measurement set-up for determining the wavelength of a light with an Avantes Spectrometer.

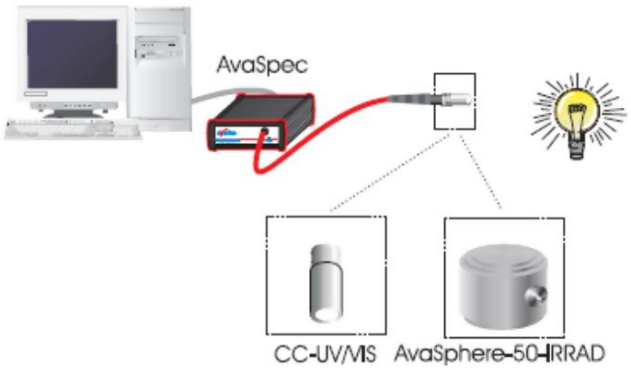

Figure 2-7: Figure showing a typical set up for irradiance measurement. The incoming light source is coupled to the AvaSpec through a fibre optics cable,the CC-UV/VIS and the Avasphere-50-IRRAD enables the coupling of the incoming light into the spectrometer. The spectrometer is connected to the computer via a USB cable and the read out of the wavelength is obtained on the computer through the Avasoft software installed for wavelength and intensity measurement.

2-3-4 Step 4 : Wavelength estimation

The fourth step involves estimating the unknown wavelength of an incoming light from a set of photodiode measurement y_k and control signal v_k generated as indicated in step 3 above. The estimation of the unknown wavelength is done using the following algorithm :

- The Nonlinear Least Square Optimisation Algorithm.
- The Neural Network Algorithm.

Wavelength estimation with NonLinear Least Square Optimisation Algorithm

From the generation of data as described in the previous step, each photodiode intensity measurement produces a non-linear equation which is represented as described in equation 2.53. Using the true transmission function $y(\lambda_0) = f(\lambda_0, v_k) + n_k$ from equation 2.4 and the true (but unknown) wavelength λ_0, the result of the set of measurements is summarised as a vector.

$$Y = \begin{bmatrix} y_1 \\ y_2 \\ \vdots \\ \vdots \\ \vdots \\ y_n \end{bmatrix} = \begin{bmatrix} f(\lambda_0, v_1) + \eta_1 \\ f(\lambda_0, v_2) + \eta_2 \\ \\ \vdots \\ f(\lambda_0, v_n) + \eta_n \\ \\ \end{bmatrix} \tag{2-8}$$

In similar manner, considering the transmission function obtained from the calibration $\hat{f}(\lambda, u_k)$ with approximate (guessed) wavelength $\hat{\lambda}$ as described in step 2, a vector with N predicted measurements values is obtained as follows:

$$\hat{Y} = \begin{bmatrix} \hat{y_1} \\ \hat{y_2} \\ \vdots \\ \vdots \\ \vdots \\ \hat{y_n} \end{bmatrix} = \begin{bmatrix} \hat{f}(\hat{\lambda_0}, v_1) + \hat{\eta_1} \\ \hat{f}(\hat{\lambda_0}, v_2) + \hat{\eta_2} \\ \\ \vdots \\ \hat{f}(\hat{\lambda_0}, v_n) + \hat{\eta_n} \\ \\ \end{bmatrix} \tag{2-9}$$

The unknown wavelength λ_0 can be estimated Solving the following equation set for λ_0:

$$\hat{\lambda}_0 = \arg\min_{\hat{\lambda}} \left\| Y - \hat{Y} \right\|_2^2. \tag{2-10}$$

The difference between the measurement vector Y and the approximation $\hat{Y}$ is defined as the cost function. The Nonlinear least square optimisation algorithm estimates the unknown wavelength by minimising the cost function starting from an initial guess λ and selecting the optimal wavelength that minimises the cost function the most as the final wavelength which corresponds to the estimated wavelength.

Wavelength estimation with Neural Network Algorithm

The Neural network employs the use of a learning process in which a set of activation functions are used to approximate the unknown multiple-variable function between the input variables intensity Y and control signal U and the expected output (λ) by means of nonlinear mapping.

In the Neural Network approach, a set of intensity measurement is presented as an input into the network and the calibrated wavelength is presented as the target (desired response) of the Network.

$$\lambda = \Upsilon_{NN}(Y, U) \tag{2-11}$$

The Neural Network fitting approach requires training of the neurons by selecting a set of weights to optimise the accuracy of the mapping. The training algorithm minimizes an error function which is the sum of squares errors between the network output vector $\lambda(y, u)$ at given input vector (y, v) and its corresponding target vector λ and this is represented in the equation below.

$$Error_{net} = \sum_{k=1}^{K} \sum_{o=1}^{o} [\lambda_n(y^k) - \lambda_n^k]^2 \tag{2-12}$$

The mean squared error is dependent on the weights and the biases of the network.

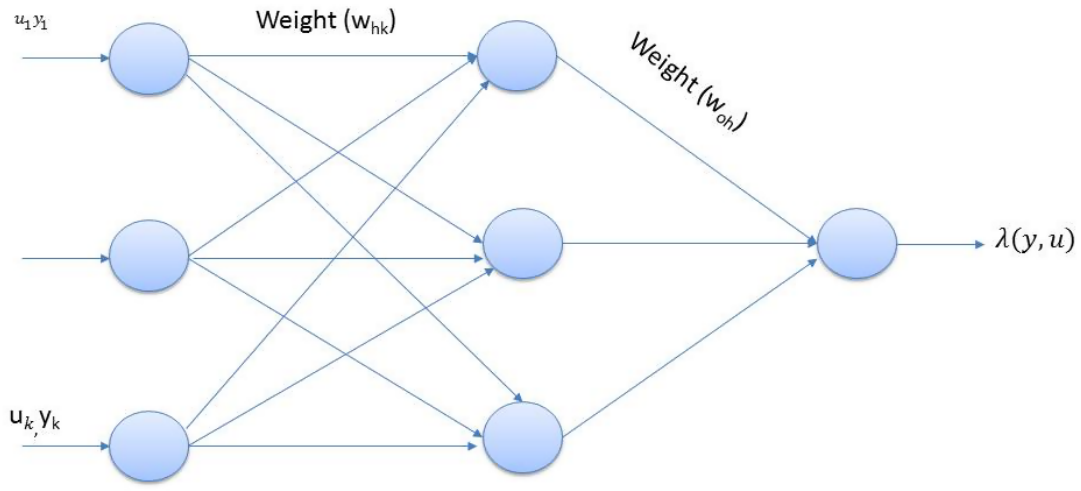

Top: The architecture of a three layer MLP with one hidden node to solve our problem

The above figure depicts a network of processing elements, neurons or nodes represented by a circle. Each circle are connected by lines known as weights. The intensity measurement y is applied to the k unit. The output layer is represented as $O = 1$ while H represents the hidden layer. The input variables y_k, for $k = 1, ...K$ multiplied by the weight w_{hk} thus generating

a vector of inputs to the units in the middle layer. The vector is transformed by a nonlinear activation function denoted as ϑ and the output of the hidden layer is written as:

$$\zeta_h = f(\sum_{k=1}^{K} w_{hk} y_k + b_h) \tag{2-13}$$

b_h is a bias or offset and the function $f()$ is the activation function (a sigmoid function) denoted as

$$\varphi(y) = \frac{1}{1 + \exp^{-y}} \tag{2-14}$$

is chosen for neurons in the hidden layer and a linear function is selected for the neurons in the output layer. The hidden layer produced an output which is multiplied by weight w_{oh}, $(o = 1)$ and bias b_o is added to the resulting vector and the network output is generated as represented in the equation below.

$$\lambda_o = \sum_{h=1}^{L} w_{oh} \zeta_k + b_o \tag{2-15}$$

The above equation is combined such that the neural network algorithm corresponds to the mapping of intensity measurements y_k to outputs λ. Hence

$$\Upsilon_{NN}(y, u) = \lambda_o(y_1, ...y_k) = \sum_{h=1}^{L} w_{oh} f(\sum_{k=1}^{K} w_{hk} y_k + b_h) + b_o \tag{2-16}$$

The limitation of the Neural Network is that the data presented to the trained network must be statistically similar to the data used to trained the Neural Network. Therefore, the network generalizes by interpolating within the range of input data and the network is not expected to give reliable results if a different data is used.

2-4 Validation of the proposed strategy

To validate our propose strategy for wavelength estimation the need for a tunable light source is not negotiable. The cost of a tunable laser source left us with no option but to design and construct a tunable light source suitable for the validation of our proposed methodology for wavelength estimation. In an effort to realise a tunable light source, two methods designs were implemented and these includes :

1. Design of tunable laser using a laser pointer.

2. Design of a tunable laser using a bandpass filter.

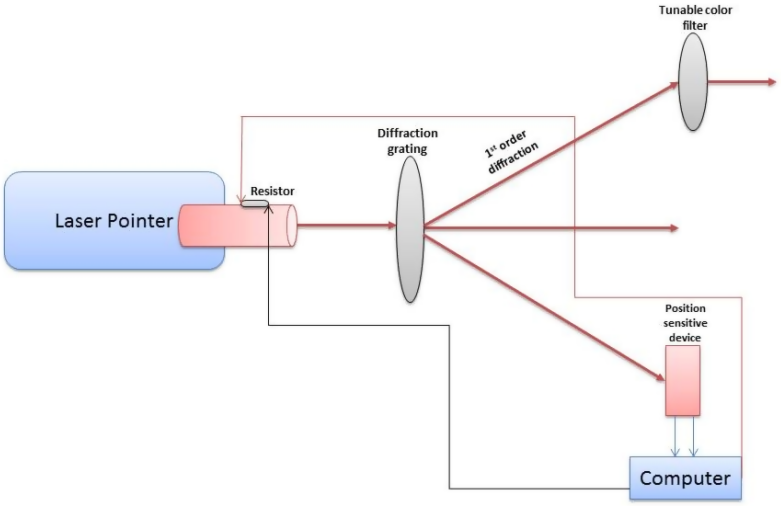

Figure 2-8: Schematic of the tunable light laser source using a laser pointer.

2-4-1 Design of a Tunable laser source using a Laser Pointer

A laser pointer is a small hand held device with a power source (usually a battery) and a laser diode emitting a very narrow coherent low-powered laser beam of visible light, intended to be used to highlight something of interest by illuminating it with a small bright spot of colored light. Power is restricted not to exceed 5 mW The laser pointer used in our experimental set-up had a centre wavelength of 632 nm and was suitable for our research.

The wavelength of the laser pointer was tuned by a heating resistor which was fixed to the cavity of the laser pointer. As the input voltage to the heating resistor was gradually increased, the temperature also increased. This caused a corresponding increase in the heat radiated to the cavity of the laser pointer and this consequently caused a drift in the wavelength of the laser pointer.

The change in the wavelength is measured by passing the light through a diffraction grating device (a low-cost compact disc).The displacement of the 1st order diffraction of the light passing through the diffraction grating corresponds to a change in wavelength. This displacement is measured by a calibrated position sensitive device whose voltage output corresponds to the wavelength. The displacement of the light on the position sensitive device therefore correspond to the wavelength of interest based on the amount of heat applied to the diode cavity of the point laser.

The displacement measured is fed into a MATLAB Algorithm which estimates the wavelength from the measured displacement and therefore keeps the temperature of the heating element constant by adjusting the voltage of the resistive element attached to the laser pointer via a Proportional-Integrator (PI)controller. Hence, the PI controller was used to set the wavelength of the laser to a user defined reference.

Though this method of realizing a tunable laser source provided the necessary wavelength shift, it however had the following limitation which made it unfit for an accurate generation of a tunable laser source suitable for generating the required data for the design of our system.

- Stabilizing a desired wavelength using a simple proportional integrator controller produced an inaccurate result due to the high sampling rate of 2.5s. The slow cooling of the heated point laser also contributed to the increased time measurement process and this constitute potential inaccuracy in measurement. Although a method of increasing the speed of cooling by incorporating a peltier element which will optimised the speed of the system was contemplated, however, this method is limited in accuracy.
- The red laser diode are tunable over the range of $+-5\ nm$ around the 650 nm optical region and thus such diodes produces effective wavelength and not single wavelength.
- Mode Hopping : When the temperature of the red laser diode was tuned, a slow shift in wavelength is observed (approximately 0.06 nm/degree). However, further increase in temperature may result to observation of discrete jumps (jumps from 0.06 nm to 0.3 nm). This mode hopping occurs when the laser switches from one longitudinal mode to another. therefore, the mode hops occurs in an erratic way with the laser switching back and forth between wavelengths. Furthermore, since the distance between two hops is about 0.25 nm and the tunable color filter has a transmission window of about 3 nm, it thus implies that about 10 modes will be oscillating unnoticed. This also causes a corresponding fluctuations in the laser output intensity which further introduces unwanted intensity noise.

Based on the inaccuracy of the designed tunable laser source a new tunable light source was designed and the design details are discussed in the following section while the experimental set-up and results are discussed in the next chapter.

2-4-2 Design of Tunable Light Source with a Bandpass Filter

The tunable light source is designed based on the transmission characteristics of an optical bandpass filter . When a portion or all of incident radiation is at an angle other than the normal to the surface of a bandpass filter a wavelenght shift occurs i.e increasing the angle θ between the filter normal and the incident rays causes a shift towards the lower wavelength according to the equation below:

$$\lambda_\theta = \lambda_0(1 - (\frac{N_e}{N}^*)^2 \sin^2\theta)^{\frac{1}{2}} \tag{2-17}$$

λ_θ is the centre wavelength at an incident angle θ. N_e and N^* denote the refractive index of the outer medium and the filter.

The optical thickness of a thin film decreases with an increase in angle of incidence; consequently, a multilayer narrow bandpass filter's center wavelength shifts toward shorter wavelengths as the angle of incidence is increased [20,21]. The magnitude of the shift in wavelength is dependent on the type of filter, the filter design, the refractive index of the coating materials used and the precision with which the coating materials are deposited [20].

Figure 2.9 below represents the schematic design of a simple tunable light source used for the validation of our proposed strategy.

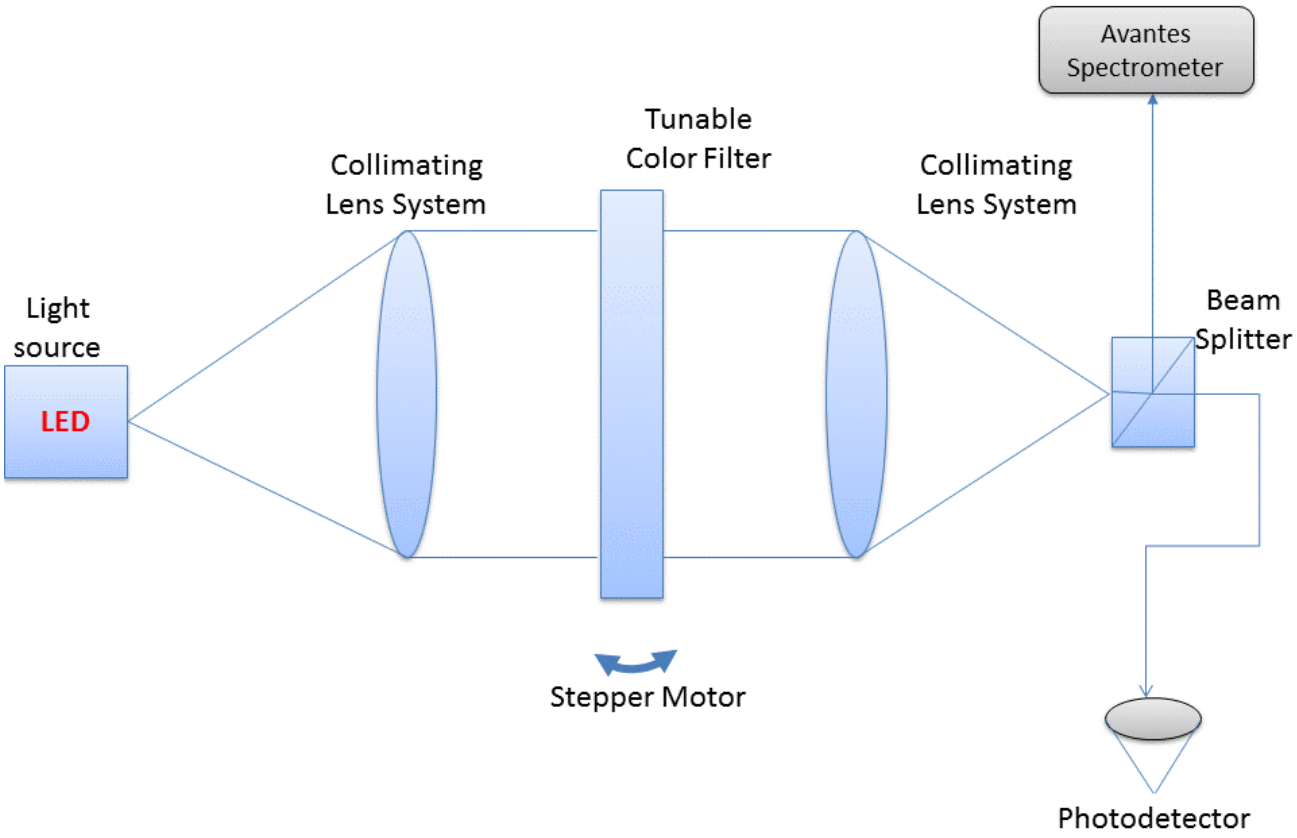

Figure 2-9: *The schematic diagram of the Tunable Light Source. The light from the red Light Emitting Diode is collimated by the collimating Lens system and then incident on the tunable color filter mounted on a stepper motor, the output from the tunable color filter is collimated again and passed through a beam splitter where. The incoming light is splitted and part is reflected to the spectrometer and part is further transmitted into the wavelength meter*[18]

The output of the light source which is a red high power Light Emitting Diode (LED) is collimated by a thin lens and the wavelength is defined and selected by a tunable color filter. The field propagating over a distance F (where F is the focal point)and thus striking the lens is the impulse response denoted as

$$h(x,y) = \frac{e^{ik_0 z}}{\lambda z} \exp(i\pi \frac{x^2+y^2}{\lambda F}) \tag{2-18}$$

The field is transformed by the lens into a plane wave by modulating it by a transmittance function $t(x,y)$. The transmittance of the lens can be derived from the phase modulation experienced by the field by propagating through the lens. The transmittance of the lens due

to its non absorbing property is denoted by $t(x,y) = \exp[i\phi(x,y)]$ where $\phi(x,y)$ is the phase delay, encountered by the field when passing through the lens at point (x,y).

The phase delay is thus

$$\phi(x,y) = (\frac{2\pi}{\lambda})(\Delta_0 - \Delta(x,y)) + (\frac{2\pi n}{\lambda})\Delta(x,y)) \tag{2-19}$$

where $\Delta(x,y)$ is the thickness of the lens at position (x,y) on the lens. $\Delta(0,0) = \Delta_0$ and n is the refractive index of lens.

From the analysis of the geometry of the lens, the phase delay propagation through the lens is approximately:

$$\phi(x,y) = \frac{2\pi}{\lambda}\Delta_0 - \frac{2\pi(n-1)}{\lambda}(\frac{1}{R_1} - \frac{1}{R_2})(x^2+y^2) \tag{2-20}$$

Denote

$$\frac{1}{F} = (n-1)[\frac{1}{R_1} - \frac{1}{R_2}](\textit{Noted as the lens maker equation}) \tag{2-21}$$

we obtain the lens transmittance as

$$t(x,y) = \exp(-i\pi\frac{x^2+y^2}{\lambda F})P(x,y) \tag{2-22}$$

Where $P(x,y)$ is the pupil function introduced to account for the finite transverse aperture and lens shape aberration of real lenses.

The pupil function

$$P(x,y) = Circ(\sqrt{\frac{x^2+y^2}{D}}) \tag{2-23}$$

Where D is the diameter of the lens. considering the first part of the schematic as shown below...

The field at the plane(x,y) is diffracted along the I_z axis through a distance z_1 to the (x_1', y_1') plane which contains a lens. The transmittance of the lens causes a modulation of the field after which the field is diffracted along the I_z axis at a distance Z_2 to the (x'', y'') plane.

Given the field $f(x,y)$ on the (x, y) plane, the field at the output represented by $g(x'', y'')$ on the (x'', y'') is computed as a linear transformation due to the transmittance of the lens and it is characterize by an impulse response.

Therefore an impulse at (x_0, y_0) in the(x,y) plane produces

$$u(x', y') = \frac{e^{ik_0 z_1}}{\lambda z_1}\exp(i\pi\frac{(x'-x_0)^2 + (y'-y_0)^2}{\lambda z_1}) \tag{2-24}$$

The field is modulated after passing through the thin lens and the field produced is a product of the impulse and the lens transmittance.

$$t(x', y'), u(x', y') = \frac{e^{ik_0 z_1}}{\lambda z_1}\exp(-i\pi\frac{x'^2 - y'^2}{\lambda F} * \exp(i\pi\frac{(x'-x_0)^2 + (y'-y_0)^2}{\lambda z_1})P(x', y') \tag{2-25}$$

The impulse response describes the linear transformation that occurs when a field passing through a lens is modulated by the transmittance of the lens [6]. The impulse response at the output plane is therefore denoted as $h(x'', y'', x_0, y_0)$ and it is obtained by convolving the modulated field with the fresnel kernel and this produces equation 2-26. For more detailed derivation, interested reader is referred to [6].

$$\begin{aligned} h(x'', y'', x_0, y_0) = \quad & \frac{e^{ik_0(z_1+z_2)}}{\lambda^2 z_1 z_2} \int\int exp(-i\pi \frac{x'^2 + y'^2}{\lambda F} P(x', y') * exp(i\pi \frac{(x'-x_0)^2 + (y'-y_0)^2}{\lambda z_1}) \\ & * exp(i\pi \frac{(x''-x')^2 + (y''-y')^2}{\lambda z_2} \delta x' \delta y' \end{aligned} \tag{2-26}$$

To further solve the above integral equation, the following assumptions were made :

- Assume $z_1 = z_2 = F$ then the impulse response is given below

$$\begin{aligned} h(x'', y'', x_0, y_0) = \quad & \frac{e^{i\frac{4\pi F}{\lambda}}}{\lambda^2 z_1 z_2} exp(i\pi \frac{x''^2 + y''^2}{\lambda z_2}) exp(i\pi \frac{x_0^2 + y_0^2}{\lambda z_1}) \\ & * \int\int P(x', y') exp[-i \frac{\pi}{\lambda F}(x'^2 + y'^2)] \\ & * exp(i \frac{2\pi}{\lambda}[x'(x_0 z_1 + x'' z_2)] + [y'(y_0 z_1 + y'' z_2)] \delta x' \delta y') \end{aligned} \tag{2-27}$$

To neglect the impact of the aperture, we assume $P(x, y) = 1$ and thus the integral becomes the fourier transform of the complex gaussian. Thus applying the similarity theorem, the impulse response becomes :

$$\begin{aligned} h(x'', y'', x_0, y_0) = \quad & \frac{e^i 2k_0 f}{i\lambda F} exp(-i\pi \frac{x''^2 + y''^2}{\lambda F}) exp(i\pi \frac{x_0^2 + y_0^2}{\lambda F}) \\ & * exp[-i\pi F \lambda (\frac{x_0}{\lambda F} + \frac{x''}{\lambda F})^2 + (\frac{y_0}{\lambda F} + \frac{y''}{F})^2] \end{aligned} \tag{2-28}$$

and $h(x'', y'', x_0, y_0)$ is the impulse response of the propagation of the incident field from the front focal plane of the lens to the back focal plane.

$$g(x'', y'') = \frac{e^{i2k_0 F}}{i\lambda F} \int f(x, y) exp[-i \frac{2\pi}{\lambda F}(xx'' + yy'')] \delta x \delta y \tag{2-29}$$

Thus $g(x'', y'')$ is the output field which is the fourier transform of the incident field evaluated at $u = \frac{x''}{\lambda F}$ and $v = \frac{y''}{\lambda F}$

2-5 Concluding Remarks

In this chapter, the strategy used for the design of the model based wavelength wavelength estimation device was proposed. The progression in steps, necessary for the actualisation of our model was also described. Furthermore, the underlying theories of the components used in our system such as the TCF, the photodiode, the Avantes spectrometer etc were discussed. To validate our system, the need for a tunable light source was emphasised and the methods deviced for the realisation of the tunable light source have been documented.

The experimental set-up of a tunable light source used to validate our system and the experimental set-up of our wavelength estimation device will be discussed in the next chapter.

Chapter 3

Wavelength Estimation

The previous chapter describes our strategies for the design of our wavelength meter with particular focus on developing a model for the calibration of the transmission function of our system using the Neural Network method. Furthermore, the Nonlinear Least Square optimisation algorithm and the Neural Network algorithm were proposed as the method of estimation of the unknown wavelengths. This chapter presents the details of the implementation of our proposed strategies described in the previous chapter and the results obtained from the experimental implementations.

3-1 Experimental set-up of Tunable light source

To validate our proposed strategy, we built a tunable light source (described in 2.42) which produces better accuracy than the tunable laser source described in 2.41. The schematic diagram is described in figure 2.9.

Light from a red light emitting diode (LED) is collimated by lens L_1 and lens L_2. The collimated laser beam is focused into a pin hole of $20\mu m$. The light emerging from the pin hole passes through the lens L_3 and thus collimated before striking the tunable optical filter surface.

The optical band pass filter allows the transmission of wavelengths in a narrow range around a specified wavelength hence it selectively transmit a defined wavelength and rejects other wavelengths. The transmission characteristic of the optical filter is tuned by changing the angle of incidence of the incoming light from the red LED via the stepper motor on which the filter is mounted. When a control signal v_k at a time instant k is sent from the computer to the stepper motor via the microcontroller, the stepper rotates in steps of 1 degrees and thus the wavelength shifts to shorter wavelengths according to equation 2.41.

The output of the filter is then passed through a beam splitter (a device which splits the incoming light beam into two halves) the first half is collimated by a collimating lens and the intensity of the collimated output beam is measured by a photodiode and the second half is

fed into an Avantes spectrometer which measures the wavelength of the output beam thus enabling the calibration of the light source.

The intensity measured by the photodiode when the Optical filter is tuned by the stepper motor is readout and transmitted to the PC via a data acquisition card. The stepper motor control signal is generated by the PC and the control voltage to the stepper motor is set via a digital to analog card connected to the PC.

All user-defined parameter for the hardware and software are written in a text file by Matlab. During the experiment, Matlab communicates with the Digital Acquisition Card (DAQ) and Digital Analogue (DA) cards and the results are also read out by MATLAB. The Avantes spectrometer is also connected to the PC via the Matlab and its Avantes software and both softwares are used interchangeably.

In our experimental set-up, the tunable color filters (Thorlabs, GmbH, Germany) is tuned by a stepper motor (Texas instrument) with a step angle of 1.0 degrees. The photodiode measurement is readout by National Instrument SCB-68.

3-1-1 Experiment and Results

The experimental set-up described in section 3.1 gives a tunable light source which generates 15 wavelengths. As the TCF is rotated, the central wavelength shifts downwards and the wavelength output shifts from 630.6235 nm to 615 nm, spanning a range of approximately 15 nm. The result is displayed in table 3.1. With a complete rotation of the TCF from 35

Table 3-1: Wavelengths obtained at control input (θ) to the Tunable color filter.

S/no	Angles (degrees)	Wavelength(nm)
1	θ_1	630.6235
2	θ_2	630.3121
3	θ_3	629.8450
4	θ_4	629.2222
5	θ_5	628.4434
6	θ_6	627.5085
7	θ_7	626.5734
8	θ_8	625.6380
9	θ_9	624.7023
10	θ_{10}	624.2344
11	θ_{11}	622.5179
12	θ_{12}	621.1127
13	θ_{13}	619.2382
14	θ_{14}	616.8933
15	θ_{15}	615.0162

degrees to 70 degrees (almost blocked transmission to the other end of blocked transmission)a repetition of the wavelength cycle is visible as depicted in figure 3.1. The limitation of the designed tunable light source is that it cannot provide a high and consistent resolution due

to the properties of the filter, the tunning of the filter and the properties of the light source. This however limits the performance of our model but gives us insight into the performance of our proposed methodology for wavelength estimation.

3-1-2 Calibration of the tunable color filter

The combined spectral function $f(\lambda_0, v)$ of the Tunable Color Filter needs to be identified. This is referred to as the calibration of the Tunable Color Filter and it provides gainful insight into the performance characteristics of the filter especially when an angular displacement is applied to it.The calibration of the TCF was done in two steps:

Calibration of $f(\lambda_0, v)$ at fixed λ_0

In this first step, wavelength λ_0 of incident light is fixed and only the bandpass filter is rotated by the stepper motor (i.e, v changes). As the incident angle of the incoming light changes, the transmitted intensity varies as shown in figure 3.3. This shows that the spectra curve $f(\lambda_0, v)$ is sensitive to the incident angle (i.e.control signal v) and thus can be used in our system set-up.

Calibration of $f(\lambda, u)$ for varying λ and u

In the second step, both λ_0 and v are varied i.e for every wavelength, a set of intensity measurement is recorded. The recorded intensity measurement y is thus used for identifying $f(\lambda_0, v)$. The results of the calibration of the color filter is depicted in figure 3.4.

3-2 Wavelength Estimation Methods

The goal of our model is to estimate the unknown wavelength of light injected into our system. As described in chapter 2, two algorithms are used for the estimation of the unknown wavelength. In this section, three approaches based on the two algorithms described in chapter two are used for wavelength estimation. The three approaches are highlighted below and described in the subsections that follows:

- Non-linear least square optimisation approach based on Neural Network.
- Single Neural Network approach.
- A hybrid (Neural-least square) approach based on two Neural Network.

3-2-1 Non-Linear Least square Optimisation approach based on Neural Network

The purpose of the NLLS optimisation approach based on Neural Network is to estimate the unknown wavelength of an incoming light by deducing the optimal wavelength which

minimises the cost function as shown in the equation below:

$$\hat{\lambda} = \arg\min_{\hat{\lambda}} \left\| Y - \hat{Y} \right\|_2^2. \tag{3-1}$$

where

$$Y = \begin{bmatrix} y_1 \\ y_2 \\ \vdots \\ \vdots \\ \vdots \\ y_n \end{bmatrix} = \begin{bmatrix} f(\lambda_0, v_1) + \eta_1 \\ f(\lambda_0, v_2) + \eta_2 \\ \\ \vdots \\ f(\lambda_0, v_n) + \eta_n \\ \end{bmatrix}, \hat{Y} = \begin{bmatrix} \hat{y_1} \\ \hat{y_2} \\ \vdots \\ \vdots \\ \vdots \\ \hat{y_n} \end{bmatrix} = \begin{bmatrix} \hat{f}(\hat{\lambda_0}, v_1) + \hat{\eta_1} \\ \hat{f}(\hat{\lambda_0}, v_2) + \hat{\eta_2} \\ \\ \vdots \\ \hat{f}(\hat{\lambda_0}, v_n) + \hat{\eta_n} \\ \end{bmatrix} \tag{3-2}$$

and

$$V = \begin{bmatrix} v_1 \\ v_2 \\ \vdots \\ \vdots \\ \vdots \\ v_n \end{bmatrix} \tag{3-3}$$

From the above equations, $Y = F(\lambda_0, V)$ and $\hat{Y} = \hat{F}(\lambda_0, V)$. This implies that equation 2.10 can be re-written as

$$\hat{\lambda} = \arg\min_{\hat{\lambda}} \left\| Y - \hat{Y} \right\|_2^2. \tag{3-4}$$

Approximating spectral function $\hat{F}(\lambda, V)$ by a Neural Network

Given the fact that the wavelength of an incoming light source was measured (calibrated) with the Avantes Spectrometer, the control input signal at each time instant was known and the intensity measurement was measured by recording the output of the photodiode, approximating the function $\hat{F}(\lambda, V)$ by a Neural Network is possible by fitting a function to the data generated.

$$\hat{F} = NN(\lambda, V) \tag{3-5}$$

The Neural Network is trained by presenting the calibrated wavelength λ and the control signal U as the input to the network and the output of the network is the intensity measurement recorded at the control signal U. The network is trained with the Levenberg marquardt algorithm and the choice of neurons which minimises the cost function is appropriately selected such that the function $(\hat{F}\lambda, U)$ is well approximated.

An incoming light with an unknown wavelength λ provides an intensity vector Y at control signal U. The difference between the measured intensity Y and the function $\hat{F}(\lambda, U)$ approximated using the Neural Network approach is minimised by using the non-linear least square

optimisation algorithm. The wavelength which minimises the cost function provides the best estimate of the unknown wavelength of the injected light.

The cost function $J = \frac{1}{N}\|Y - \hat{F}(\lambda, U)\|_2^2$ is defined as the Mean Square Error (MSE) between the measurement vector Y and the approximation at certain guess λ and the purpose of equation 3.4 is to find the suitable $\hat{\lambda}$ such that the cost function is close to zero as much as possible.

Pseudo Algorithm for NLLS approach

1. Initially known parameters are : $\hat{F}(\lambda, U)$ which is the result obtained from calibration using Neural Network algorithm, intensity measurement Y and control signal U.
2. Initialise parameter : λ_0 as initial guess.
3. Run Levenberg Marquardt algorithm to optimise$\hat{\lambda}_x = \arg\min_{\hat{\lambda}_x} \left\|Y - \hat{Y}\right\|_2^2$.
4. Store λ_{final}.

3-2-2 The Neural Network Approach

Section 2.4 gives an overview on the principles of Neural Network and how to fit a Neural Network.

For this Neural Network approach for wavelength estimation, a Neural Network is trained with inputs Y which is the measured set of intensity data and the output of the network λ (the calibrated wavelength measured with the Avantes Spectrometer) is the desired response or the target response of the Network. This approach allows the estimation of the optimal wavelength λ when a set of intensity measurement is presented to the trained network.

In this approach, the control signal U is known and it corresponds to $Y(U)$.

$$\lambda = NN(Y(U)) \tag{3-6}$$

The unknown wavelength is estimated with the Neural Network approach by deducing the inverse of the calibrated function as depicted in the equation below:

$$\lambda = \hat{F}^{-\lambda}(Y(U)) \tag{3-7}$$

$$\lambda = \hat{F}^{-\lambda}\begin{bmatrix} f(\lambda, u_1) \\ f(\lambda, u_2) \\ \vdots \\ \vdots \\ \vdots \\ f(\lambda, u_m) \end{bmatrix} \tag{3-8}$$

Training and Validation.

Neural Network fitting adopted for the estimation of wavelength in our wavelength meter requires two-phase handling which are :

1. Training.
2. Validation.

Training

The training involves using a large database of intensity measurement and control signal to teach the neural network to perform a mapping. In the training phase, a learning process is completed and a hyper-surface is constructed. The constructed hyper-surface which is as a result of optimising the free parameters of the network, fits to the training data points.

The primary goal of the Training phase is to minimize the error function (which is the sum of squares of the errors between the output vector $\lambda(y^p)$ (at a particular sets of intensity measurement of the network which represents our input vector y^p) and the corresponding target vector λ^p (which is our calibrated wavelength at a specified intensity).

Validation

The Validation phase is the phase where a set of intensity measurement from a light source with an unknown wavelength is presented to the trained network.

The unknown wavelength is deduced from the interpolation on the constructed hyper-surface. The process of validation is completely equivalent to computing the unknown wavelength of an incoming light since the weights or the parameters of the network have been determined after the completion of the training process.

For the network to generalize to new data such that the unknown wavelength can be estimated, it is essential that the training data spans the input space where the mapping is to be applied because Neural Network are poor at extrapolating beyond their training experience and are very efficient at interpolating within their training examples.

3-2-3 The Hybrid Method

In this method , the two wavelength estimation methods discussed above are combined.

Two Neural Networks are combined with the Non Linear Least square algorithm to provide an estimation of the unknown wavelength of an incoming light. The first Neural Network NN_1 is fitted with the intensity measurement Y as the input to the network, while the output (desired response) of the network is the calibrated wavelength λ as described in section 3.2.2.

The first Neural Network is used to compute the initial estimate of the optimal wavelength λ thus providing an educated guess for the Non Linear Least Squares optimisation algorithm.

The provision of an educated initial guess ensures that the an abstract initial guess is not selected.The provision of an educated guess ensures convergence to a unique solution. It

also allows the iterative method to converge in fewer iterations. This method could prevent convergence to the wrong solution since the initial guess is well predicted by the Neural Network.

The second Neural Network NN_2 is as described in (3.21) The second Neural Network has calibrated wavelength λ and the control input signal U as the input to the network to produce an estimate $\hat{Y}$ of Y which is the output of the second Neural Network. This Neural Network is used in Non-Linear Least Square optimisation to deduce the approximate of the function $\hat{F}(\lambda, U)$ such that

$$\|Y - \hat{F}(\lambda, U)\|_2^2 \tag{3-9}$$

is formed.

Difference between the Least square approach,the Neural network approach and the Hybrid Solution

- Least square approach to curve fitting requires optimization for every set of data points to be fitted.
- The Neural network approach to curve fitting performs one - time optimization which is sufficient to solve a whole class of fitting problems.
- Once the neural network is trained it can very quickly perform the curve fitting operation on a new data.

3-3 Performance Measures

Two performance indices are defined to evaluate the performance of our model.

The optimisation algorithm for finding the unknown wavelength uses the sum of squares as minimisation criteria. Although this performance index can be used for evaluating the performance of our model, another performance index which is the Variance-Accounted-For (VAF) is defined. The sum of squares can indicate that a perfect model is not performing well if the signal is noisy. The VAF however is less sensitive to this and it gives a better model judgement when we have noisy signals.

3-3-1 Variance-Accounted-For

The Variance Accounted For is often used to verify the correctness of a model, by comparing the real output with the estimated output of the model. VAF weights the variance of the residual with the variance var(λ) of the measured wavelength λ. The maximum VAF is 100, but for an inaccurate model the VAF can even become negative.

The VAF is calculated as:

$$v = (1 - \frac{var(\lambda_{real} - \hat{\lambda}}{var(\lambda_{real})}) * 100 \tag{3-10}$$

where λ_{real} is the calibrated wavelength and $\hat{\lambda}$ is the predicted wavelength. The VAF of two signals that are the same is 100. If they differ, the VAF will be lower.

Inputs:

- λ_{real} Signal 1, often the real output which is the wavelength calibrated by the Avantes spectrometer.
- $\hat{\lambda}$ Signal 2, often the estimated output of our model.
- Output: v is the Variance-Accounted-For, computed for the two signals

3-3-2 Sum of Squares

Sum of Squares is applied as performance evaluation (cost function) for the minimisation of the prediction error in the nonlinear calibration procedure. This cost function is minimised by the Levenberg Maquardt algorithm to estimate the unknown wavelength with the nonlinear least squares optimisation technique. The sum of squares is defined as follows:

$$J(\lambda) = \frac{1}{N}\sum(\hat{y}(k,\lambda) - y(k))^2 \tag{3-11}$$

where k is the time index of the sampled data, λ is the parameter to be estimated, $\hat{y}(k,\lambda)$ is the predicted spectral curve, $y(k)$ is the measured data and N is the number of samples.

The absolute error is computed from the Sum of Squares error by dividing the summation of the absolute value of the error by the number of measurements.

$$J(\lambda) = \frac{1}{N}\sum(\hat{y}(k,\lambda) - y(k)) \tag{3-12}$$

3-4 Experiments and results

An experimental setup has been built in DCSC Smart optics Laboratory for a proof of concept of our proposed wavelength estimation method.

A high power LED (4.6 Watt) is used as our light source. The Light source is collimated by various collimating lens and therefore passed through a Tunable Color Filter (FL632.8-3, Thorlabs) mounted on a stepper motor (RDK-Stepper Motor,Texas Instrument) which enables the realisation of a tunable light source with a tunning range of $15nm(630nm - 616.1114nm)$. The light at every wavelength is transmitted through the wavelength meter assembly. The set-up is depicted in figure 3.5.

Spectral sensitivity function $F(\lambda,\theta)$ is identified from a set of input-output data $\{\lambda, y\}$ at $\theta = 30 : 1.0 : 60\ deg$.

For each fixed θ, λ is scanned from 616.6nm to 630.3 nm with an inconsistent increment of approximately 0.6 nm (the resolution is limited by our light source, motor steps (approximately 1.8 degrees) and the resolution of our wavelength calibration equipment).

The range $[616.6\ nm, 630.3\ nm]$ is selected because the Tunable color filter produces optimal tunability when it is tuned over the range of 18 degrees. Each $\{\lambda, y\}$ curve is approximated by a neural network.

3-5 Data for calibration and wavelength estimation

To demonstrate the performance of our proposed optical wavelength meter, four data set were generated. The first two dataset A and B generated are used for the calibration of our function and the for the validation of our model respectively.

Dataset A and B are limited in terms of the recorded transmission data points hence the number of measurements made is reduced as compared to dataset C and D. This therefore reduces the prediction accuracy of our proposed wavelength estimation algorithms.

To observe the impact of the number of measurements on the accuracy of our wavelength estimation algorithm, data set C and D are generated. Dataset C and D have high number of recorded transmission data point.

While dataset C is used for the calibration of our Model, dataset D is used for the validation of our proposed. Further details are discussed in the section that follows.

3-5-1 Data set A

Data set A is the transmission data points (intensity measurement) recorded at varying wavelength λ_0 i.e for every wavelength selected by the first tunable color filter a complete rotation of the second tunable color filter produces a transmission data point which is recorded by the photodiode.

Dataset A is mathematically depicted by equation 3-13 and the measured data includes the intensity measurement Y, the calibrated wavelength λ and the control signal V.

The overview of the measurement profile of the data set is represented mathematically in equation 3-13 below.

$$\begin{bmatrix} Y_1 \\ Y_2 \\ \vdots \\ \vdots \\ \vdots \\ Y_{18} \end{bmatrix} = \begin{bmatrix} F(\lambda_1, V) \\ F(\lambda_2, V) \\ \\ \vdots \\ F(\lambda_{18}, V) \\ \end{bmatrix} \tag{3-13}$$

For a given set of angles that is set by the inputs $U_{1:18}$ where U is the control input signals to the stepper motor which generated the wavelength from the red LED, wavelength λ_i for $i = 1:18$ is generated.

For each λ_i, corresponding set of intensity measurement $Y = y_{(1:1:15)}$ are recorded at control signal $V = v_{(\theta_1:1:\theta_{15})}$ where V is the control signal to the color filter used for the wavelength estimation.

This process is repeated for a different angle set by a different control signal U. To ensure accuracy of our system more intensity measurements were generated by repeating each intensity measurement 18 times for the same λ_i. In total we have 15 settings of angle, repeated 18 times for each 18 wavelengths generated. It is important to note also that the transmission data points were recorded while the light source (LED) is kept at constant power.

Data set A is used for the calibration of our system such that the nonlinear least square algorithm can adequately estimate the optimal wavelength that minimises the cost function. In the neural network approach however, this data set is used for training the neural network since the need for calibration is not necessary.

3-5-2 Validation Data set B

Data set B is measured under similar condition as data set A and it is mathematically represented as equation 3-13.

Data set B was used for the validation of our model therefore, it is not used for calibration or for training. Data set B was recorded 72 hours after data set A was measured. The time difference between measurement A and B is deliberately done so that allowance is given for drifts in measurement which may arise as a result of temperature variation, vibrations, displacements etc.

Using data set B as our validation data gives us insight into the accuracy of our model and how our model will behave when data which are completely different from the data used for calibration and wavelength estimation are used to predict the wavelength in our proposed wavelength estimation methods.

3-5-3 Data set C

Data set C is similar to the Data set A (which is the recording of the intensity measurement at varying wavelength λ).

While the transmission data point in data set A is recorded for the power of the light source set at a constant value, the transmission data points in data set C is measured while the power of the light source is varied. The variation in the power of the light source results in measurements of the transmission data points through the range of 13 different power levels (watts) and this results into a large database of transmission data points used for the calibration of our system and the estimation of the unknown wavelength.

For data set C, the control signal is designed such that 30 intensity measurements are taken at each wavelength which also makes data C different from data A where only 15 intensity measurements are recorded. A set of intensity measurement $Y = y_{(1:1:30)}$ is measured given a set of control signal $U = u_{(\theta_1:1:\theta_{30})}$ thus giving rise to 30 angles which implies that N_{angles} = 30. For the generation of data set C, 15 wavelengths are used.

$$\begin{bmatrix} Y_1 \\ Y_2 \\ \vdots \\ \vdots \\ \vdots \\ Y_{18} \end{bmatrix} = \begin{bmatrix} F(P\lambda_1, U) \\ F(P\lambda_2, U) \\ \\ \vdots \\ \\ F(P\lambda_{15}, U) \end{bmatrix} \tag{3-14}$$

Table 3-2: Four data set used for system calibration and wavelength estimation

Dataset	No.Angles	No.Wavelength	No.Duplicates	Intensity Val.	Pwr.Levels
DS A	15	18	18	4860	1
DS B	15	18	18	4860	1
DS C	30	15	18	105300	13
DS D	30	15	18	8100	1

3-5-4 Data set D

Data set D is measured under similar condition as data set C and like data set B, data set D is also used to validate and test our model.

A complete cycle (30 intensity measurement at each of the wavelength selection which is repeated for 18 duplicates) is recorded while the light source is at constant power (arbitrary power (watt) setting of the light source). This measurement was done one week after the data set C dataset was generated because this will simulate a more realistic situation and will proffer better insight into the performance of our model in terms of accuracy.

3-6 Data Processing

To gain more useful insight into the performance of our wavelength estimation method, the recorded transmission data points (light intensity and calibrated wavelength) were processed and the results of the processed data points are compared with the results obtained from the unprocessed data points.

3-6-1 Normalizing the transmission data points

To ensure consistency in our data and to see the impact of introducing consistency into our data analysis, the entire set of data was normalized by deducing the maximum intensity value in each channel and dividing the entire measurement in a channel by its maximum intensity measurement.

This analysis reduces the database to a consistent maximum value of 1 for every channel. Normalization was performed on each of the data set (intensity measurement) in the above table and the result will be discussed in the subsequent section on experimental results. The normalisation procedure is mathematically described below :

for each Y_i :

$$Y_{normalized} = \frac{Y_i}{max(Y_i)} \tag{3-15}$$

3-6-2 System of equation

Equation for the calibration of our system with $\hat{y}$ normalized :

$$\hat{y_k}(\lambda) = \hat{f}(\lambda_0, v_k) = w_1 tanh(w_2\lambda_0 + s_1) + s_2 \tag{3-16}$$

Set of non-linear equation derived from the physics of our system.

$$\begin{aligned} y_1 &= f(\lambda_0, v_1) + \eta_1 \\ y_2 &= f(\lambda_0, v_2) + \eta_2 \\ &\vdots \\ y_n &= f(\lambda_0, v_n) + \eta_n \end{aligned} \tag{3-17}$$

Equations denoting the set of approximated transmission curve.

$$\hat{y} = \begin{bmatrix} \hat{y_1} \\ \hat{y_2} \\ \vdots \\ \vdots \\ \vdots \\ \hat{y_n} \end{bmatrix} = \begin{bmatrix} \hat{F}(\hat{\lambda_0}, v_1) + \hat{b_x} \\ \hat{f}(\hat{\lambda_0}, v_2) + \hat{b_x} \\ \\ \vdots \\ \hat{F}(\hat{\lambda_0}, v_3) + \hat{b_n} \\ \end{bmatrix} \tag{3-18}$$

Available measurements

- θ_k : Control input at time instant k for tunning the tunable color filter.
- y_k : Intensity measurement at time instant k recorded by the photodiode.
- λ : Calibrated wavelength measured by the Avantes spectrometer.
- Power : The power (watts) of the light source at various time instant k.

Parameters to be estimated

- λ : Unknown wavelength of a tunable light source.
- $\hat{y}$: $\hat{F}(\lambda, \theta)$ spectra sensitivity of combined color filter and photodiode.

Cost function

$$\hat{\lambda}_x = \arg\min_{\hat{\lambda}_x} \left\| Y - \hat{Y} \right\|_2^2. \tag{3-19}$$

3-7 Results for Data Set A and Data Set B

This section presents the wavelength estimation results using the Neural Network estimation algorithm where data set A (with 4806 recorded transmission data points) was used for the training of the Neural network.

The estimation algorithm has been tested with data set B which was generated at the same control input signal θ and wavelength λ but the measurement was performed 3 days after data set A was generated. The dataset B is therefore referred to as the validation data set which is used to validate the accuracy and the performance of the Neural Network estimation algorithm for wavelength estimation.

3-7-1 Result of trained Neural Network with validation data set A

The validation data set used to test our trained network is thesame as the dataset used to train the network (i.e a part of the generated data was used for training the network while the other part was used for the validation of the model.)

The Neural network is trained with Dataset A, using 20 Neurons and the computed variance -Accounted-For between the wavelength measured by the Avantes Spectrometer and the wavelength estimated by the Neural Network is 99.9971 percent. The wavelength estimation error which is the difference between the calibrated wavelength and the predicted wavelength is depicted in Figure 3-6.

Figure 3-6 shows the plot of the estimation error and the histogram of the errors when the trained neural network is tested with similar data used for the training. The maximum estimation error for the validation set is about 0.4 nm. 98% of the estimation error is between -0.1 nm 0.1 nm.

3-7-2 Result of trained Neural Network with validation data set B

A validation data set measured 72 hours later was used to validate the Neural Network estimation algorithm. When a completely different data set which is measured under different environmental conditions (such as drift in temperature, humidity, vibrations, drift in the power of light source,etc) is used to measure the accuracy of the prediction of the unknown wavelength the performance of our trained Neural Network dropped and this is obvious in the decrease of the value of the computed VAF and the increase in the absolute error.

The plot and the histogram of wavelength estimation error in figure 3-7 depicts the performance of our model. The Variance-Accounted-For between the estimated wavelength using data set B and the calibrated wavelength is 91.4740 the absolute error is 1.4044.

3-7-3 Neural Network algorithm validation data set B Normalized

To observe the impact of processing the data sets on the performance of our model, data set A was normalized before it was used for the training of the neural network. The training of the neural network was done under similar conditions as when the data sets were not normalised

Table 3-3: Summary of Neural Network training process.

Modelling dataset	Number of Neurons	Algorithm
Data set A	20	Levenberg-Marquadt
Data set A Normalised	20	Levenberg-Marquadt

Table 3-4: Results of the Neural Network estimation Algorithm.

Modelling dataset	Validation dataset	VAF	Absolute error
Data set A	Data set A	99.9971	0.2 nm
Data set A	Data set B (72hrs later)	91.4740	1.4044 nm
Data set A Normalised	Data set B normalised	99.1892	0.5942 nm

(i.e, 20 neurons were used for the training and the Levenberg Marquardt method was used). The data set used for the validation (i.e data set B) was also normalised before it was used to validate the performance of our model. The plot and the histogram of the wavelength estimation error are depicted in Figure 3-8 below.

For the normalised data sets, the Variance-Accounted-For is equal to 99.1892 percent,the absolute error = 0.5942. Normalizing the data used for training and for validating the Neural network is important to the accuracy and the performance of neural network algorithm.

Data normalisation ensures consistency in the statistical properties of the data set used for training and the data set used for validation of the trained network.

3-7-4 Hybrid (Neural Network - Nonlinear least square optimisation) algorithm validation data set B Normalized

The combination of the Non-linear least square optimisation and the neural network algorithm was validated with the normalised dataset B. The Neural network provided the initial guess needed to minimise the cost function. The variance accounted for is 99.6535 and the computed absolute error is equal to 0.4446.

The results for the wavelength estimation of different data sets are compared in the table 3.4 and 3.5. The table shows the Variance-Accounted-For and the absolute error for each data set. The performance of Neural Network when the training dataset was used as the validation dataset provides the best VAF and the minimum absolute error. This is not the case however when real validation data generated 72 hours later were presented to the trained network.

Table 3-5: Table 3.4: Results of the Hybrid (NNNLS).

Modelling data set	Validation data set	VAF	Absolute error
Data set A Normalised	Data set B normalised	99.6535	0.4446 nm

The network generalizes best when the data presented to the network are statistically similar to the data used to train the network.

Processing the data by normalizing it as discussed earlier improves the performance of the Neural Network model when presented with a new data set. From the table 3.4 it can be deduced that the accuracy and the VAF improved significantly when the data set presented to the trained NN was normalized.

The NLLS algorithm provides a good estimate of the wavelength as depicted in table 3-5. A VAF of 99.6535 depicts how accurate the model is for wavelength estimation. It is important to note also that the accuracy of the estimation algorithm is limited by the accuracy of the calibration equipment (Avantes Spectrometer which has an accuracy of 1 nm) and the tunable light source designed to validate our methodology. This implies that a more accurate tunable light source (Tunable laser) with a high resolution and accurate optical spectrum analyser is needed for a better performance of the Neural network wavelength estimation algorithm.

3-7-5 Results for Data Set C and Validation Data Set D

This section describes the results for Data set C (the large transmission data points of $1.05*10^5$ is recorded for different settings of power (watts) of the light source). Data set C is used for the following purposes in the wavelength estimation methodology.

1. The training of Neural Network required for wavelength estimation.
2. The calibration of our system required for the approximation of the spectral curve needed for non-linear least square optimisation algorithm method of wavelength estimation.
3. The training of the neural network used to predict the wavelength required for the initial guess of the optimisation algorithm.(Hybrid method to wavelength prediction).

Data D is measured three days after data C was generated and it was used for the validation of the proposed wavelength estimation methodology. The data set will be analysed using the following proposed wavelength algorithm:

1. Neural Network Algorithm.
2. The Non-linear least square optimisation algorithm.
3. The Hybrid (Neural-Non-Linear least square optimisation algorithm).

3-7-6 Neural Network Algorithm with Dataset D

Dataset C is used to train the Neural network, the network input is the recorded intensity measurement and the output (target) of the network is the calibrated wavelength measured using the Avantes Spectrometer. The network is trained with 80 neurons in 156 iterations and the trained network is stored.

Data set D containing the intensity measurement of an unknown wavelength is presented to the trained network. The trained network predicts the unknown wavelength and the performance measures is estimated providing the following results:

The Variance-Accounted-For is 99.7998, the absolute error =0.1941 and the computational time = 0.010175sec.

3-7-7 Non-linear least square optimisation algorithm

The non-linear least square optimisation algorithm was used to estimate the unknown wavelength in the following steps :

- Calibration of transmission curve using the Neural network to fit an analytical function to the recorded transmission data points. The Neural network is trained with data set C where the input to the neural network is the vectorised form of the calibrated wavelength and the control input signal θ. The output of the network is the intensity measurement recorded by the photodiode.
- The selection of appropriate $\lambda_{initialguess}$ requires human intervention such that the lower and the upper bound of the initial guess is selected to avoid the convergence of the algorithm to a wrong solution due to the wrong selection of initial guess. Two initial guess are selected and the impact of the selection choices is observed as documented in table 3-6.

The wavelength estimation error obtained when data set D is used to validate the optimisation algorithm is depicted in the figure 3-12.

With an initial guess of 625nm, the Variance-Accounted-For is equal to 96.1761, the absolute error is equal to 0.5048 and the computational time is 0.862121 seconds.

3-7-8 Hybrid solution (Educated - iterative method)

Due to the fact that the a wrong choice of an initial guess can cause the algorithm to converge to a wrong solution then a hybrid solution estimation algorithm is proposed. This educated-iterative algorithm increases the convexity of the optimisation algorithm. The neural network is trained with the data set C and the input used for the training is the recorded intensity measurement and the output is the calibrated wavelength. When a set of intensity measurement needed for the estimation of unknown wavelength is presented to the trained network a wavelength needed for use as the initial guess in the optimisation algorithm is estimated. The educated-iterative method involves the following steps.

1. Calibration of the system by training the Neural network with vectorised form of the calibrated wavelength and control input signal as the input to the network.
2. Selection of an appropriate initial guess by training the neural network with data set C and estimating $\lambda_{initialguess}$.

Table 3-6: Results of the estimation algorithm on Data set C and D..

Algorithm	VAF	Absolute error	Computational time
NN	99.7998	0.1941 nm	0.0107 sec
$NLLS_{625}$	96.1761	0.5048 nm	0.8621 sec
$NLLS_{620}$	17.4174	4.1603 nm	0.3773 sec
HYBRID (NN+NLLS)	99.5971	0.3972	0.2002 sec

3. Present data set D for the estimation of the unknown wavelength and estimate optimal lambda that minimises the cost function the most.

The result obtained from the hybrid method is tabulated in table 3-6.

It can be deduced that the estimation accuracy of the unknown wavelength using the Hybrid NLLS aproach depends on the number of measurements for solving Eq. (3.18), the initial guess of λ_0 and the weighting matrix W_k used for the calibration of the system. The number of measurements determines the shape of the cost function J (e.g., how many local minima in J). A good initial guess of λ_0 ensures that Eq. 3-18 converges to λ_0 if the model is accurate.

3-8 Concluding Remarks

In this chapter, wavelength has been estimated with a single tunable color filter and a single photodiode. The Neural Network and the NonLinear Least Squares optimisation algorithms are used to estimate the unknown wavelength of an incoming light.

The Neural Network provides a good estimation of the unknown wavelength but it is observed that the NN approach provides excellent approximation when the data presented to the trained network is statistically similar to that which formed the dataset used to trained the neurons.

This implies that the network generalizes by interpolating within the range of the input data and as such the network is not expected to give reliable results if substantially novel input data are used. When a validation data set measured three days later was used to validate the trained network, the result shows a clear decline in the performance of the model.

Processing the modelling and validation data set by normalizing the data however, improves the accuracy of the estimation of the unknown wavelength with noticeable improvement in the Variance-Accounted-For as depicted in tables 3.1-3.4. The nonlinear parameter estimation problem is tackled by minimising a cost function based on the sum of squares. An optimisation technique called Levenberg Marquardt is used for minimising the cost function. The validation results shows that it is possible to obtain a good model which predicts the unknown wavelength with good accuracy.

From the result obtained, it is clear that the estimation accuracy improves with the number of measurements and a good initial guess of the wavelength λ. When an initial guess chosen by human intervention was used, it was observed that the accuracy of the estimation of the

unknown wavelength can not be predicted. For example an initial guess of 625 nm provides a good estimate of the unknown wavelength and an initial guess of 620 nm provides a bad estimate of the unknown wavelength as depicted in the table. Hence the use of an educated guess provides a better estimation of the unknown wavelength.

Now that the system has been calibrated and the wavelength estimation algorithms have been tested, in the next chapter we predict the performance of our proposed wavelength estimation algorithms when a temperature drift is introduced into the system.

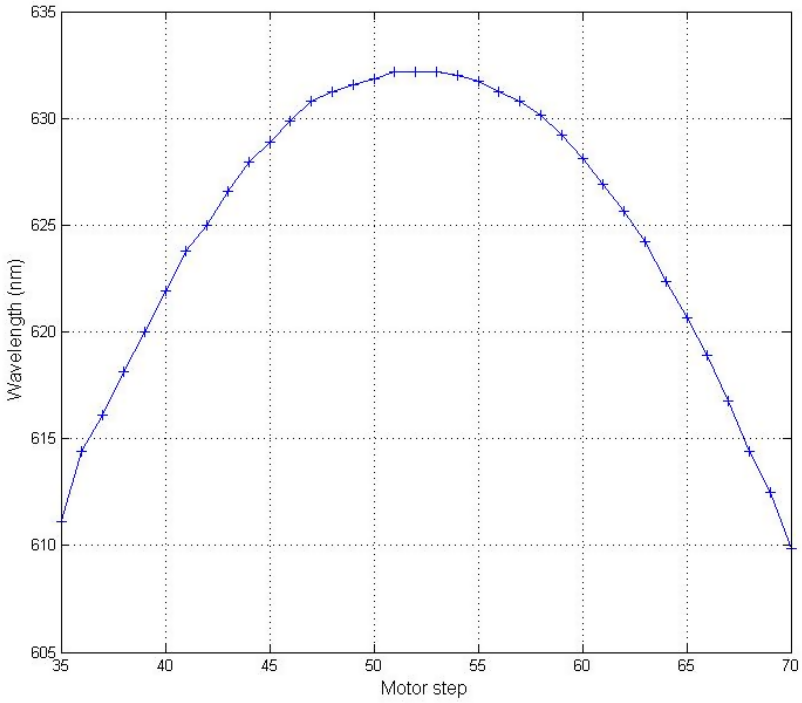

Figure 3-1: Figure showing the plot of wavelength obtained by tuning the tunable color filter,the color filter is mounted on a stepper motor which provides the control input signal θ thus generating a total of 18 wavelengths when the angle is displaced from normal angle. Maximum wavelength obtained is 632.3nm and the minimum is 609.3nm. For our application, 15 wavelengths were selected and the rest discarded. Although this does not proffer a very accurate tunable light source for the calibration of our system, it however gives an opportunity to develop a proof of concept in the DSCS Optics Lab.

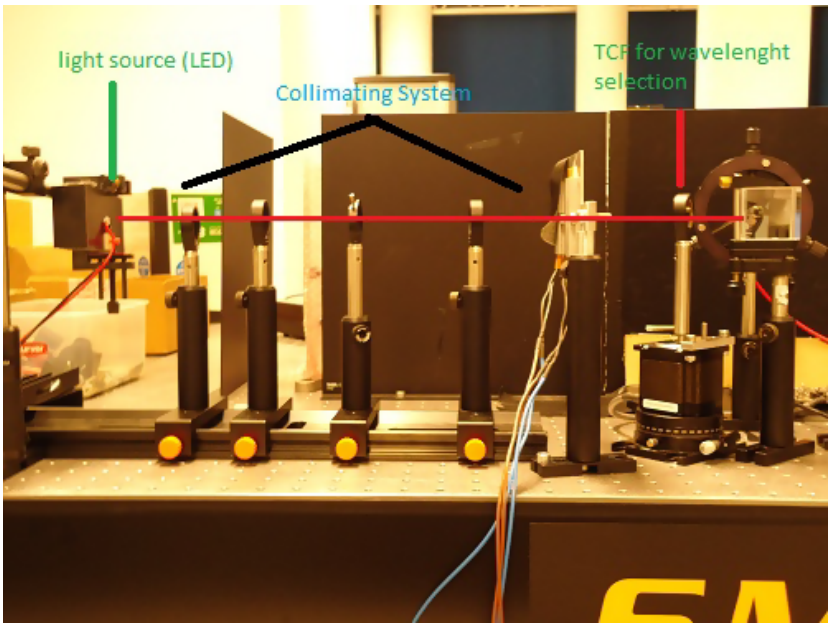

Figure 3-2: Figure showing the system set-up comprising of the tunable light source

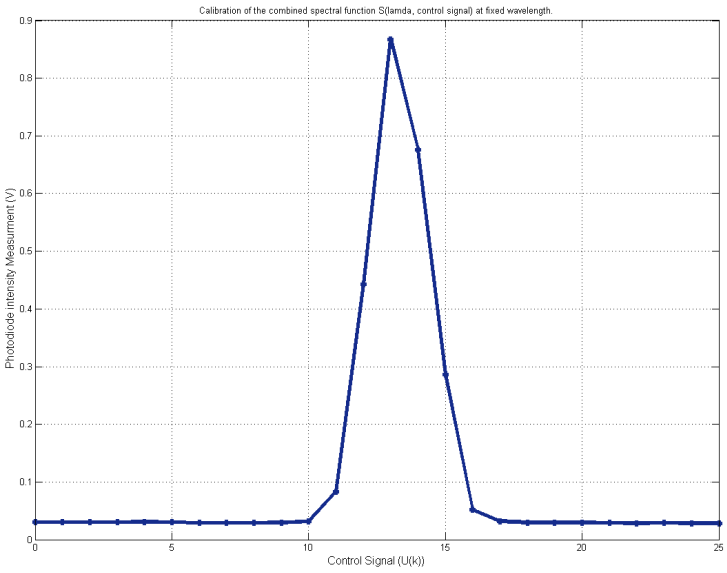

Figure 3-3: Spectra curve $f(\lambda, v)$ for different motor angle u at fixed wavelength λ. 1 angle step is approximately equal to 1 degree. Intensity varies from 0 (all blocked),to maximum;

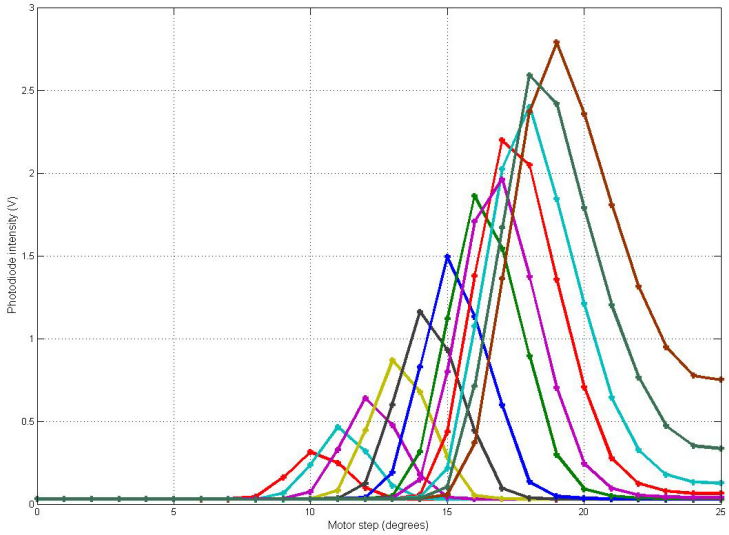

Figure 3-4: Spectra curve $f(\lambda, u)$ for different motor angle u at varying wavelength λ.

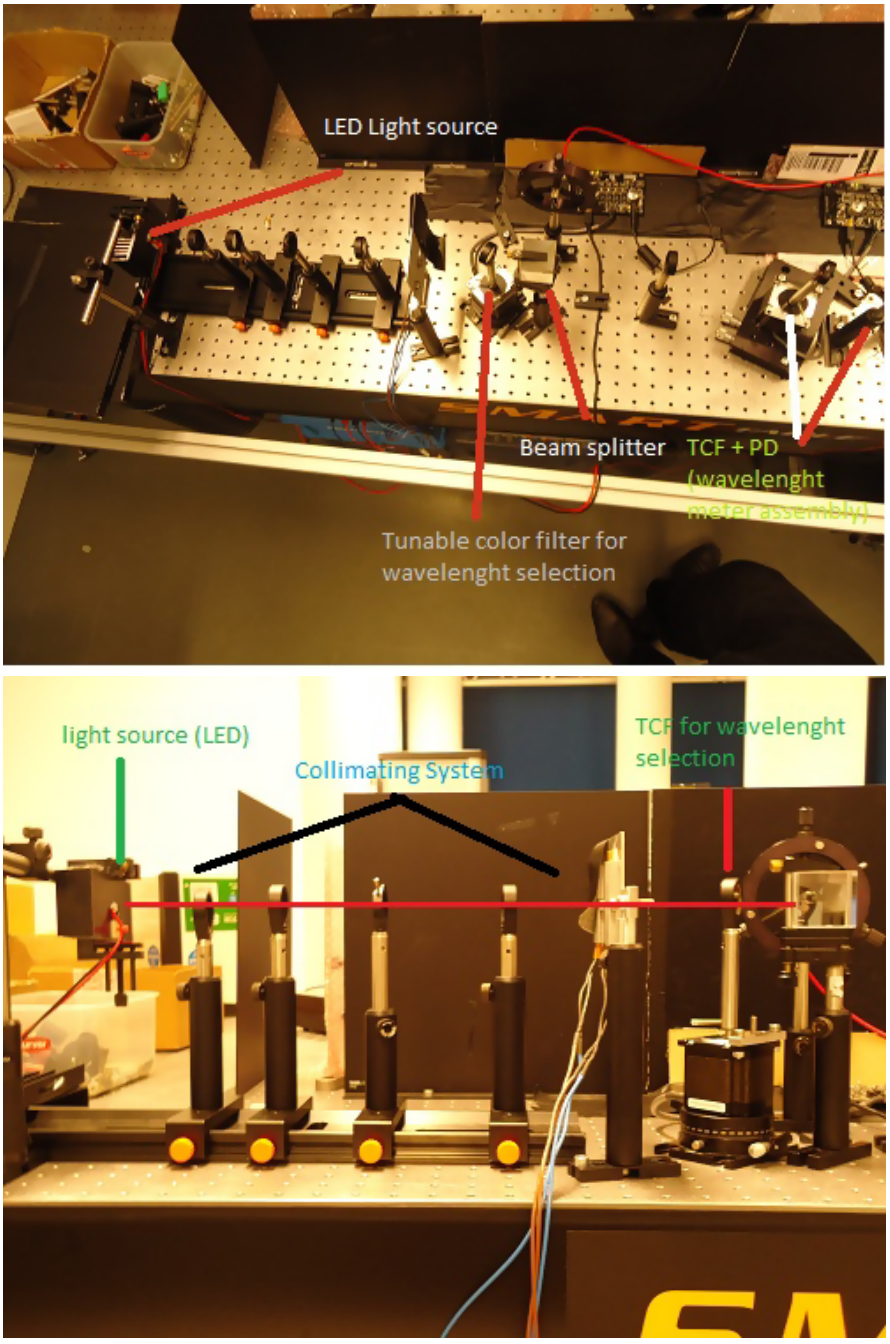

Figure 3-5: Top: Figure showing the system set-up comprising of the tunable light source and the wavelength meter on the optical bench in the DSCS Lab; bottom: Figure showing the system set-up comprising of the tunable light source.

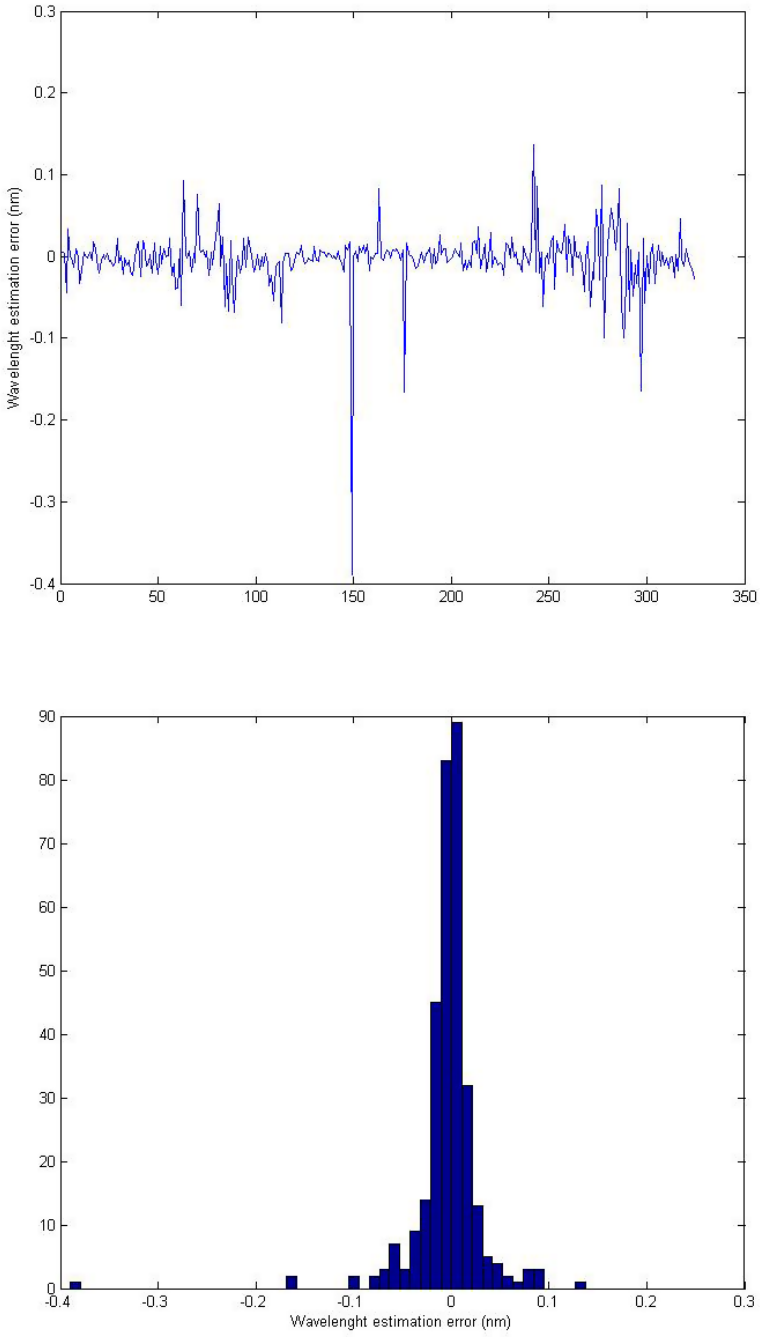

Figure 3-6: Top: the plot of wavelength estimation error in the modeling data set; bottom: histogram of the wavelength estimation error in the modeling data set.

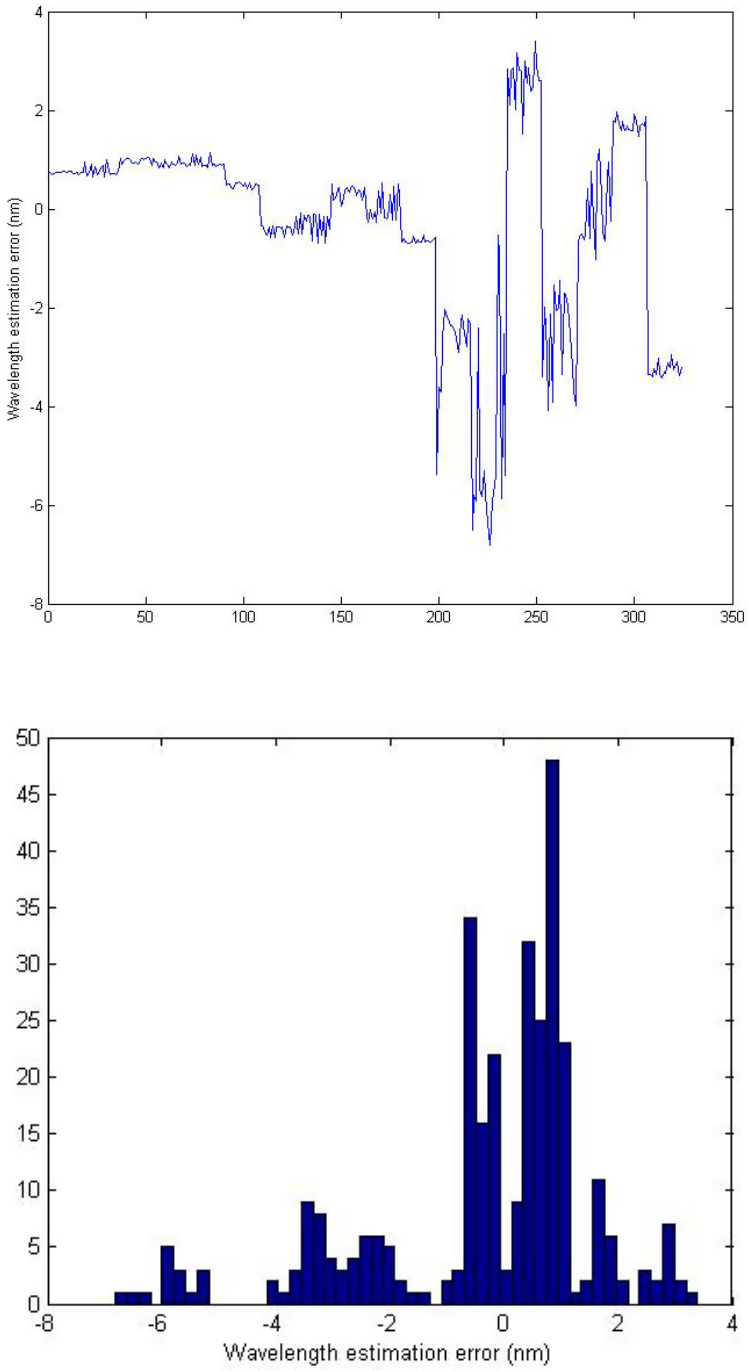

Figure 3-7: Top: the plot of wavelength estimation error using the data set B generated 72 hours later; bottom: histogram of the wavelength estimation error in the data set B.

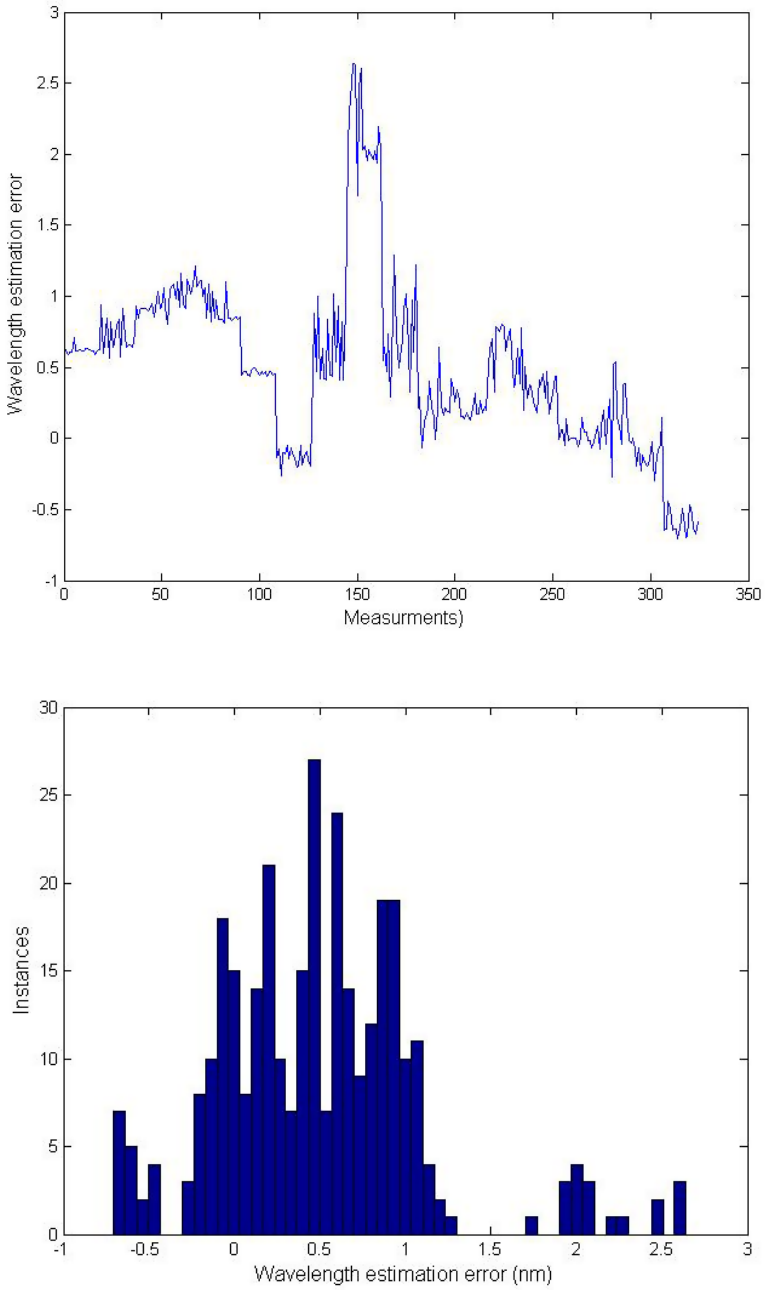

Figure 3-8: Top: the plot of wavelength estimation error using the normalised data set B generated 72 hours later; bottom: histogram of the wavelength estimation error in the normalised data set B.

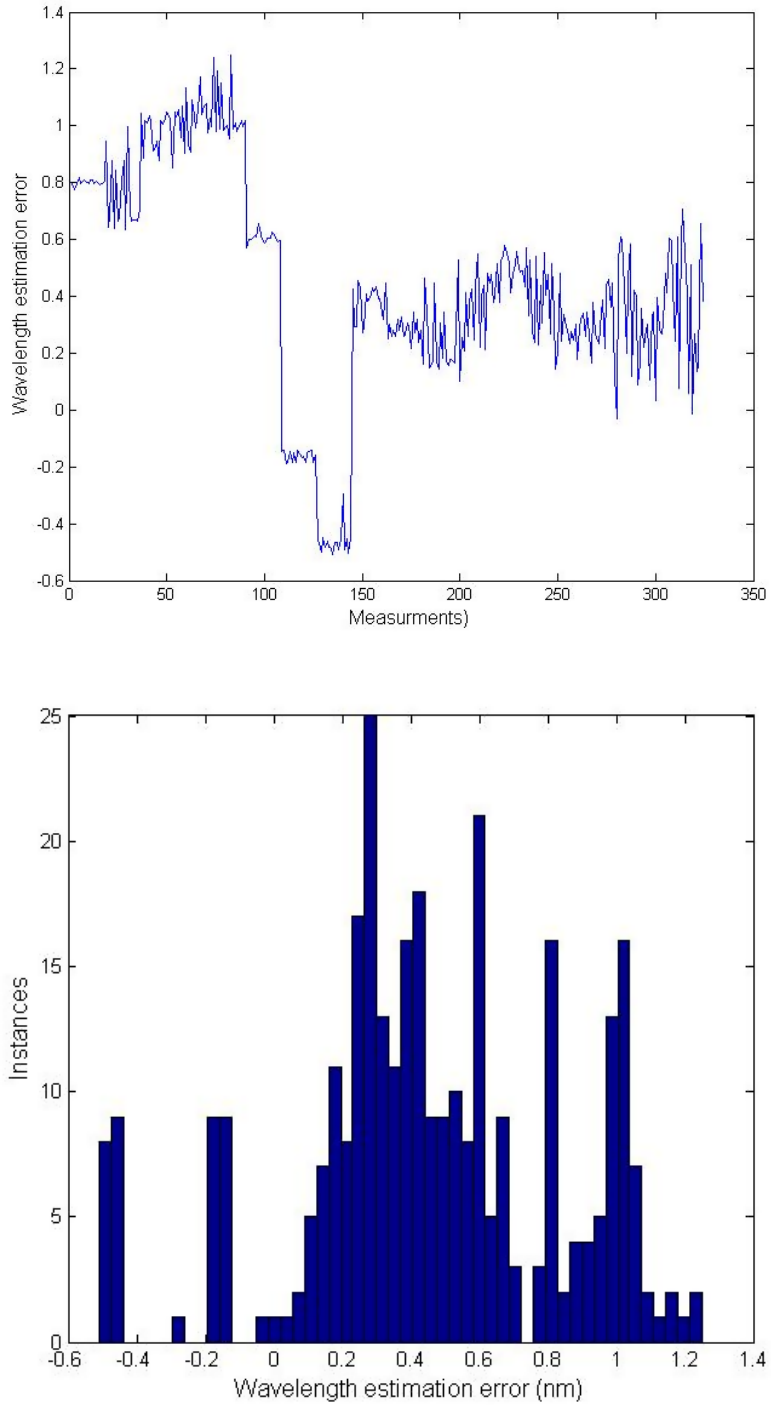

Figure 3-9: Top: the plot of wavelength estimation error using the normalised data set B recorded 72 hours later; bottom: histogram of the wavelength estimation error in the normalised data set B. Hybrid solution (NN+NLLS)is used to estimate unknown wavelength

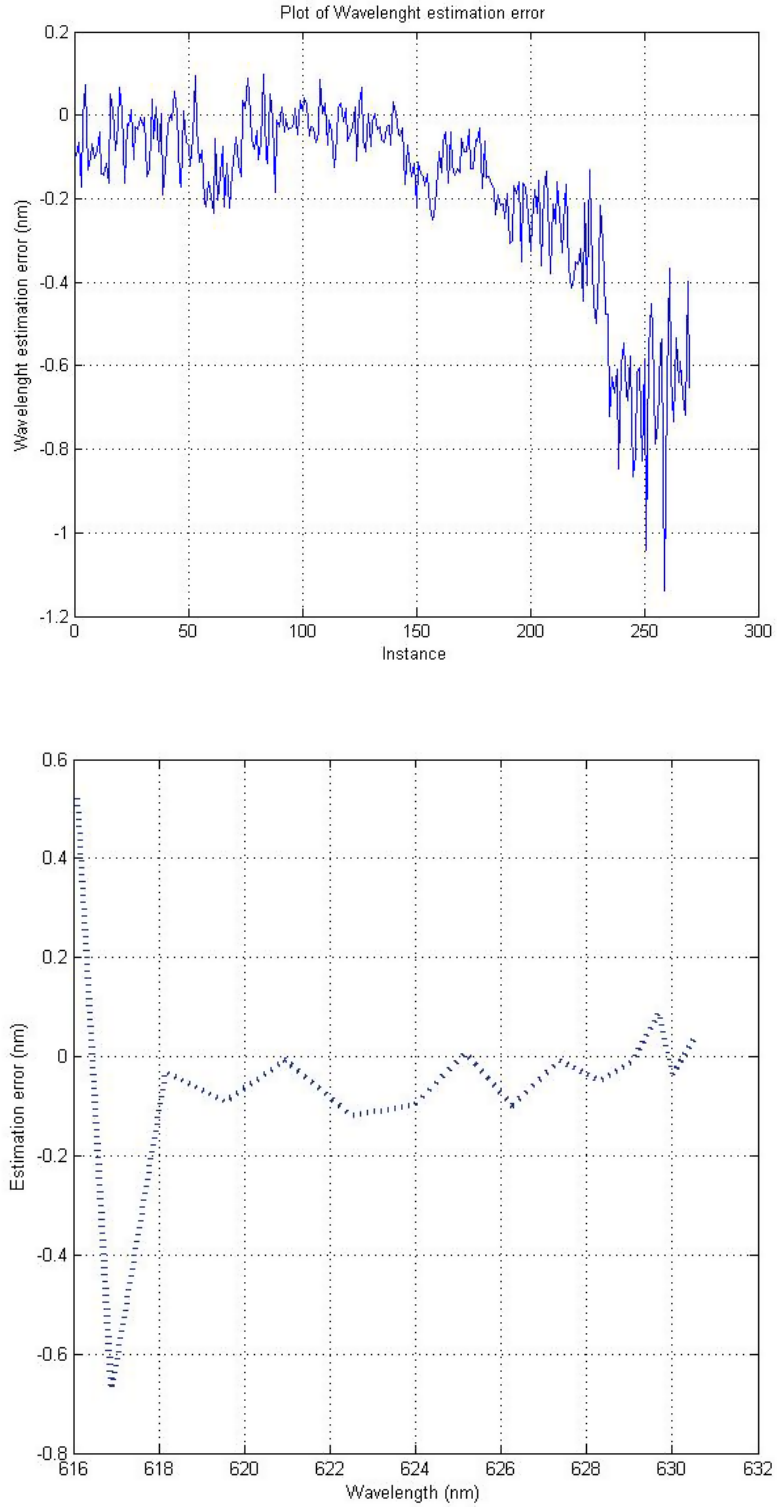

Figure 3-10: Top: the plot of wavelength estimation error using data set D ; bottom: the plot of the wavelength estimation error as plotted against wavelength.Neural Network trained with data set C and validated with data set D

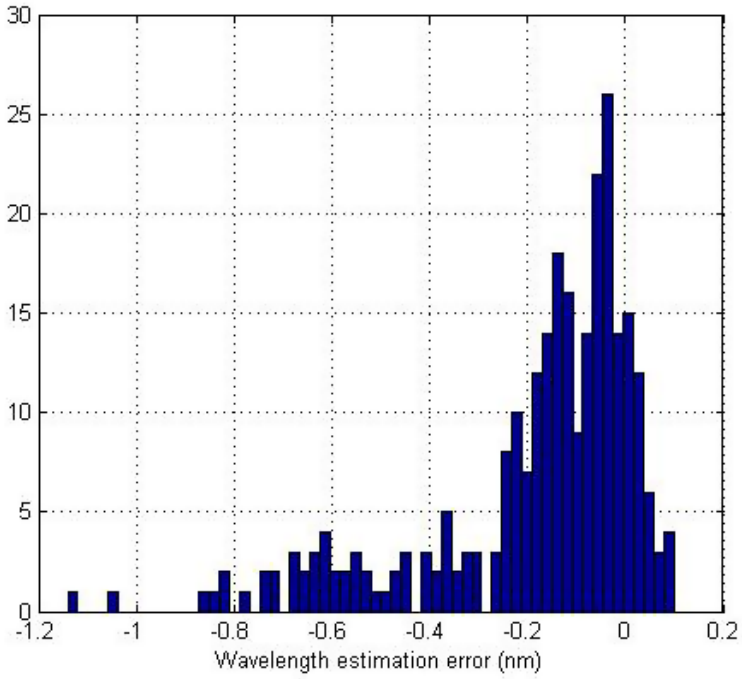

Figure 3-11: Top: the histogram of wavelength estimation error using data set D.

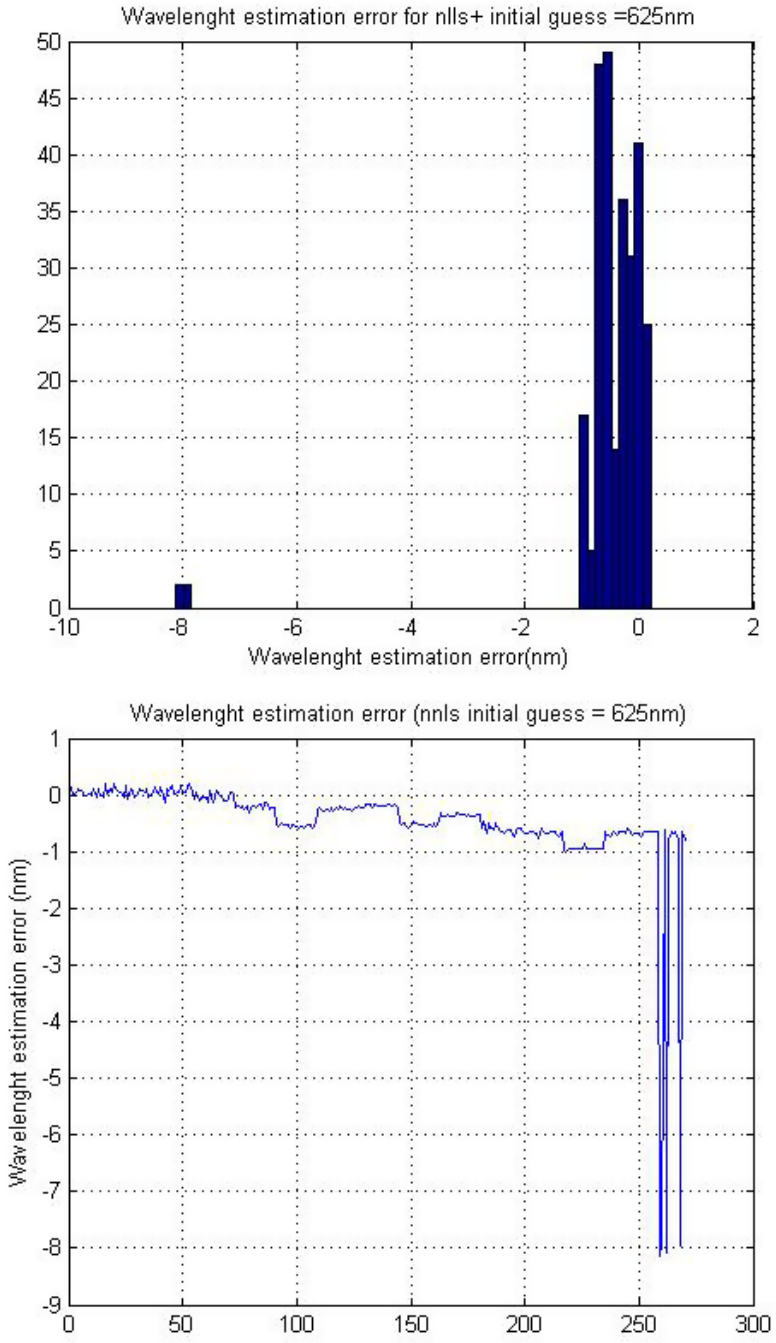

Figure 3-12: Top: the plot of wavelength estimation error using data set D ; bottom: the plot of the wavelength estimation error when an initial guess of 625nm is used for the wavelength estimation algorithm. Nonlinear least squares algorithm used to estimate unknown wavelength in data D at an intial guess of 625 nm

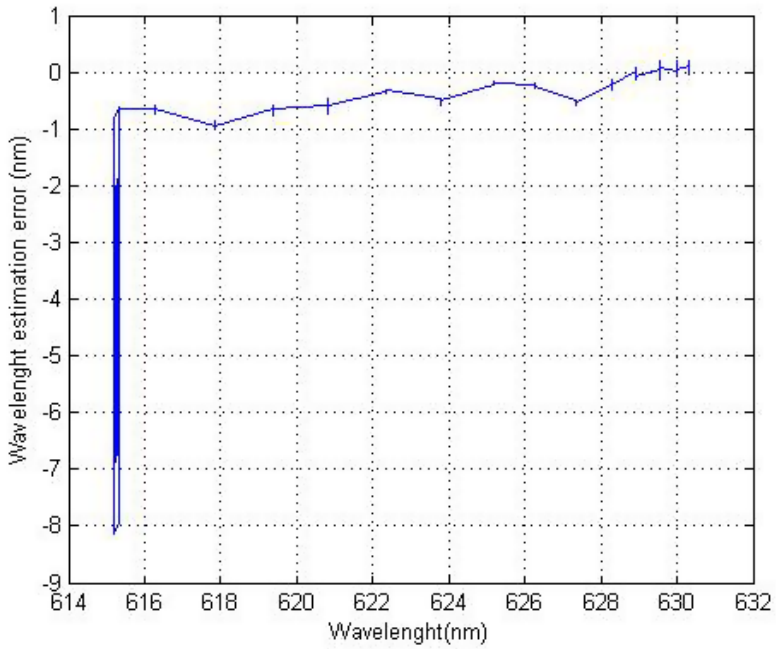

Figure 3-13: Top: the histogram of wavelength estimation error plotted against wavelength.

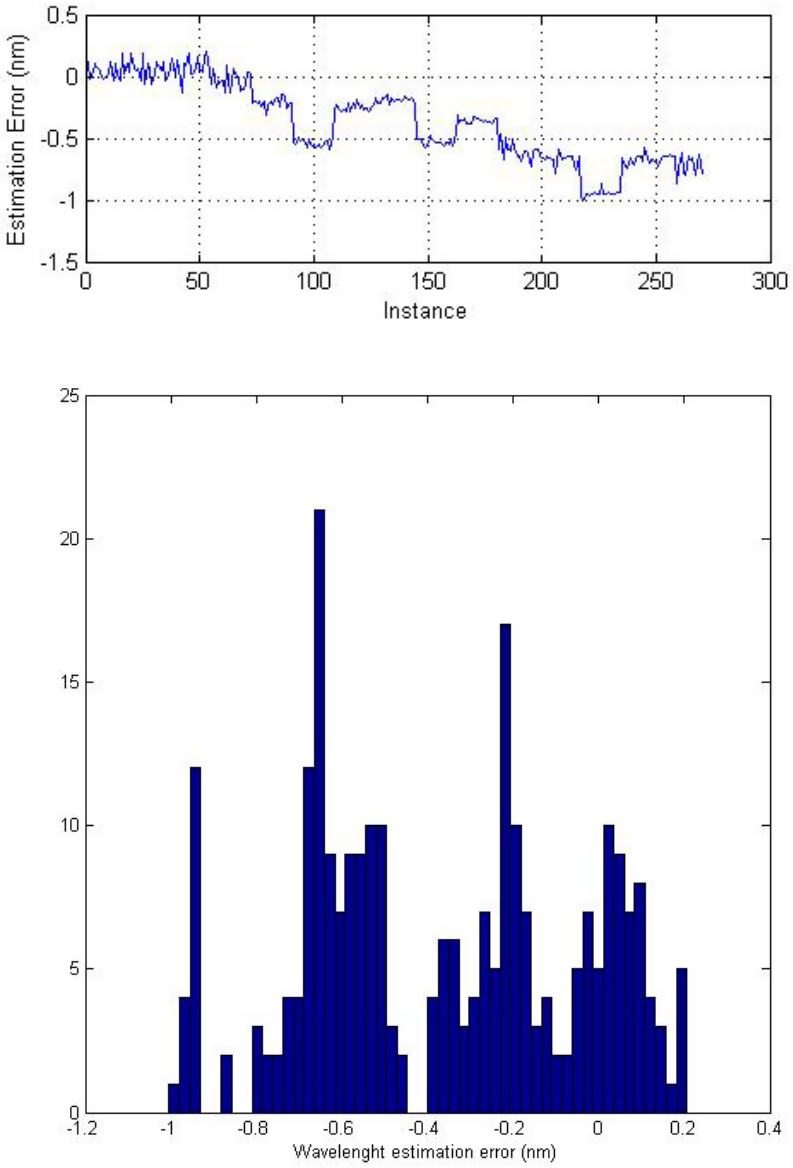

Figure 3-14: Top: the plot of wavelength estimation error using data set D ; bottom: the plot of the wavelength estimation error when NN is used to predict the initial guess needed to deduce the optimal wavelength. Using the Hybrid algorithm to estimate unknown wavelength in Data D

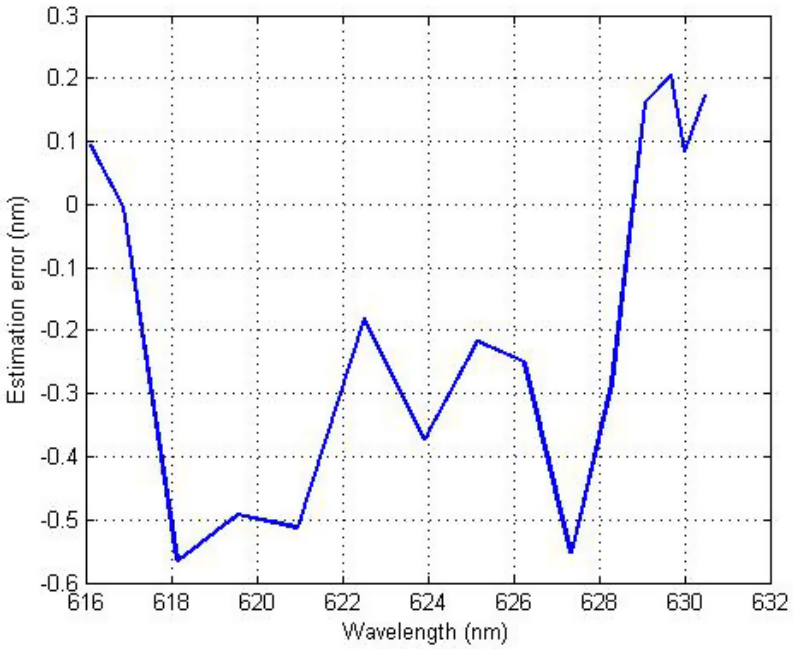

Figure 3-15: The wavelength estimation error plotted wavelength.

Chapter 4

Temperature Drift

4-1 Bandpass Filter Performance

Water, temperature, and other environmental conditions can affect the performance of Tunable Color Filters. The actual coating processes have a definite influence on the details of the interaction between the coating performance and the environment to which the filter is exposed .

The transmission characteristics of the bandpass filter is altered as the coating absorbs moisture. If the filter is subsequently dried either by heating in a warm oven or by leaving it in a dry box for a longer period of time, the performance shifts back toward the preexposure values [33].

Of particular interest to our application is the temperature response of a bandpass filter since temperature change provides the fastest alteration in the transmission characteristics of the bandpass filter.

The following subsection provides an overview on the impact of Temperature on the performance of the bandpass filter.

4-1-1 Impact of Temperature on the performance of Bandpass filter

Temperature can affect the performance of bandpass filters because both the index of refraction and the thickness vary as a function of temperature. The center of a narrow wavelength structure may shift by a large fraction of its width owing to changes in the optical thickness of the layers in the coating.

The optical thickness of each layer varies with temperature as a result of

1. The change in the refractive index induced by the temperature $\frac{dnl}{dT}$.
2. The linear coefficient of expansion $\frac{dl}{dT}$ which affects the physical thickness.

As the temperature of the bandpass filter increases, the refractive index become smaller and on the other hand, the expansion coefficients increases which leads to a corresponding increase in the path length. $\frac{dnl}{dT}$ becomes negative while $\frac{dll}{dT}$ is positive [33]. Thus, the change in optical thickness change with temperature. The result is that for most materials, the performance of a filter shifts to longer wavelengths as the temperature is increased. This implies that the transmission characteristics of the bandpass filter is altered when the temperature is considerably increased beyond the normal room temperature.

Introducing the Temperature Drift to the Bandpass filter

To measure the performance of our wavelength estimation algorithm, a temperature drift was intentionally introduced to the filter performance in the following procedure.

1. A small aluminium housing was designed just big enough to contain the bandpass filter. The size of the aluminium housing is chosen to be very small so that the movement of airflow in the aluminium box can be significantly reduced. The incoming light is allowed to pass through the aluminum to the bandpass filter and to exit the aluminum box to the photodiode through a small hole on the aluminium box. The filter was inserted into the aluminum box which also allows the free rotation of the bandpass filter mounted on the stepper motor.

2. A heating blower (Temperature range of 50 degrees to 660 degrees) was used to heat the aluminum box to specific temperature of choice. Three temperatures selected were 50 degrees, 70 degrees and 90 degrees. The temperature measurement is as an approximate of the desired values as the heat was manually applied.

3. A thermocouple was inserted into the aluminum box and attached to the metallic ring of the bandpass filter without making contact with the surface. The thermocouple measures the temperature of the air in the aluminium box and since the air flow in the box is restricted, the temperature of the air in the box is the temperature on the surface of the bandpass filter inserted into the aluminium box.

4. The thermocouple is connected to a voltmeter and the temperature measured in the box is read from a voltmeter connected to the thermocouple.

Overview on Thermocouple

A thermocouple is a sensor for measuring temperature, that consists of two dissimilar metals that are joined together at the sensing end. Thermocouple indicate temperature by providing a very small voltage signal generated by a junction of dissimilar metals [32].

Thermocouple work because heat creates a thermoelectric voltage in a wire. This is the Seebeck effect. Anywhere there is a temperature gradient, there will be a voltage because electrons want to flow from hot to cold. The voltage value per degree temperature difference is the Seebeck coefficient and depends on the characteristics of the specific wire alloy. Bringing both ends of the wire to a voltmeter gives the temperature desired temperature reading [32].

4-2 Experimental details

To see the performance of our wavelength estimation algorithm when a temperature drift is introduced, intensity measurements of an incoming light source with unknown wavelength were recorded. The unknown wavelength was estimated using the Nonlinear Least square Algorithm and the Neural Network Algorithm and the wavelength estimation error, the Variance-Accounted-For and the absolute error were estimated. The performance measures provides useful insight to the performance of our designed system when a temperature drift occurs. The following subsections describes the results of these experiments.

4-2-1 Function $\hat{F}(\lambda, U)_{RT}$ with Validation dataset generated at high temperature.

The function calibrated at room temperature was used to estimate the unknown wavelength from a set of data generated at high temperature. This is mathematically described in equation 4-1 below:

$$\|Y_{HT} - \hat{F}(\lambda, U)_{RT}\|_2^2 \tag{4-1}$$

Y_{HT} is the intensity measured at high temperature and the function was calibrated with dataset (intensity) recorded at room temperature. Data set E is the intensity measurement which was recorded at varying wavelength λ under increased temperature of 50 degrees, 70 degrees and 90 degrees. While the transmission data point in data set A is recorded for the power of the light source set at a constant value, the temperature was increased . For data set E, the control signal is designed such that 30 intensity measurements are taken at each wavelength and at specific temperatures set of intensity measurement $Y = y_{(1:1:30)}$ is measured given a set of control signal $U = u_{(\theta_1:1:\theta_{30})}$ thus giving rise to 30 angles which implies that $N_{angles} = 30$ at specified temperature.

$$\begin{bmatrix} Y_1 \\ Y_2 \\ \vdots \\ \vdots \\ \vdots \\ Y_3 \end{bmatrix} = \begin{bmatrix} F(\lambda_1, V) \\ F(\lambda_2, V) \\ \\ \vdots \\ \vdots \\ F(\lambda_{15}, V) \\ \\ \end{bmatrix} \tag{4-2}$$

The data set E measured when the temperature was increased, was used to validate our model and the details of Dataset E is summarized in table 4.1 below.

The above validation data set were processed (normalized) to validate the performance of our estimation algorithm.

The Nonlinear least square algorithm with calibration data and its initial guess estimated with Neural Networks trained with dataset recorded at room temperature and the Neural Network which was trained with data set measured at room temperature were used to estimate the unknown wavelength of the validation dataset E. The result of the performance of the wavelength estimation algorithm is compared and tabulated in the following tables.

Table 4-1: Dataset measured at various temperatures drift.

Dataset	No.Angles	No.Wavelength	No.Duplicates	Intensity Val.	Temp (deg)
DS E	30	15	3	1620	50
DS F	30	15	3	1620	70
DS G	30	15	3	1620	90

Table 4-2: Results of the estimation algorithm at Temperature 50 degrees with the photodiode offset (dark current) removed.

Algorithm	VAF	Absolute error
Hybrid (NN+NLLS)	99.7009	0.2065 nm
Neural Network	93.046	1.1648 nm

Table 4-3: Results of the estimation algorithm at Temperature 70 degrees with the photodiode offset (dark current) removed.

Algorithm	VAF	Absolute error
Hybrid (NN+NLLS)	99.6878	0.2482 nm
Neural Network	90.168	1.1639 nm

Table 4-4: Results of the estimation algorithm at Temperature 70 degrees with the photodiode offset (dark current) removed.

Algorithm	VAF	Absolute error
Hybrid(NN+NLLS)	99.7952	0.3499 nm
Neural Network	89.8516	1.2425 nm

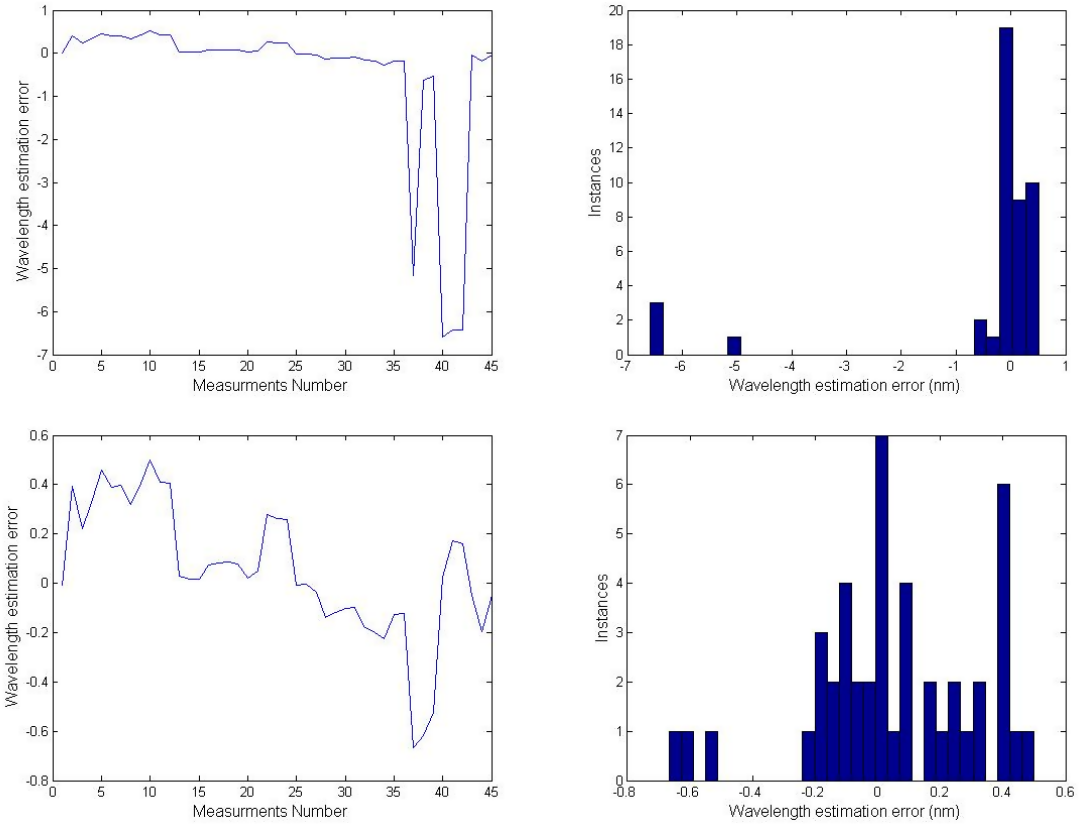

Figure 4-1: Wavelength estimation error and the corresponding histogram at Filter temperature of 50 degrees (top left: Wavelength estimation error with offset), 2 (top right:Wavelength estimation error histogram with offset), 3 (bottom left:Wavelength estimation error with offset of the photodiode removed) and 4 (bottom right:Wavelength estimation error histogram with offset removed). Case 1 :The performance of the Non-linear least square algorithm is validated when temperature drift is introduced to the system.

4-2-2 Case Scenarios

To observe the impact of the temperature drift on the accuracy of the wavelength estimation, two case scenarios were tested.

Case 1

The first case scenario is represented by the equation below :

$$\|Y_{90} - \hat{F}(\lambda, U)_{RT}\|_2^2 \tag{4-3}$$

The validation dataset was recorded at 90 degrees and the algorithms calibrated and trained with data set recorded at Room Temperature are used for wavelength estimation. The result is presented in table 4-8:

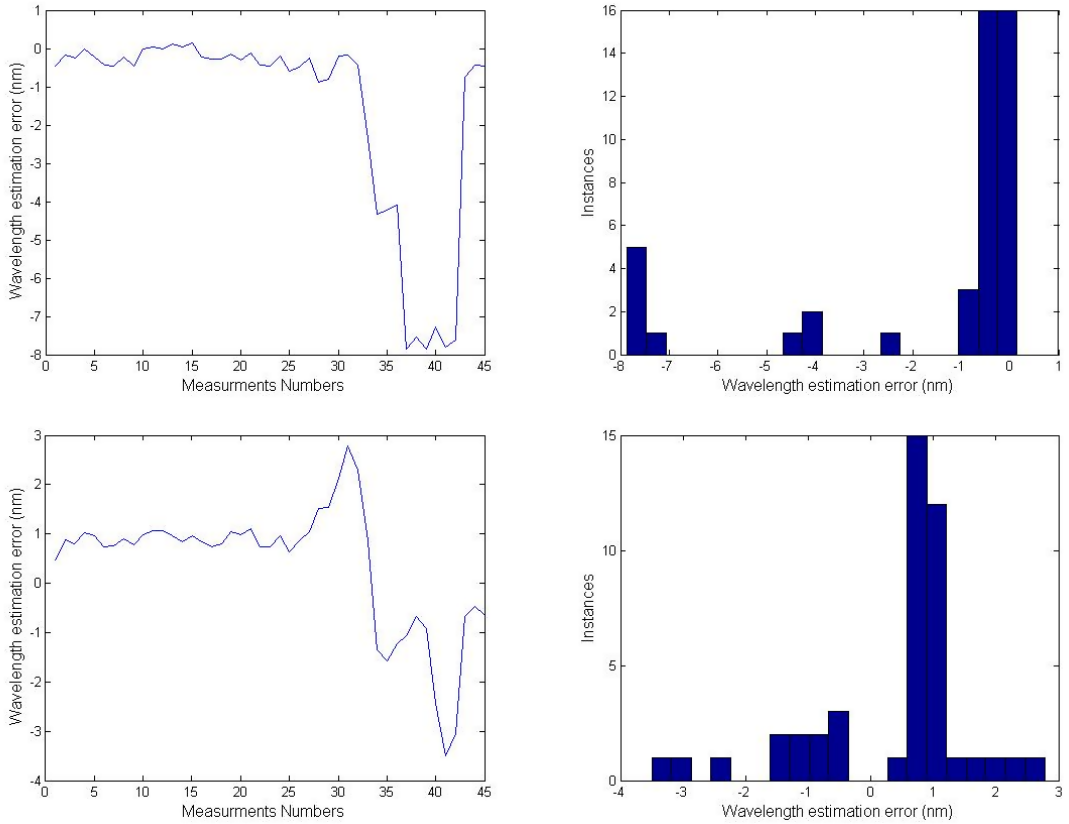

Figure 4-2: Wavelength estimation error and the corresponding histogram at Filter temperature of 50 degrees (top left: Wavelength estimation error with offset), 2 (top right:Wavelength estimation error histogram with offset), 3 (bottom left:Wavelength estimation error with offset of the photodiode removed) and 4 (bottom right:Wavelength estimation error histogram with offset removed). Case 1 :The performance of the Neural Network algorithm is validated when temperature drift is introduced to the system.

Case 2

The second case scenario is represented by equation 4-4 :

$$\|Y_{90-degrees} - \hat{F}(\lambda, U)_{90-degrees}\|_2^2 \tag{4-4}$$

The validation dataset was generated at 90 degrees and the calibration of our model was done with dataset generated at 90 degrees also. The unknown wavelength is estimated from the generated validation dataset at high temperature using the calibrated function $\hat{F}(\lambda, U)_{90-degrees}$.

The result is presented in table 4.8 and table 4.9.

The estimated wavelength is compared with the calibrated wavelength at various temperature and the plot is shown in figure 4-7 and 4-8.

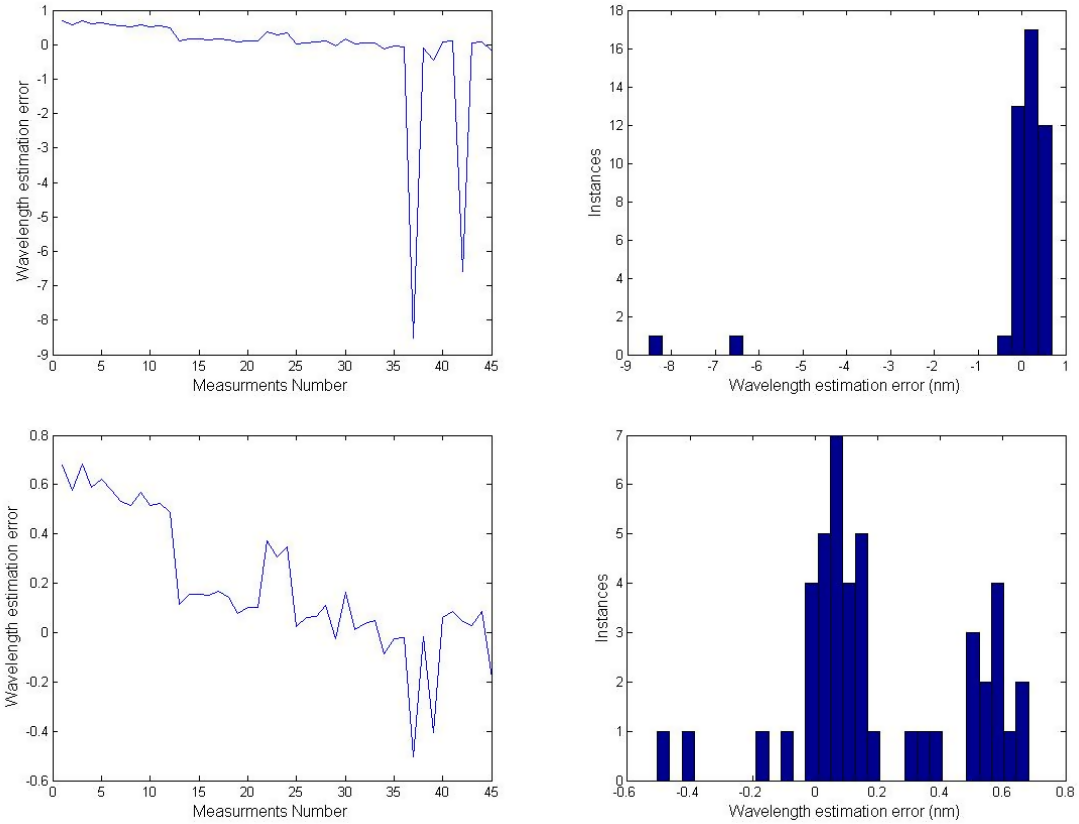

Figure 4-3: Wavelength estimation error and the corresponding histogram at Filter temperature of 70 degrees (top left: Wavelength estimation error with offset), 2 (top right:Wavelength estimation error histogram with offset), 3 (bottom left:Wavelength estimation error with offset of the photodiode removed) and 4 (bottom right:Wavelength estimation error histogram with offset removed). Case 1 :The performance of the Non-linear least square algorithm is validated when temperature drift is introduced to the system.

4-3 Concluding Remarks

In this chapter we have shown that the Hybrid approach (Nonlinear Least Square + Neural Network), provides a good estimate of an unknown wavelength despite the intense temperature drift introduced into the component of the measurement system.

The performance measures (VAF), shows that the Neural Network approach performs quite badly when a temperature drift is introduced into the system because the Neural Network is similar to the look-up table approach and its performance is enhanced when validation data set statistically similar to the training data set are used to validate the trained network.

The noise sources that influences the performance of our wavelength estimation algorithm includes the dark current and read out noise of the photodiode. The dark current and the read out noise which influences the photodiode was compensated for by calibrating the photodiode before every measurement. The offset (i.e the output voltage of the photodiode measured when no light is incident on it) is therefore deducted from the intensity measurement used for

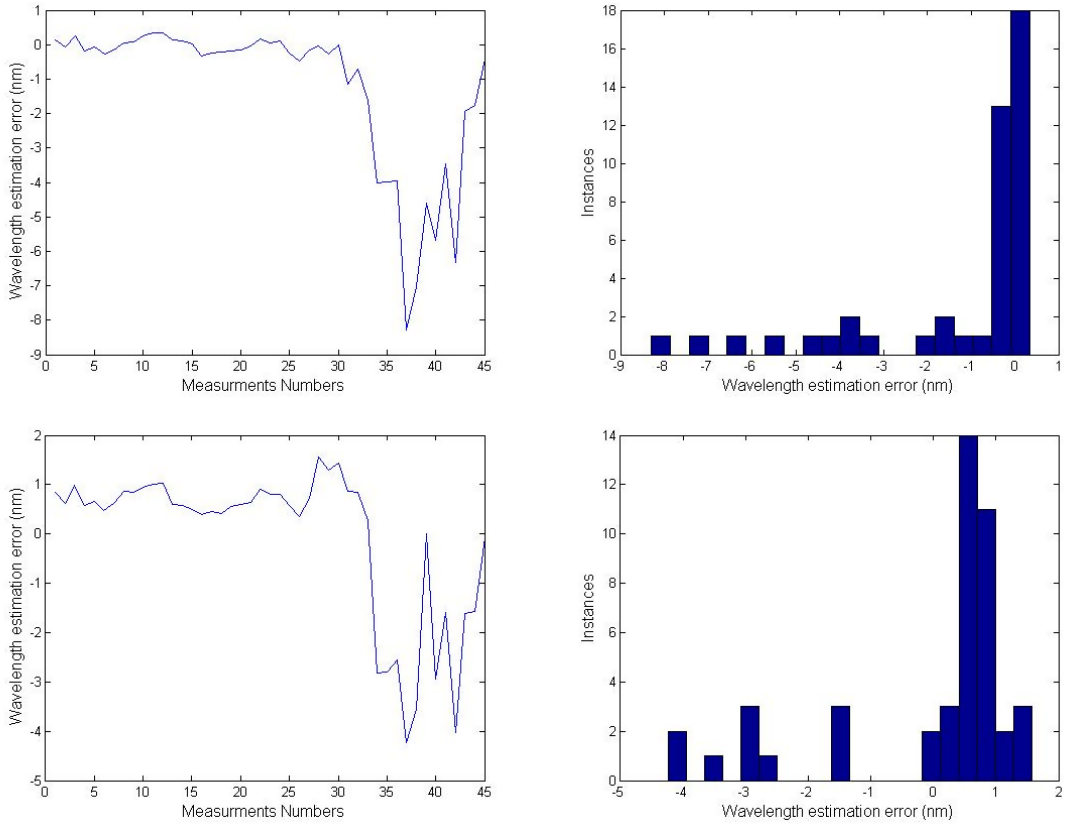

Figure 4-4: Wavelength estimation error and the corresponding histogram at Filter temperature of 70 degrees (top left: Wavelength estimation error with offset), 2 (top right:Wavelength estimation error histogram with offset), 3 (bottom left:Wavelength estimation error with offset of the photodiode removed) and 4 (bottom right:Wavelength estimation error histogram with offset removed). Case 1 :The performance of the Neural Network algorithm is validated when temperature drift is introduced to the system.

our estimation. The calibration of the photodiode a priori enables the realisation of a more accurate model which generally predicts the wavelength more accurately than when the dark current and read out noise is unaccounted for.

From the temperature drift experiment, it was observed that the spectral sensitivity curve of the Tunable Color Filter was altered at increased temperature. This constituted a drift in the performance of the TCF. The NLLS Algorithm provided a good estimate of the unknown wavelength at high temperature when the NLLS was calibrated with data recorded at room temperature. The performance of the NLLS Wavelength estimation algorithm is better improved when the calibration is done with data set generated at high temperature.

The Neural Network Algorithm did not give a good estimate of the wavelength because the data used to trained the network differs considerably from the data used for the validation.

Conclusively,the increased temperature of the filter caused a change in the refractive index of the filter and thus the filter transmission characteristics was altered However, this alteration is only observed at high temperature of 70 degrees and above. At such drift, the Nonlinear

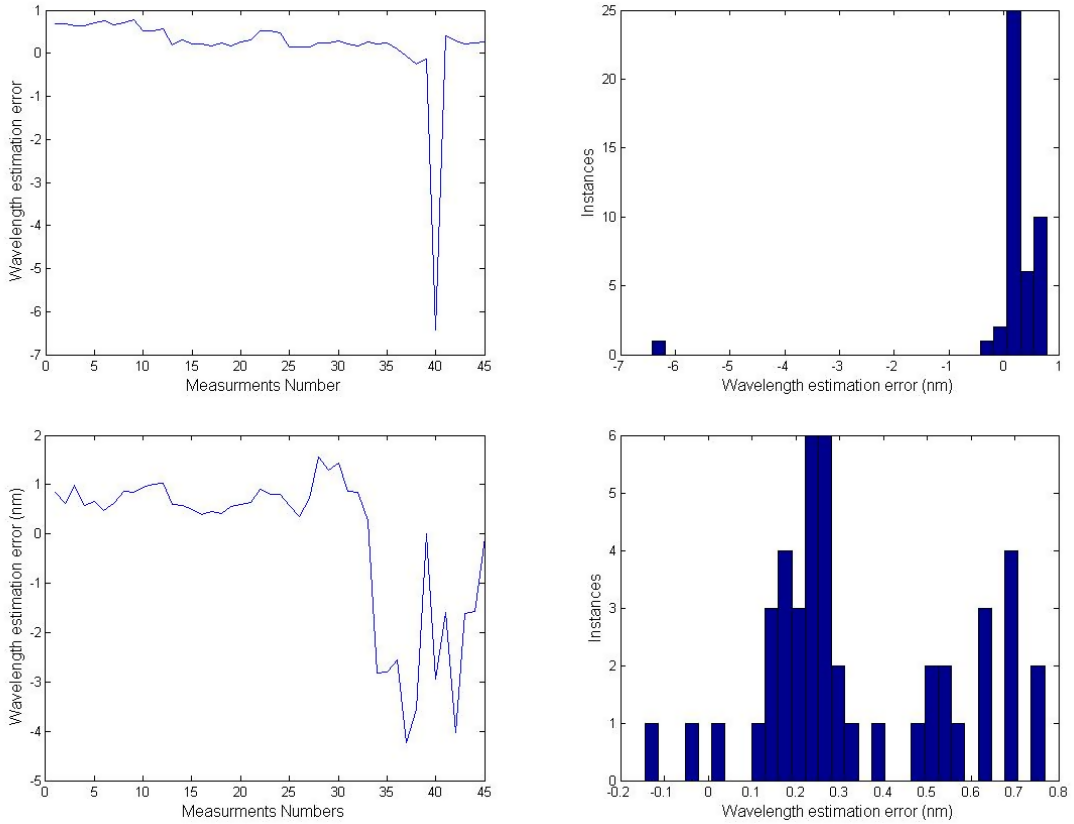

Figure 4-5: Wavelength estimation error and the corresponding histogram at Filter temperature of 90 degrees (top left: Wavelength estimation error with offset), 2 (top right:Wavelength estimation error histogram with offset), 3 (bottom left:Wavelength estimation error with offset of the photodiode removed) and 4 (bottom right:Wavelength estimation error histogram with offset removed). Case 1 :The performance of the Non-linear least square algorithm is validated when temperature drift is introduced to the system.

Least square algorithm provides a good estimate of the unknown wavelength of an incoming light source with good accuracy.

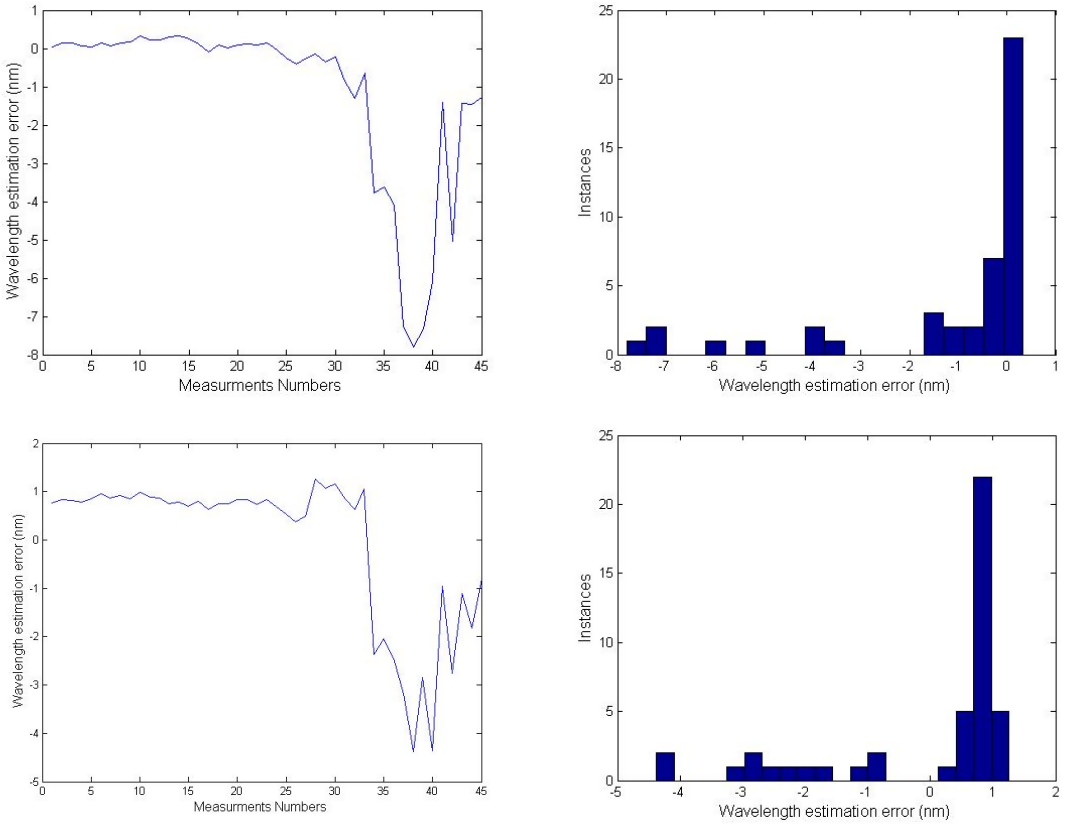

Figure 4-6: Wavelength estimation error and the corresponding histogram at Filter temperature of 90 degrees (top left: Wavelength estimation error with offset), 2 (top right:Wavelength estimation error histogram with offset), 3 (bottom left:Wavelength estimation error with offset of the photodiode removed) and 4 (bottom right:Wavelength estimation error histogram with offset removed). Case 1 :The performance of the Neural Network algorithm is validated when temperature drift is introduced to the system.

Table 4-5: Results of the estimation algorithm at Temperature 90 degrees.$\|Y_{90} - \hat{F}(\lambda, U)_{RT}\|_2^2$

Algorithm	VAF	Absolute error
Hybrid (NN+NLLS)	98.6770	0.4520 nm
Neural Network	93.7520	1.4862 nm

Table 4-6: Results of the estimation algorithm at Temperature 90 degrees.$\|Y_{90} - \hat{F}(\lambda, U)_{90}\|_2^2$

Algorithm	VAF	Absolute error
Hybrid (NN+NLLS)	99.9572	0.1285 nm
Neural Network	99.3244	0.3220 nm

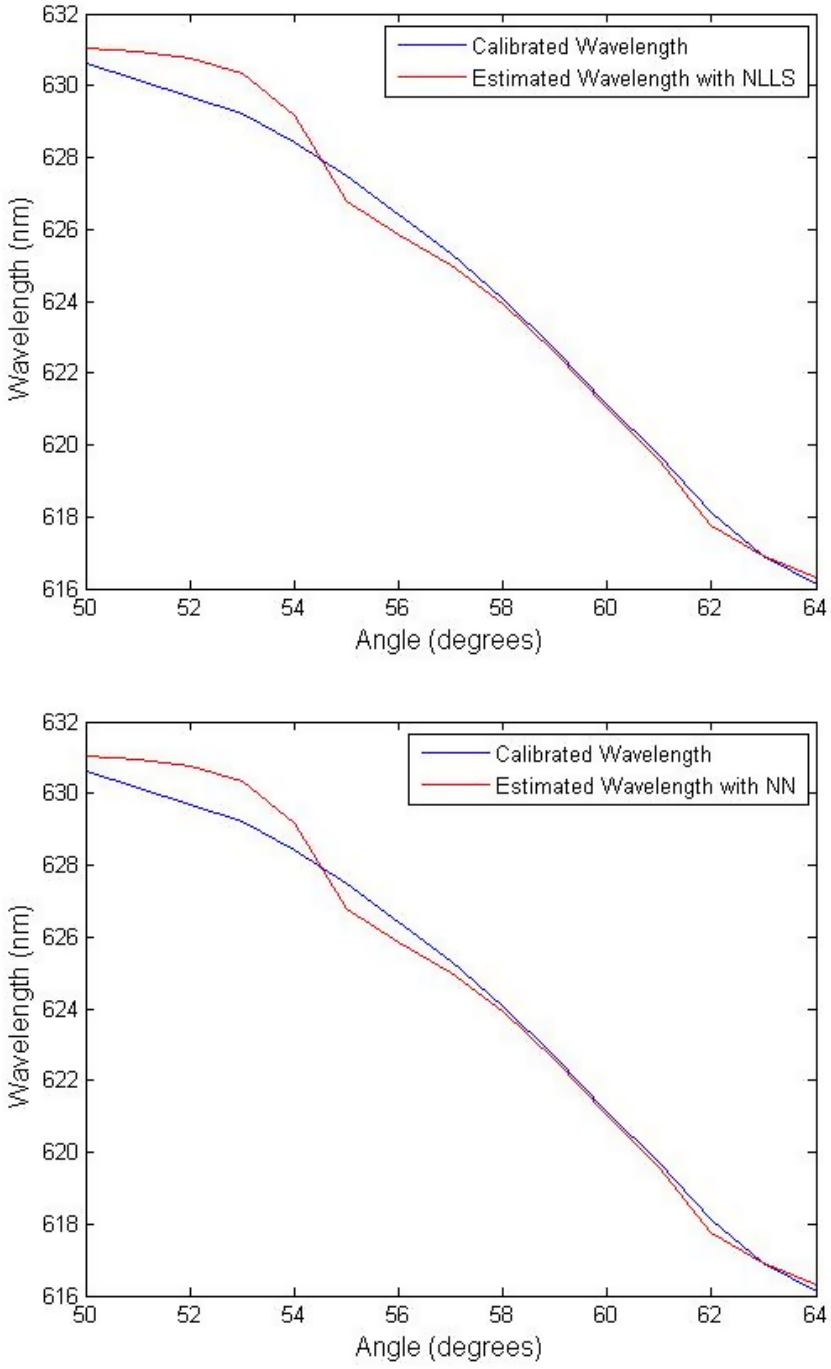

Figure 4-7: Plot of Estimated wavelength compared with the calibrated wavelength using the NNLS 3 (bottom :Plot of Estimated wavelength compared with calibrated wavelength using NN.)

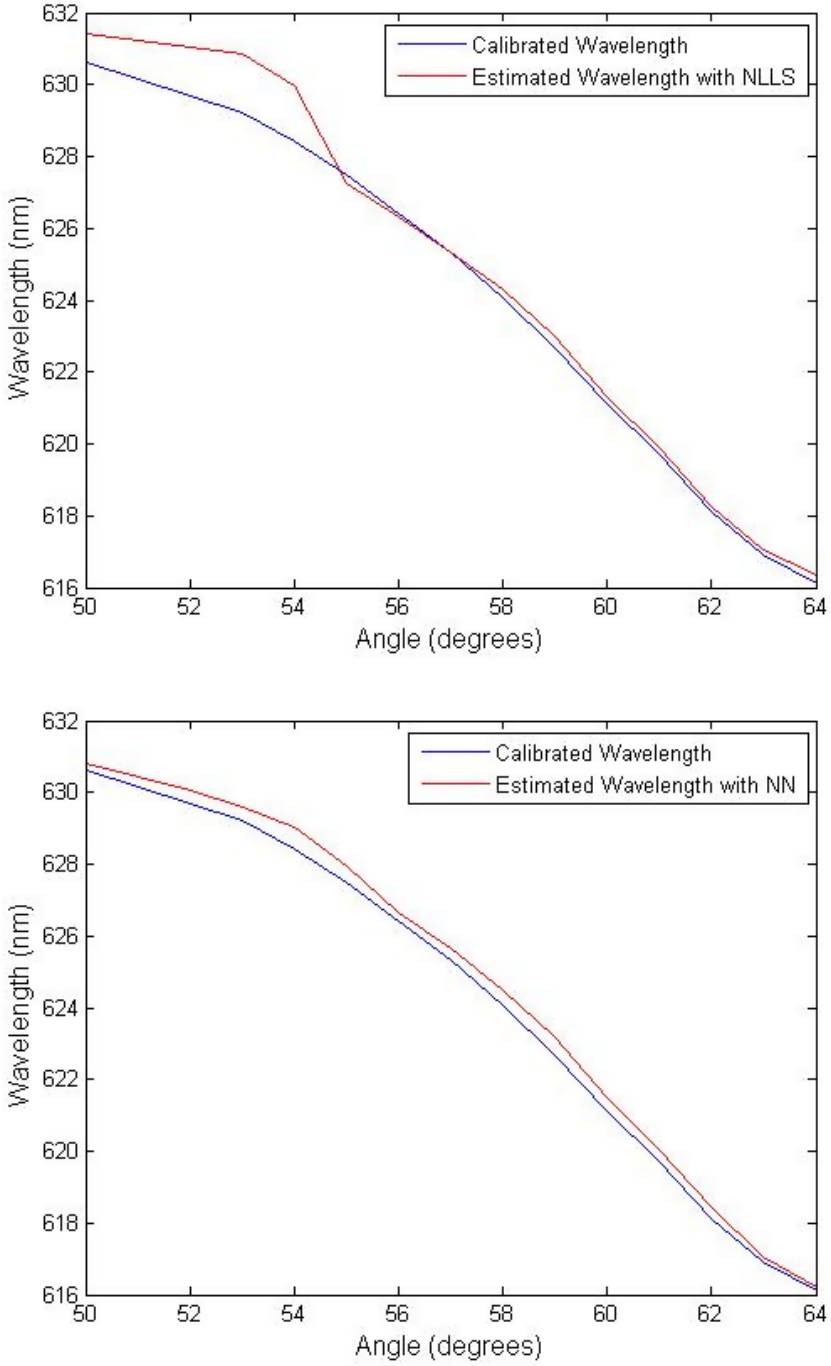

Figure 4-8: Plot of Estimated wavelength compared with the calibrated wavelength using the NNLS estimation algorithm (bottom :Plot of Estimated wavelength compared with calibrated wavelength using NN algorithm.)

Chapter 5

Conclusions

The development of cheap semiconductor laser in recent times is on the increase and therefore the need for a low-cost wavelength measurement device that will accurately measure the spectral purity of low-cost semiconductor laser is irreplaceable in this world of laser technological advancement.

Most of the Wavelength measurement device currently available measure the wavelength with high precision, resolution and accuracy but the the challenge is the trade off that arises as a result of the cost and performance of the device.

This thesis focuses on the design of a simple low-cost wavelength measurement device that estimate an unknown wavelength with an accuracy and resolution as good as the high cost spectrum analyser. It is also the focus of this thesis to ensure the simplicity of the integration of this device.

This thesis describes four necessary steps to realise this simple device : Problem formulation, Function Calibration, Data generation and Wavelength estimation. To estimate the wavelength of an incoming light source three algorithms are proposed : The Neural Network, The Non-Linear Least Square algorithm and the Hybrid (Nonlinear-Neural) algorithm.

The contribution of this thesis are summarised in section 5-0-1. Consequently, the answer to the research question below is given in section 5.2.

1. To what degree of resolution and accuracy does our proposed wavelength estimation algorithm estimates an unknown wavelength.

more detailed research objectives are :

1. Development of a model for the estimation of unknown wavelength.
2. Selecting an appropriate wavelength estimation algorithm that will provide a wavelength estimation with good accuracy.

3. Investigation of the model accuracy and accounting for the drifts that could cause inaccurate estimation. Selection of the most accurate model.

Finally this chapter ends with a recommendation for future research.

5-0-1 Thesis Contribution

Chapter 3

In chapter 3, an integral model of the complete system is developed using the Neural Network.

This technique allows the estimation of an unknown wavelength of an incoming light source . The Nonlinear least square algorithm and the Neural Network were the estimation algorithm used for wavelength estimation and the performance of the algorithms on validation data set were measured.

The Nonlinear least square algorithm provides good estimation of an unknown wavelength but the Neural Network's performance does not differ from the conventional look-up table approach. This chapter also provides a simple technique of improving the performance of the Nonlinear Least Square optimisation technique by incorporating an educative initial guess.

The proposed method is called the Hybrid method which is the combination of the NLLS and NN. This wavelength estimation technique provides a good estimation of the unknown wavelength than the single Nonlinear Least Square method.

Chapter 3 also provides a simple technique of data processing (data normalisation) which improves the accuracy of our model. A tunable light source was also designed and implemented and the details are described in chapter 3.

Chapter 4

In chapter 4, the performance of our wavelength estimation algorithm when presented with data generated at high temperature is investigated. A temperature drift was introduced by increasing the temperature of the Tunable color filter beyond 50 degrees.

The performance of our developed model was measured on a set of validation data set generated at such high temperatures.

We show that for the Nonlinear least square optimisation algorithm, we are able to reliably estimate the unknown wavelength even when the validation data set were measured at high temperature.

The Neural Network's performance to validation data set generated at high temperature is unreliable and does not provide a good estimate of the unknown wavelength.

5-1 Conclusions

In this thesis work, a control-based approach using a black-box model is used for wavelength estimation and the following conclusion can be drawn.

- The proposed method of wavelength estimation provides the possibility of having a simple high precision wavelength meter at low-cost. The technique used in realising this measurement devices enables its compactness and ease of optical integration.
- Estimating an unknown wavelength of an incoming light source requires three algorithms : While the single Non-linear least square algorithm provides a good estimate of the unknown wavelength based on the developed black-box model, the challenge however is the issue of convergence to the wrong solution if the initial guess of the wavelength λ is far from the true estimate.

  The NLLS approach to wavelength estimation provides a good estimate of an unknown wavelength if the initial guess of λ and the weighting matrix W_k are well selected. A good initial guess of λ ensures convergence if the model is accurate.

  The Single Neural Network provides a good estimate of the wavelength only if it is presented with a validation data set which has similar statistical properties with the data used for training the network therefore the trained Neural Network provided a bad estimate of the unknown wavelength when validation data generated at high temperature were presented to the network.
- The Hybrid Algorithm which essentially consisted of two Neural Network combined with the Nonlinear Least Square Algorithm uses one of the Neural network as an educative guess.

  This algorithm provides a more accurate estimate of the unknown wavelength since the initial guess of λ is done by Neural network and this enables convergence to the right solution.
- The accuracy of the estimation algorithm is well improved when the offsets in the system are compensated for. For example,compensating for the dark current and the read out noise in the photodiode by measuring the photodiode offset significantly improves the performance of the model thus improving the accuracy of the wavelength estimation.
- It was shown that normalising the data by dividing the measured intensity in each channel by the maximum intensity in that channel provides a maximum intensity of 1 in each channel and this improved the calibration of the function, and the estimation of the unknown wavelength.
- A proof of concept is developed and the result obtained shows that this wavelength estimation method measures the wavelength with high precision and resolution.

5-2 Recommendation

With regard to the work done in this thesis, the following research directions are suggested.

- In the experimental set up, the tunable light source used is limited in resolution and accuracy and as such for the deployment of this system it is important to take it further by purchasing a tunable light source from which a resolution of 0.01 nm can be generated such that the systems specification as relevant to wavelength resolution can be estimated.

- In this thesis, a low-cost spectrometer which is limited in accuracy and resolution is used for the generation of our calibration data set. This however limits the performance of our system since the calibration data are limited in accuracy and in resolution.

  Obtaining a high cost optical spectrum analyzer which provides better resolution and and improved accuracy will also improved the resolution and accuracy of our system model.

- In this thesis, tunning the spectral function of the color filter was done with stepper motor which has steps that correspond to 1.8 degrees. Fine tuning the angular displacement of the stepper motor might provide a better spectral property of the filter.

- In this thesis, the intensity measured by the photodiode are amplified and transferred to the computer for analysis in Matlab. Taking the cost of a PC, a National Instrument Data Acquisition card and the cost of purchasing the license of the Matlab software into consideration, the overall system will cost much more than 2000 euros.

  To further simplify the cost of this device and derive the low-cost benefit, miniaturisation of the system should be considered.

Appendix A

Basic idea of the Neural Network

A-1 An Appendix Section

A neural network is a massively parallel distributed processor made up of simple processing unit which has a natural propensity for storing experiential knowledge and making it available for use [10]. Hence neural network acquires knowledge from its environment through a learning process and the knowledge acquired are stored by the interneuron connecting strengths which are known as synaptic weights.

Neural network are non linear since they are made up of an interconnection of non-linear neurons, therefore the neural network can be used to develop a learning algorithm which is suitable for the analysis of our system. The intensity measurement versus wavelength which is the input to the neural network is non-linear. The learning process in the neural network which is of particular interest to the wavelength estimation in our system is the supervised learning which involves the adjustment of the synaptic weights of the network by applying a set of labelled training samples.

Each sample has a unique input signal and a desired response. When the network is presented with an example picked at random from the set of input the synaptic weights of the network are adjusted such that the difference between the desired response and the actual response of the network is minimized. Network training is done again and again for many examples in the set of input until a steady state is reached. The steady state is a point where no further change is observed in the synaptic weights.

A-1-1 Advantages of the Artificial Neural Network.

- Nonlinearity : The ANN exploits nonlinearity (i.e a nonlinear system in which the effect of external factors is not purely additive and may be disruptive, hence it cannot be decomposed into parts and reassembled into the same unit and a change in its output is not proportional to a change in its input) Since real-life problems are mostly nonlinear in nature, we therefore need nonlinear computational unit to solve the nonlinear

computational problems. The ANN provides an interconnection of non-linear Neurons and the non-linearity is distributed throughout thus making it very suitable for solving non-linear equations or problems.

- Input - Output mapping : An input is fed into the input of the system and a corresponding output or desired response is specified. When there is a difference in the actual output and the desired output, then the free parameters of the system can be modified accordingly such that for a given input, an output output closest to the desired output can be obtained. First time a pattern is fed into the system, the system has no prior knowledge of the pattern therefore what the desired output should be is also fed into the system but the actual output of the system will be different from the desired output.

  The difference between the actual output and the desired output is therefore minimized by adjusting the free parameters and this has to be done several times thus giving rise to a process of learning which involves a teacher. The role of the teacher is to specify the output corresponding to a set of a given input such that if the system output does not correspond to what has been specified by the teacher then the teacher places a demand for the adjustment of the free parameters such that when the same input is fed again into the system, an output closer to the desired output will be obtained and then deviation between the actual and the desired response corresponding to a given set of input is minimised. The learning ability of the neural network distinguishes it from other conventional computational units. Learning can also be done with association where a given set of input is associated with a desired output.

- Adaptivity : Neural network can adapt the free parameters to the changes in its surrounding environment.

- Evidential Response : The Neural network associates a great percentage of confidence measures to its decision.

- Ability for Fault Tolerance : A failure of one neuron will not result into a catastrophic failure but might result into a degradation in performance which is referred to graceful degradation (meaning the number of fault is proportional of degradation such that if the number of fault is minimal then the degradation is also very reduced)which is contrary to the computer unit where a failure of a single processing unit can cause a catastrophic failure.

- VLSI implementable :VLSI (is the process of creating integrated circuits by combining thousands of transistors into a single chip) A very large number of neurons can be integrated together using integrated circuits. This is achievable because the neurons are absolutely parallel computational units (i.e the neurons can do independent computation).

A-1-2 Non-linear model of a neuron

The neuron is the information-processing units which very key to the operation and performance of a neural network. The neuron model (a functional description of various elements that constitute the model of a neuron) has three fundamental elements which are very important for its operation.

The above figure depicts the non-linear model of a neuron with its three basic elements.

- The connectivity link (Called synapses):The synapse decide the strength of the connection i.e how strong or how weak the connecting link is hence the strength of the connection is called the synaptic weights and it is proportional to its value. The larger the value, the stronger the connection and vice versa.The synaptic weights are defined for the connection between the input and the neuron under consideration and are represented as shown above as w_{kj} Where w_{kj} is the connection between neuron k and input j. Each of the connecting link has the weight of its own such that the input signal x_j is multiplied by the connecting links to produce an input signal which is weighted by the connecting links such that .
- The Adder : Sums up the weighted input signals of the respective input so that the sum total is the summation of all the weighted input and effectively linearly combining them together.
- The activation function: It squashes the output of a neuron thus limiting its amplitude to 1 or 0 such that the response of the neuron is absolutely binary in nature, if the output of the neuron requires a threshold function limiting is output to -1 and 1 then activation function is defined as a signal function.

The bias b_k increase or lowers the net input of the activation function, it is often used as input into the system. The neuron k can be described in mathematical terms by the following equation :

$$U_k = \sum_{j=1}^{\infty} W_{kj} X_j \tag{A-1}$$

and the output $y_k = \varphi(U_k + b_k)$ Where the input signal are $x_1, x_2, x_3, ...x_n$ and the connecting links or synaptic weights are $w_{k1}, w_{k2}....w_{km}$.

The adder produces an output U_k after summing the input signals weighted by the respective connecting links. The bias is represented by b_k and the activation function is denoted as $\varphi(\dot{})$. While y_k is the output of the neuron. The activation function employed in our Neural network algorithm is the sigmoid function. The S-shaped sigmoid activation functions exhibits a good balance between linear and non linear behaviour [34].

An example of the sigmoid function is the logistic function defined by

$$\varphi(v) = \frac{1}{1 + exp(-av)} \tag{A-2}$$

where a is the slope parameter of the sigmoid function.

The hyperbolic tangent function expressed as $\varphi(v) = tanh(v)$ is the corresponding form of the sigmoid function.

A-1-3 Knowledge Representation of the Neural Network

The neural network has a predominant task of learning a model of the environment where it is embedded and to maintain the model such that it is sufficiently consistent with the

real world thus achieving its goal of interest. Prior information is a type of knowledge of the Neural Network which provides fact about what information is and what information has been known. Measurements or observations of the world are also obtained by sensors designed to probe the environment in which the neural network is supposed to operate thus providing a pool of information from which examples used to train the network are drawn. This is another type of information that forms the knowledge of the network. A set of training data therefore contrast of a set of input-output pairs with each pair consisting of an input signal and a corresponding desired response.

A-1-4 Learning Process of a Neural Network

Learning is a process by which the free parameters of a Neural network are adapted through a process of stimulation by the environment in which the network is embedded. Hence a learning algorithm is a prescribed set of a well-defined rules for the solution of a learning problem. The difference in learning algorithm is rooted in the way in which the adjustment to a synaptic weight of a neuron is formulated. The learning algorithm of our neural network is based on the error-correction rule.

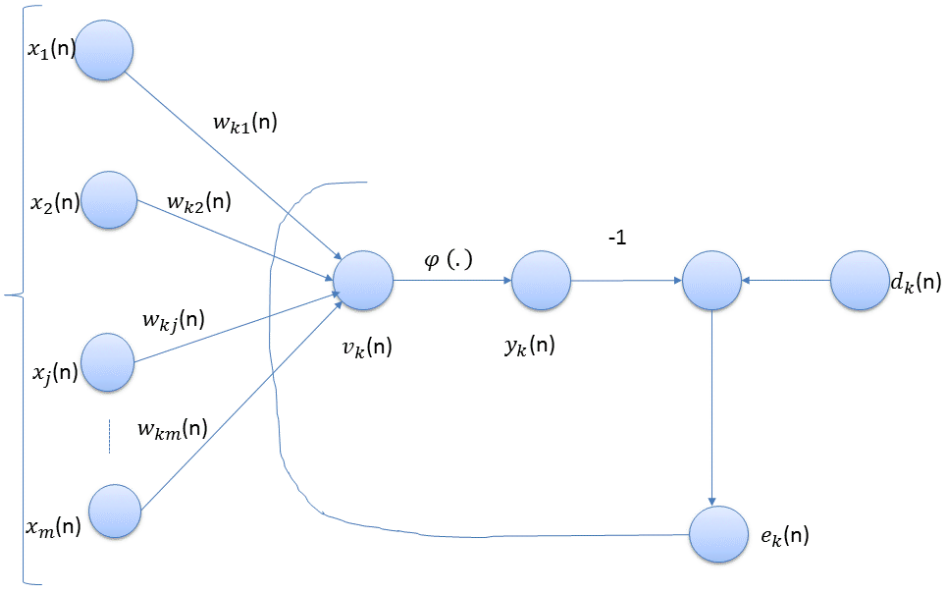

Figure A-1: *The schematic diagram of the Neural Network error correction learning* [18]

Figure depicts a neuron K which represents the only computational node in the output layer of the neural network

x(n) a signal vector is the output of the hidden layer of neuron driven by an input vector applied to the input layer of the network. The output Neuron K is thus driven by the signal vector x(n). Where n is an argument denoting the time step of an iterative process used for the adjustment of the synaptic weights of neuron k. The output neuron k produces an output

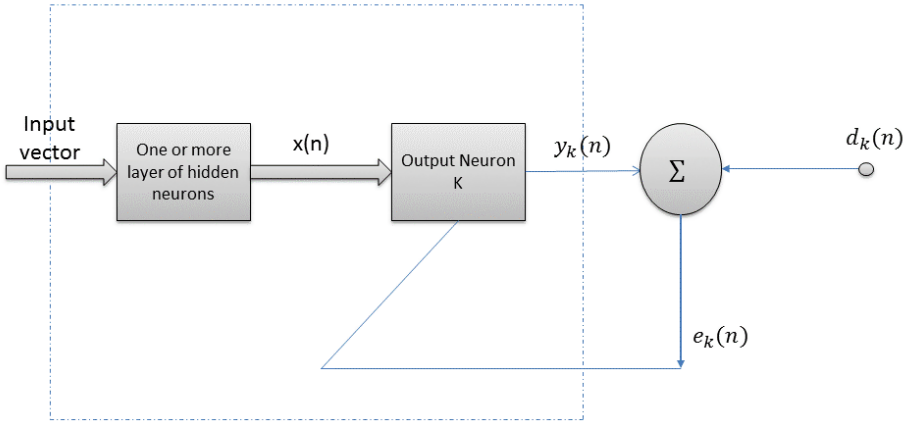

Figure A-2: *The schematic diagram of the Neural Network error correction learning* [18]

signal denoted by $y_k(n)$. The output $y_k(n)$ is compared to the desired response or target output denoted by $d_k(n)$ in the diagram. This comparison gives rise to an error-signal which by definition is represented as :

$$e_k(n) = d_k(n) - y_k(n) \tag{A-3}$$

The error signal $e_k(n)$ activates the control mechanism which is aimed at applying a sequence of corrective adjustment to the synaptic weights of neuron k. The corrective adjustment aims at making the output signal $y_k(n)$ come closer to the desired response in a sequential manner. This aim is achieved when the cost function defined in terms of error signal is reduced. The learning process is however terminated when the step -by-step adjustment to the synaptic weights of neuron k brings the system to a steady state i.e the synaptic weights are essentially stabilized.

This learning rule is commonly known as the Widrow-Hoff Rule which is defined as (the adjustment made to a synaptic weight of a neuron is proportional to the product of the error signal and the input signal of the synapse in question). Let $w_{kj}(n)$ be the value of the synaptic weight w_{kj} of neuron k excited by element $x_j(n)$ of the signal vector $x(n)$ at time step (n). The adjustment $\Delta w_{kj}(n)$ applied to the synaptic weight w_{kj} at time step n is defined by :

$$\Delta w_{kj}(n) = \eta e_k(n) x_j(n) \tag{A-4}$$

and η is a positive constant determining the learning rate. Since the synaptic adjustment $\Delta w_{kj}(n)$ is computed then updating it is done as follows.

$$\Delta w_{kj}(n+1) = w_{kj}(n) + \Delta w_{kj}(n) \tag{A-5}$$

$w_{kj}(n)$ is the old value of synaptic weight and $w_kj(n+1)$ is viewed as the new value of synaptic weight w_{kj}

A-1-5 The Back Propagation Algorithm

The back propagation algorithm is an algorithm based upon the error-correction learning rules and it is employed to train neural network which have one or more hidden layers between the input layer of the computational nodes and the output layer of computation nodes, such multilayer network is called a multilayer perceptron. The multilayer perceptron has three characteristics :

- The model of each neuron in the network includes a non-linear activation function.
- The network contain one or more layer of hidden neuron which are excluded from the input or output of the network. The ability of the network to learn complex tasks is enhanced by the hidden layer.
- A high degree of connectivity determined by the synapsis of the network is exhibited by the network

Appendix B

Methods for solving the Non Linear Least Square

The non-linear least square method involve an iterative improvement to parameter values in order to reduce the sum of the squares of the errors between the approximated function and the measured data points. Methods for solving the Non-linear least square problems include :

1. Gradient-descent method.
2. Gauss -Newton method.
3. Levenberg-Marquardt Algorithm.

The above highlighted algorithms are reviewed in the next subsection according to the following references [29,30,31]

B-0-6 Gradient Descent Method

The Gradient Descent Method is a general minimization method which updates parameter values in the direction opposite to the gradient of the objective function. It is an iterative method that is given an initial point, and follows the negative of the gradient in order to move the point toward a critical point, which is hopefully the desired local minimum. It is a highly convergent algorithm for finding the minimum of simple objective functions. Its major disadvantage is that it can take a long time to converge.

B-0-7 Gauss-Newton Method

The Gauss-Newton Method is a method of minimizing a sum-of-squares objective function. It presumes the objective function is approximately quadratic in the parameters near the optimal solution.It is an algorithm that converges much faster than the gradient-descent methods.

B-0-8 Levenberg-Marquardt Method

The Levenberg-Marquardt curve-fitting method is actually a combination of two minimization methods: the gradient descent method and the Gauss-Newton method. In the gradient descent method, the sum of the squared errors is reduced by updating the pa- rameters in the direction of the greatest reduction of the least squares objective. In the Gauss-Newton method, the sum of the squared errors is reduced by assuming the least squares function is locally quadratic, and finding the minimum of the quadratic. The Levenberg-Marquardt method acts more like a gradient-descent method when the pa- rameters are far from their optimal value, and acts more like the Gauss-Newton method when the parameters are close to their optimal value.

The LM algorithm was chosen for our NLLS optimisation technique because its solution typically converges rapidly to the local minimum and the ease in implementing it in Matlab.

Local Minima

The local minima is the smallest value that the function takes at point either within a given neighborhood. Non-linear optimisation may result in a local minimum or have multiple solutions therefore it is important to keep the initial guess (λ) bounded so that the initial guess can be randomly chosen between an interval [λ_{min} and λ_{max}].

List of Abbreviations

- FP : Fabry Perot.
- DG : Diffraction grating.
- OSA : Optical Spectrum Analyzer.
- TCF : Tunable Color Filter.
- PD : Photodiode.
- NLLS : NonLinear Least Square.
- DCSC : Delft Centre for Systems and Controls.
- DS : Dataset
- No.Angles : Number of Angles.
- No. Wavelength : Number of Wavelength.
- No. Duplicates : Number of Duplicates.
- Intensity Val : Intensity Value.
- Pwr.Levels : Power Levels.

Bibliography

[1] Roberto Bartali *Fabry-Perot Interferomter*available at// *http* : $//www.scribd.com/doc/6715522/Fabry-Perot-Interferometer$

[2] Discovery of Light,Thinkquest. Available at *http* : $//www.library.thinkquest.org/27356/p_index.htm$

[3] Introduction to FTIR Spectroscopy,Newport available at // *http* : $//newport.com/store/gencontent.aspx?id = 405840'I\&'lang = 1033'I\&'print = 1.$

[4] R.M Oldenbeuving. *Spectral Control of Diode Lasers Using External Waveguide Circuits.* PhD thesis, University of Twente , February 2013.

[5] V.N. Tkachenko.*Optical Spectroscopy Methods and Instrumentations.*Elsevier 2006.

[6] J.Brady.*Optical Imaging and Spectroscopy.*John Wiley 'I&'Sons 2009.

[7] E.Nicolescu, M;J Escuti.*Compact Spectrophotometer using polarization-independent crysal tunable optical filters* In Proceedings of SPIE, Vol.6661,no.666105(2007)

[8] P.Griffiths 'I&' J.D.Haseth.*Fourier Transform Spectrometry.*Wiley 'I&' Sons, 1986.

[9] E.Hecth.*Optics*,Addison Wesley 2002.

[10] Fourier Transform NIR Available at *http* : $//www.nicoletcz.cz/userfiles/file/ruzne/FourierTransfor$

[11] Introduction to Laser beam and Spectral Measurement, available at www.cvimelllesgriot.com.

[12] J.F. James. *A students guide to Fourier transforms.*Cambridge 2011.

[13] J.James.*Spectrograph Design fundamental.*Cambridge 2007

[14] I.Ashdown, P.Eng,L.C.*Photo 'I&' Radiometry : A tour guide for computer Graphics Enthusisasts*

[15] P.J Olver./textitIntroduction to Partial Differential Equations, Available online at *http* : *//www.math.umn.edu/ olver/pd/ft.pdf*

[16] What is Spectral resolution, available at http://www.horiba.com/scientific/products/raman-spectroscopy/ //tutorial-faqs/raman-faqs/what-is-spectral-resolution-and-when-is-it-needed/

[17] Fabry-Perot Interferometers available online at *http* : *//www.rp − photonics.com/fabry_perot_interferometers.html*

[18] R.Hui,M.OâĂŹSullivan. *Fibre optics measurement technique.*Elselvier 2009.

[19] Diffraction grating available online at *http* : *//www.olympusmicroscopy*

[20] E.Baker,M;V. Yen.*Effects of the variation of Angle of Incidence and Temperature on Infrared Filter Characteristics* Applied Optics, Vol.6,no.8(1967)

[21] J Brauers, T. Aach.*Multispectral Imaging with Optical Bandpass Filters: Tilt Angle and Position Estimation//* In Proceedings of SPIE, Vol.7241,no.72410Z-1(2011)

[22] Laser Wavelength Measurement using a Colored filter Glass available online at *http* : *//www.assets.newport.com/webDocuments − EN/images/TN6810B − 7_Measure_Color_Filter_IX.pdf*

[23] Noise in photodetectors available online at *http* : *//www.optical − technologies.info/noise − in − photodetectors*

[24] Optical Detectors available online at *http* : *//www.depts.washington.edu/mictech/optics/sensors/detec*

[25] Unravelling sensitivity, signal to noise and dynamic range available online at *http* : *//www.emccd.com/what_is_emccd/unraveling_sensitivity/Signal_to_Noise_in_CCDs/*

[26] B.E Saleh, M.C Teich.*Fundamental of Photonics,*Willey 2002.

[27] UV/VIS Bandpass and Laser Line Filters:340-694.3nm Center Wavelength available online at *http* : *//www.thorlabs.com/NewGroupPage9.cfm?ObjectGroup_ID* = 1001/

[28] The Light Sensor available online at*http* : *//www.electronics − tutorials.ws/io/io_4html*

[29] Gradient Descent available online at*http* : *//homes.soic.indiana.edu/classes/spring*2012/*csci/b*553*− hauserk/gradient_descent.pdf*

[30] M. Lourakis,A.Argyros *Is Levenberg-Marquardt the Most Efficient Optimization Algorithm for Implementing Bundle Adjustment?*

[31] H.Gavin *Levenberg-Marquardt method for nonlinear least squres curve fitting problems*

[32] Understanding the tricky thermocouple available online at *http* : *//www.controlengeurope.com/article/*21976/*Tutorial − −Understanding − the − tricky − thermocouple.aspx*

[33] *Optical Thin Films.*SPIE Press 1996.

[34] *Neural Networks : A Comprehensive Foundation.* Prentice Hall 1994.